Applications of Vectorcardiography for Diagnosis and Risk Stratification in Subpopulations at Risk for Life-Threatening Arrhythmias

Cortez, Daniel

2020

Document Version:
Publisher's PDF, also known as Version of record

Applications of Vectorcardiography for Diagnosis and Risk Stratification in Subpopulations at Risk for Life-Threatening Arrhythmias

DANIEL CORTEZ
FACULTY OF MEDICINE | LUND UNIVERSITY

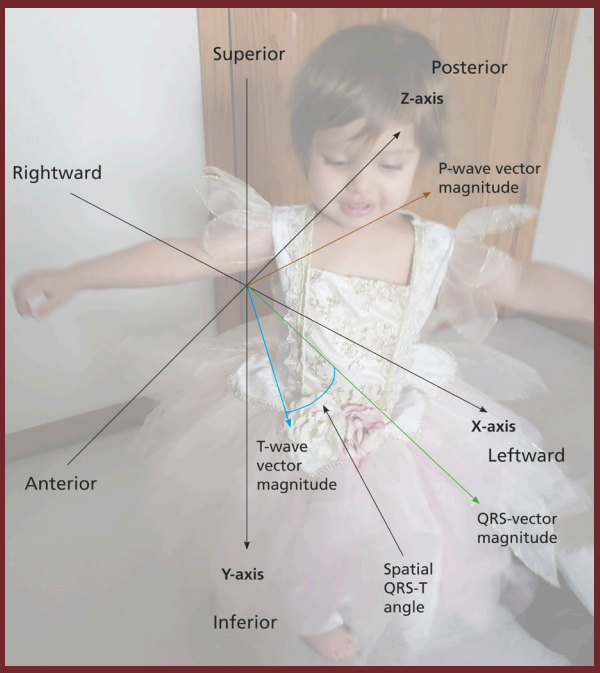

Printed by Media-Tryck, Lund 2020 NORDIC SWAN ECOLABEL 3041 0903

FACULTY OF MEDICINE

Lund University, Faculty of Medicine
Doctoral Dissertation Series 2020:73
ISBN 978-91-7619-935-0
ISSN 1652-8220

Applications of Vectorcardiography for Diagnosis and Risk Stratification in Subpopulations at Risk for Life-Threatening Arrhythmias

Applications of Vectorcardiography for Diagnosis and Risk Stratification in Subpopulations at Risk for Life-Threatening Arrhythmias

Daniel Cortez

LUND
UNIVERSITY

DOCTORAL DISSERTATION

By due permission of the Faculty of Medicine, Lund University, Sweden.
To be defended at Segerfalksalen, Biomedicinskt Centrum, Lund University

Monday 08/06/2020 and time 14:00.

Faculty opponent
Jens Cosedis Nielsen, MD, PhD

Organization LUND UNIVERSITY	**Document name** DOCTORAL DISSERTATION
	Date of issue 6-8-2020
Author(s) Daniel Cortez, MD, Pyotr Platonov MD/PhD	Sponsoring organization Lunds Universitet

Title and subtitle: Applications of Vectorcardiography for Diagnosis and Risk Stratification in Subpopulations at Risk for Life-Threatening Arrhythmias

Abstract

Introduction: Vectorcardiography, or 3-dimensional electrocardiography is a tool which can be used to identify subtle changes in the electrical forces of the heart, and which can be applied to atrial depolarization, ventricular depolarization and ventricular repolarization for prognostic and diagostic purposes.

Methods: Kor's regression-related and quasi orthogonal methods was used to derive vectorcardiographic parameters from the 12-lead electrocardiogram and applied to a cohort of cryptogenic stroke patients to assess atrial fibrillation, hypertrophic cardiomyopathy patients to assess for ventricular arrhythmias, applied with right-precordial directed quasi orthogonal method to arrhythmogenic right ventricular dysplasia/cardiomyopathy (ARVC/D) patients for diagnosis, and applied to ventricular repolarization only to patients with genotype-positive/phenotype-negative Long QT2 syndrome (KNCH2 mutation) to assess for cardiac events. Parametric and non-parameteric parameters were presented as mean ± standard deviation and median (1st to 3rd interquartile ranges). Pearson and Spearman correlation coefficients were used for parametric and non-parametric data, respectively. Odds ratios with univariate and multivariate analyses as well as hazard ratios and Kaplan-Meier curves are presented. P-values under 0.05 were represented as significant.

Results: In cryptogenic stroke patients, first atrial fibrillation event was predicted by baseline P-wave duration divided by P-wave vector magnitude ($p<0.05$). In hypertrophic cardiomyopathy patients, the spatial peaks QRS-T angle differentiated sustained ventricular arrhythmias (VA) from no VA ($P < 0.001$) and at 124.1 degrees gave positive and negative predictive values and an odds ratio of 36.7%, 96.1%, and 14.2 (95% confidence interval: 3.1-65.6), respectively. Combined right precordial-directed parameters were able to identify ARVD/C patients who otherwise met criteria but did not meet any ECG-specfiic 2010 Taskforce criteria from controls with a positive predictive value of 90.0% and negative predictive value of 83.3%. In patients with genotype positive KCNH2 mutations, without prolongation of the QTc, when dichotomized by the median of 0.30 mV, a low T-wave vector magnitude (TwVM) was associated with elevated cardiac event risk compared to those with high TwVM (HR=2.55, 95%CI 1.07-6.04, p=0.034) and the genotype-negative family members (HR=2.64, 95%CI 1.64-4.24, $p<0.001$).

Conclusion: Vector magnitudes and spatial angles, involving atrial and ventricular depolarization as well as ventricular repolarization, can be helpful in identifying disease as well as first-onset arrhythmia in subpopulations at risk for sudden death or stroke.

Key words Vectorcardiography, atrial depolarization, ventricular depolarization/repolarization

Classification system and/or index terms (if any)

Supplementary bibliographical information	**Language** English
ISSN and key title 1652-8220 Lunds University, Faculty of Medicine Doctoral Dissertation Series 2020:73	**ISBN** 978-91-7619-935-0

Recipient's notes	**Number of pages** 82	Price
	Security classification	

Signature  Date 2020-05-04

Applications of Vectorcardiography for Diagnosis and Risk Stratification in Subpopulations at Risk for Life-Threatening Arrhythmias

Daniel Cortez

LUND
UNIVERSITY

Cover photo Natalia Cortez Sharma

Faculty of Medicine
Department of Clinical Sciences Lund

ISBN 978-91-7619-935-0
ISSN 1652-8220

Printed in Sweden by Media-Tryck, Lund University
Lund 2020

To Nandita, Natalia and Mom

Table of Contents

List of publications:

I. **Cortez, D**, Baturova M, Lindgren A, Carlson J, Shubik Y, Olsson B, Platonov PP. Atrial time and voltage dispersion are both needed to predict new-onset atrial fibrillation in ischemia stroke patients. BMC Cardiovascular Disorders (2017) 17:200 DOI 10.1186/s12872-017-0631-1

II. **Cortez D,** Graw S, Mestroni L. In hypertrophic cardiomyopathy, the spatial peaks QRS-T angle identifies those with sustained ventricular arrhythmias. Clin Cardiol (2016) 39:459-463 DOI 10.1002/clc.22549

III. **Cortez D,** Svensson A, Carlson J, Graw S, Sharma N, Brun F, Spezzacatene A, Mestroni L, Platonov PG. Right precordial-directed electrocardiographical markers identify arrhythmogenic right ventricular cardiomyopathy in the absence of conventional depolarization or repolarization abnormalities. BMC Cardiovascular Disorders (2017) 17:261 DOI 10.1186/s12872-017-0696-x

IV. **Cortez D,** Zareba W, McNitt S, Polonsky P, Rosero SZ, Platonov PG. Quantitative T-wave morphology assessment from surface ECG is linked cardiac events risk in genotype-positive KCNH2 mutation carriers with normal QTc values. J Cardiovasc Electrophysiol (2019) 30:2907-2913. DOI 10.1111/jce.14210

Populärventenskaplig Sammanfattning

Nära hjärtat - nytt tredimensionellt EKG för diagnostiken närmare hjärtat, för att rädda barns liv

Vi har alla hört talas om den där vännen, familjemedlemmen, ungen i kvarteret eller sportstjärnan som plötsligt föll död ner på en basketplan, fotbollsplan, löparbana eller under något annat idrottsevenemang. Den som är frisk som en nötkärna, med fina stipendier och stora drömmar hägrandes vid horisonten. Som sedan plötsligt kollapsar, död, ner på marken på grund av plötslig hjärtdöd.

Plötslig hjärtdöd skall inte nonchaleras. Det kan hända vem som helst - även de där idrottarna som ser så friska ut. Den vanligaste orsaken till att dessa människor dör är kardiomyopati (en avvikande förtjockning eller uttänjning av hjärtat, som finns hos färre än en av 500 personer). Det kan också bero på att personen har en avvikande hjärtrytm (arytmi). Bara hos 50 % av dem som har någon av dessa sjukdomar upptäcks dessa vid rutinmässig screening. Med den låga sannolikheten för att dessa farliga sjukdomar identifieras, används rutinmässig screening med elektrokardiogram (EKG, ett 200-kronorstest där en uppsättning elektroder visar hjärtats elektriska impulser) inte av vare sig skolor eller vårdcentraler, och rekommenderas heller inte av the American Heart Association (AHA).

Elektrokardiogrammet visar överföringen av elektriska impulser via hjärtats muskelfibrer. Dock ses och avläses detta av de flesta kardiologer (hjärtdoktorer) oftast i endast två dimensioner. Liksom TV-spelet Mario Bros eller andra spel visar mycket mer information i 3D, kan man se mycket mer av hjärtat om man tittar på dess elektricitet också i en tredje dimension. Hjärtats elektriska impulser hos patienter som plötsligt dör av hjärtattacker har undersökts i tre dimensioner under flera år års tid nu. Samtidigt är det endast nyligen som man har börjat göra detta även med personer som riskerar att dö plötsligt på grund av kardiomyopati eller en avvikande hjärtrytm. Användning av tredimensionellt EKG har hjälpt oss att avgöra vem som riskerar att få en förtjockning eller uttänjning av hjärtat, vem som kommer att utveckla arytmier samt vem som riskerar att dö en plötslig död. I stora grupper med personer som har dessa sjukdomar, har tredimensionellt EKG jämförts med *the golden standard* - hjärtultraljud (ekokardiogram, 10000 kronor per test). Detta i syfte att jämföra hur väl det kan diagnosticera kardiomyopati hos idrottare i Kalifornien.

Om användning av tredimensionellt EKG visar sig vara lika effektivt som ekokardiogram, kan det förändra hur vi screenar idrottare eller unga människor som är i riskzonen för att få dessa dödliga sjukdomar. Hittills visar forskningen att när en tredje dimension inkluderas, kan EKG upptäcka såväl kardiomyopati som eventuell risk för arytmier (något som ekokardiogram inte kan identifiera särskilt

väl). Som en konsekvens av detta kan fler personer som löper stor risk att drabbas av plötslig hjärtdöd identifieras genom användning av EKG.

Endast tiden kan avgöra huruvida *the European Society of Cardiology* inför en rekommendation att använda tredimensionellt EKG. Hittills har det visat lovande resultat - det ser ut som att det en dag kan komma att användas för att för att identifiera huruvida en patient löper risk att drabbas av arytmi, samt för att underlätta tidigare behandling eller att förhindra att du får svårare komplikationer av sjukdomen.

Abbreviations:

ACA:	Aborted cardiac arrest
AF:	Atrial fibrillation
ARVD/C:	Arrhythmogenic right ventricular cardiomyopathy/dysplasia
ECG:	Electrocardiography
HR:	Hazard ratio
ICD:	Implantable cardioverter defibrillator
LQTSD:	Long QT-related sudden death
LQTS:	Long QT syndrome
LQT2:	Long QT type 2
MD:	Medical Doctorate
MRI:	Magnetic resonance imaging
Mm:	millimeter
ms:	milliseconds
mV:	millivolt
Pd:	P-wave duration
PhD:	Doctor of Philosophy
PVM:	P-wave vector magnitude
QRSd:	QRS duration
QRSVM:	QRS vector magnitude
QTc:	corrected QT duration
RBBB:	Right bundle branch block
SAECG:	Signal average electrocardiogram
SPQRS-T angle:	Spatial peaks QRS-T angle
TAD:	Terminal activation delay
TwVM:	T-wave vector magnitude
VA:	ventricular arrhythmias
VCG:	Vectorcardiography

Introduction

Vectorcardiography

Most people are familiar with the 12-lead electrocardiogram. Vectorcardiography, however, is similar but gives us a way of assessing the electrocardiogram in 3-dimensional space. It was first described in 1934 by Wilson through a communication describing the method of analysis on an electrocardiogram to yield more information than had been previously described (1). The concept described by Wilson was the ventricular gradient and was barely understood by clinicians and only understood by some researchers. This concept of the ventricular gradient and concepts related were further developed in the 1950's which lead to development of the understanding of repolarization and depolarization concepts in routine electrocardiographic (ECG) tracings (2-3). This basis of the ventricular gradient stems from overall concept of electromotive force, which is the difference in electrical potential that gives rise to a current (4). Electromotive force can be demonstrated visually by drawing an arrow with the length of the arrow proportional to the magnitude of the force in a particular direction (Figure 1). The body itself is a volume conductor with an irregular limiting boundary surface with the thorax of which a large portion is taken up by the heart, having multiple electromotive forces generated simultaneously. Thus, any electrical tracing represents an approximation, typically of the largest forces at that particular time of measure (4). However, the maximum deflection of the vectors of depolarization and repolarization can be seen visually and represented in 3-dimensional space by the vectorcardiogram (1). Each lead representing the X, Y and Z planes of 3-dimenstional space, are called orthogonal leads. Each orthogonal lead should be mutually perpendicular to the other leads for each point in the heart and each should retain the same magnitude and direction for all points where electromotive forces are generated (4).

The vectors representing the electromotive forces at any instantaneous time may have a different direction during each phase of the cardiac cycle, which include atrial depolarization, atrial repolarization, ventricular depolarization, and ventricular repolarization. Typically, atrial repolarization (the tau wave) is not well visualized due to significant overlap with ventricular depolarization, thus clinically it is not very practical to try to measure the tau wave in those with intact atrioventricular conduction. Thus, we will focus on the vectorcardiograms representing atrial depolarization (represented by the P-wave on the electrocardiogram (ECG). The

ventricular depolarization (represented by the QRS-wave on ECG), and the ventricular repolarization (represented by the T-wave on ECG) will also be discussed. For each complex represented on the ECG (P, QRS and T-waves), a vectorcardiogram can be drawn for depolarization/repolarization direction in space and magnitude at each particular time occurrence of the depolarization/ repolarization. The maximum deflection from the origin of the electrical signal (first atrial or ventricular myocardium depolarized, ie. the superior aspect of the left ventricular septum for initiation of ventricular depolarization) can be demonstrated by a vector that passes through this point from the origin, with the length of the vector representing the maximum voltage deviation from the origin. This maximum vector voltage deviation from the origin, in a particular direction, can be called a vector maximum, which has its own inherent magnitude, measured in millivolts (mV) (4).

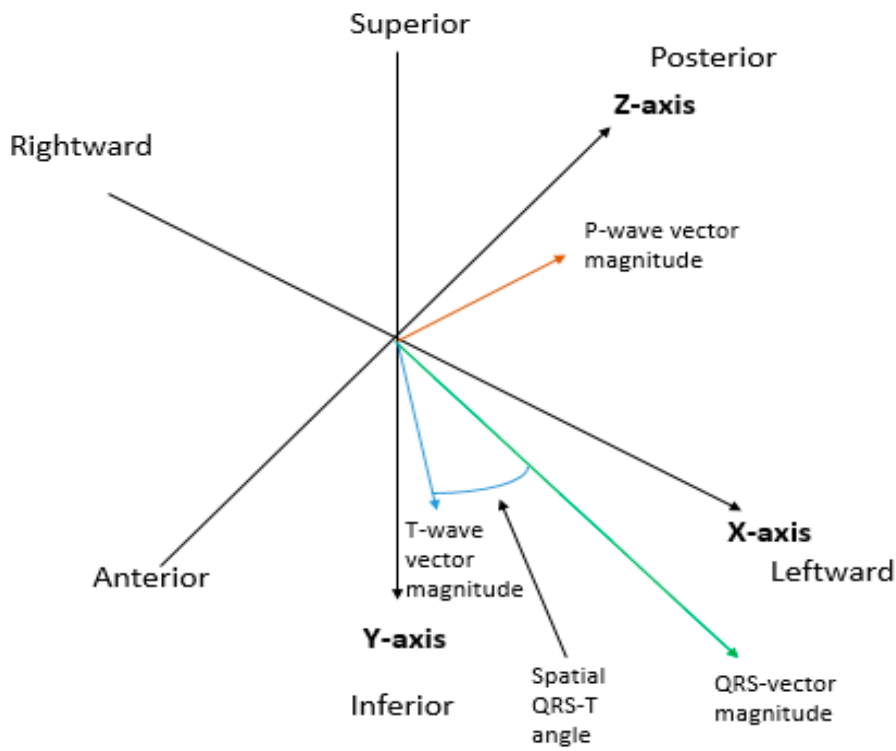

Figure 1: P-wave, QRS and T-wave vector magnitudes.

Although, the vector maxima, have a direction and magnitude, they can each be reported separately, including the P-wave vector maximum (Pvm), the QRS vector

maximum (QRSVM) and the T-wave vector maximum (TwVM). The magnitude of the each of the maximum vectors can change based on increased size of atria or ventricles with increasing size or with increased scar burden typically causing change in global vector direction and lower maximum deflection from the origin of the magnitude of the depolarization or repolarization magnitudes (4). The loop for the P-wave during the atrial depolarization is usually mostly located in the left infero-posterior quadrant with Pvm of around 0.20mV (4). The loop for the QRS-wave during depolarization typically is located mostly in the left infero-posterior quadrant with QRSVM of around 1.95 millivolts (mV), whereas the T-wave loop typically is mostly located in the left infero-anterior quadrant with TwVM of close to 0.76mV in adults (4). An angle can be calculated between the vector maxima, called the spatial peaks QRS-T angle (SPQRS-T angle), which can be calculated utilizing a transform by assessing the heights of the maximum deflection of the QRS and T-waves in lead I, II, V1-V6 (Figure 2).

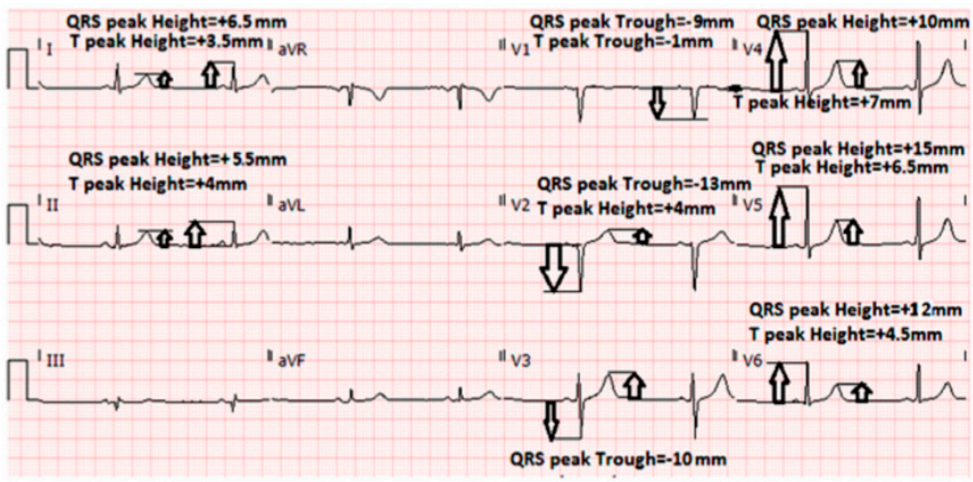

Figure 2: QRS-T components in calculation of the spatial QRS-T angle using Kors' regression-related method.

The magnitude of the QRSVM can also be affected by left ventricular hypertrophy, which can cause an increase in the magnitude and change in direction of this maximum vector, especially in the setting of asymmetric left ventricular hypertrophy and as compared by an angle between the QRS and T-wave maximum vectors, again, called the spatial peaks QRS-T angle (4,5,6). The spatial QRS-T angle can be viewed as a way to quantify the difference between a shift in the maximum QRS axis compared to a shift in the maximum T-wave axis, thus allowing one to assess early changes in either the QRS or T-wave axes, prior to more obvious changes such as T-wave inversions (4). For example, in someone with asymmetric left ventricular hypertrophy, the depolarization vector may shift to a more septal position, prior to T-wave vector shift as exemplified in Figure 3.

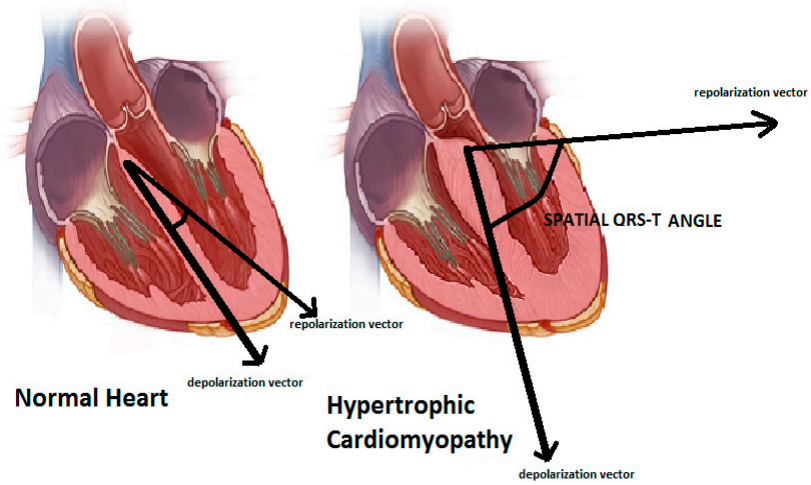

Figure 3: Change in depolarization and repolarization vectors in the normal heart and hypertrophic cardiomyopathy.

Variability of the T-wave amplitude has been associated with dilated cardiomyopathy and events in this patient population, while data is scant regarding predictive value of the TwVM (7). In paediatric patients, a lower TwVM was associated with Kawasaki disease compared to control patients who had higher TwVM values (8).

Table 1: Spatial QRS-T angle calculation based on the Kors' regression-related formula.

RMSQRS = QRS vector magnitude (QRSVM)	$\sqrt{(QRS_X^2+QRS_Y^2+QRS_Z^2)}$
RMST = T-wave vector magnitude (TwVM)	$\sqrt{(T_X^2+T_Y^2+T_Z^2)}$
SPQRS-T angle (peaks)	$\text{cosign}^{-1}[(QRS_X*T_X\_QRS_Y*T_Y+QRS_Z*T_Z)/(RMSQRS*RMST)]$
QRS_X	$0.38*QRS_I-0.07*QRS_{II}-0.13*QRS_{V1}+0.05*QRS_{V2}-0.01QRS_{V3}+0.14*QRS_{V4}+0.06*QRS_{V5}+0.54*QRS_{V6}$
QRS_Y	$0.07*QRS_I+0.93*QRS_{II}+0.06QRS_{V1}-0.02*QRS_{V2}-0.05*QRS_{V3}+0.06*QRS_{V4}-0.17*QRS_{V5}+0.13*QRS_{V6}$
QRS_Z	$0.11*QRS_I-0.23*QRS_{II}-0.43*QRS_{V1}-0.06*QRS_{V2}-0.14*QRS_{V3}-0.20*QRS_{V4}-0.11*QRS_{V5}-0.31QRS_{V6}$
T_X	$0.38*T_I-0.07*T_{II}-0.13*T_{V1}+0.05T_{V2}0.01T_{V3}+0.14*T_{V4}+0.06*T_{V5}+0.54*T_{V6}$
T_Y	$0.07*T_I+0.93*T_{II}+0.06T_{V1}-0.02*T_{V2}-0.05*T_{V3}+0.06*T_{V4}-0.17*T_{V5}+0.13*T_{V6}$
T_z	$0.11*T_I-0.23*T_{II}-0.43*T_{V1}-0.06*T_{V2}-0.14*T_{V3}-0.20*T_{V4}-0.11*T_{V5}-0.31T_{V6}$

Arrhythmogenesis and vectorcardiography

Atrial abnormality: Atrial fibrillation

Atrial fibrillation (AF) is an irregularly irregular atrial rhythm with atrial impulses between 350 and 600 beats per minute and tends to exhibit irregular ventricular responses with fine or course atrial "f" waves in lead V1, as demonstrated in Figure 4 (9). The two most common mechanisms include cause by unifocal/multifocal rapidly discharging foci or by single or multiple re-entry wavelets (10,11, 12).

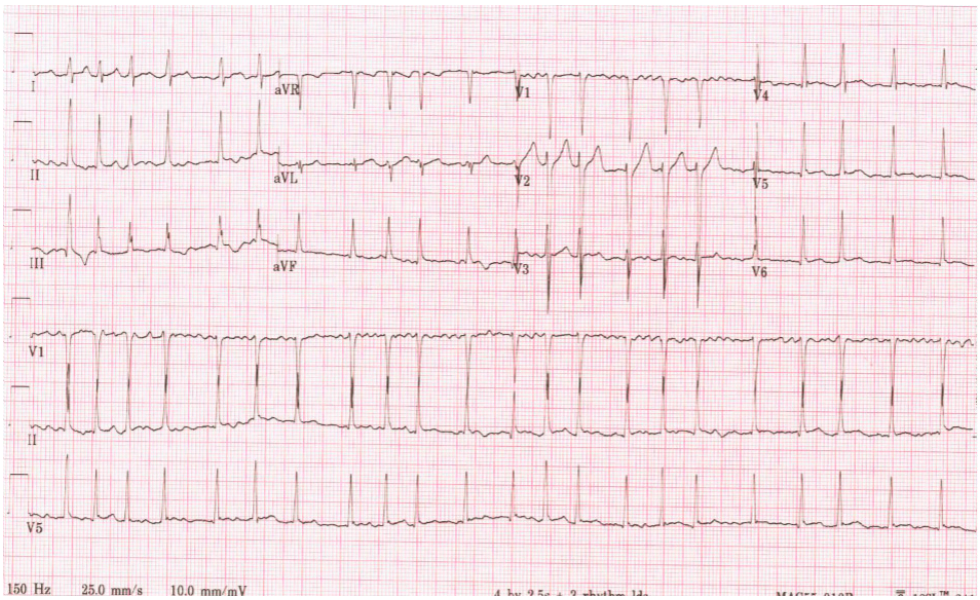

Figure 4: example of atrial fibrillation, note irregularly irregular QRS intervals and F-waves

Figure 5A-C demonstrates different possible mechanisms for atrial fibrillation. One fairly acceptable mechanism for persistence of wavelet re-entry suggests that increase in ryanodine expression and single channel open-probability increase risk of sarcoplasmic reticulum Ca2+-release events, causing delayed after depolarizations (similar to an R on T phenomenon but P on Tau in the case of atrial cells), as well as triggered events which may lead to paroxysmal atrial fibrillation (13).

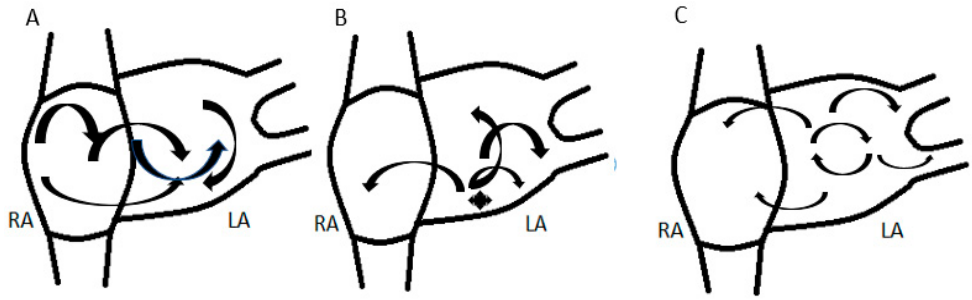

Figure 5: A-multiple wave re-entry, B-single ectopic focus, C-single wave re-entry

Atrial dilation, increase ventricular diastolic pressures and increased scar burden, can increase heterogeneity of atrial repolarization which can increase the probability of atrial delayed after depolarization (premature depolarization on phase 3 of the atrial action potential, Figure 6B). Furthermore, patients with sinus node disease can also have an increased burden of ectopic atrial beats, thus worsening atrial fibrillation as well (Figure 5A shows sinus node action potential, whereas Figure 5B is a typical atrial myocardial cell action potential). Electrical remodelling which can cause the above changes in the atrium, can also be caused by repetitive or incessant episodes of atrial fibrillation, and atrial fibrillation can beget further atrial fibrillation. Thus, treatment of atrial fibrillation can prevent further atrial fibrillation.

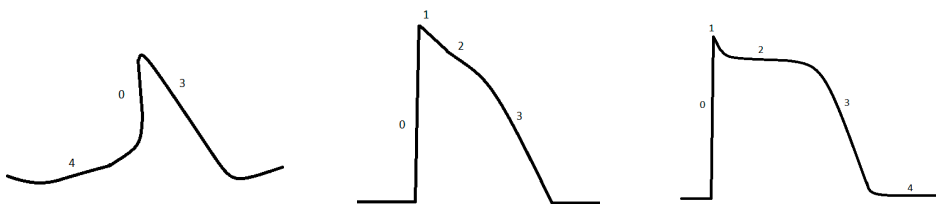

Figure 6 A:Sinus node/pacemaker cell, B: Atrial myocardium, C: Ventricular action potential, 0-4 represent phases of the ventricular action potential mediated by the SCN5A (sodium voltage-gated channel alpha subunit 5, phase 0), ITO (transient outward potassium current, phase 1), ICA (L-type calcium channel, phase 2), IKr (rapid delayed rectifier, KCNH2, phase 2,3) and Iks (slow delayed rectifier, KCNH1, phase 3) cellular ion-channels. action potential

Stroke and atrial fibrillation.

AF is a known risk factor for ischemic stroke with a high prevalence noted in these patients (14). Furthermore, the impact of ischemic stroke on the risk of subsequent development of AF is only beginning to become clear (15,16) with up to 90% of patients with ischemic strokes demonstrating ECG diagnosis of atrial fibrillation at a median follow-up of 35 days after diagnosis of stroke (3). However, given increased risk of repeat stroke and importance of decision to start preventative anticoagulation, ability to predict atrial fibrillation and thus start earlier treatment is of utmost importance.

12-lead ECG and atrial fibrillation

Atrial substrate leading to atrial fibrillation which can involve enlarged atrial, scarred atria or an atrium capable of multiple or one ectopic focus, can lead to changes which might be reflective on the 12-lead electrocardiogram. Most of the focus has been on identifying changes which can lead to atrial fibrillation with assessment at the P-wave regarding its duration, morphology, and irregularity in particular ECG leads (17-19).

P-wave duration has been assessed in a large population of patients 60 years and older, as a sub-study of the Framingham Heart Study (17). This unfortunately, was not a significant predictor of atrial fibrillation nor mortality outcomes, except when very extreme (top 5%) prolonged P-wave durations were assessed (17). One recent association found, was that of stroke and advanced intra-atrial block (18). Intra-atrial block is defined as a delay of conduction which occurs over the Bachmann bundle and the left atrium which is depolarized by retrograde activation via muscle connections near the coronary sinus (18). This is seen as P-wave duration of at least 120ms with biphasic (positive-negative) morphology in leads II, III and aVF or biphasic (positive negative) morphology in leads III and aVF and with a notched P-wave in lead II, and which was recently associated with incident stroke risk as an independent risk factor and independent of atrial fibrillation burden (18). Please see Figure 7 for example of normal and inter-atrial block depolarization schematic, vectorcardiogram and lead aVF P-wave example, respectively from top to bottom.

Another marker of stroke risk is the P-wave terminal force in V1, defined as downward deflection duration (ms) of the P-wave in lead V1 multiplied by the downward deflection amplitude (absolute value) as seen in Figure 8 (19).

The P-wave terminal force, P-wave duration (mean and maximum), along with P-wave total area (calculated by the sum of the upward and downward deflection areas in each of the 12-lead ECG) have both been prospectively assessed for risk of ischemic stroke in 6741 patients in the multi-ethnic study of atherosclerosis (19). Otherwise, when tested prospectively, the P-wave duration measures (mean and maximum) and the P-wave area did not demonstrate significance for prediction of stroke, however the P-wave terminal force did identify a significant hazard ratio per 1 standard deviation increase of 1.21 (95% CI 1.03 to 1.21).

Thus, although there have been models to assess incident stroke, there have not been good models for the prediction of atrial fibrillation or risk of repeat stroke in patients with prior cryptogenic stroke. Furthermore, vectorcardiography, derived from the 12-lead ECG has yet to be used for atrial fibrillation or stroke prediction. And given the P-wave change in vector in advanced inter-atrial block and other such conditions leading to increased atrial fibrillation, it would make sense that these changes could be quantified and may have subtle differences earlier on when measured by vectorcardiography.

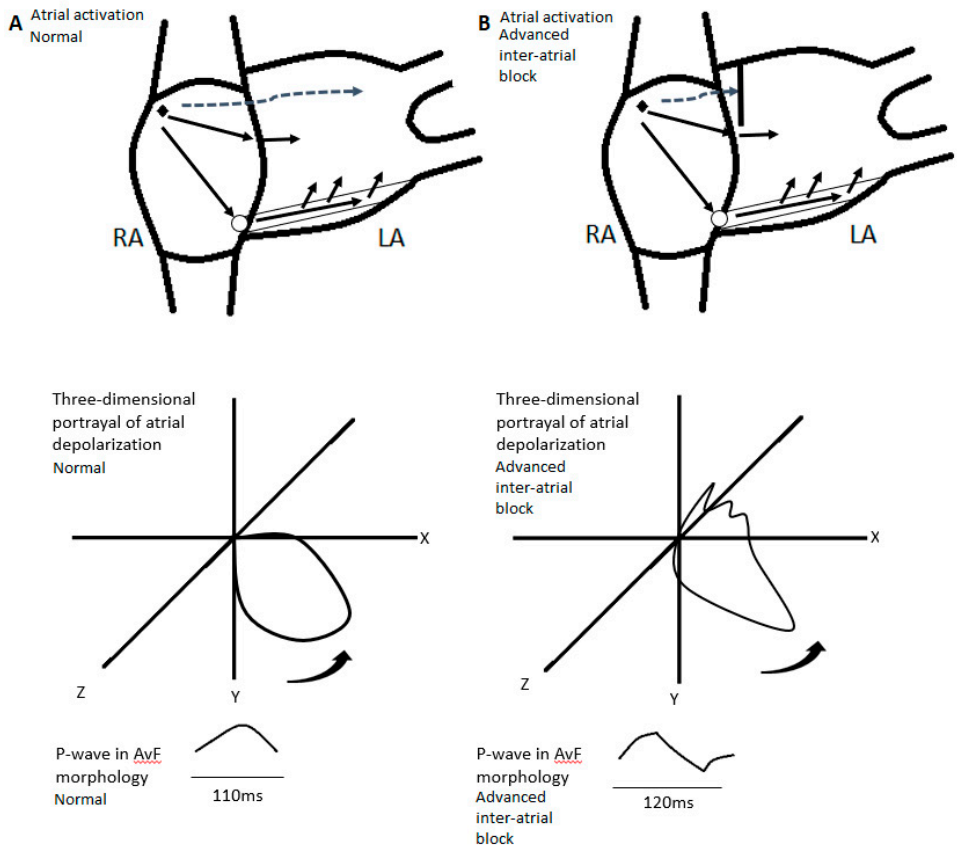

Figure 7: Example of normal (A, left) and inter-atrial block (B) in regard to inter-atrial conduction (top), vectorcardiogaphic depiction of atrial depolarization (middle) and P-wave morphology/duration (bottom).

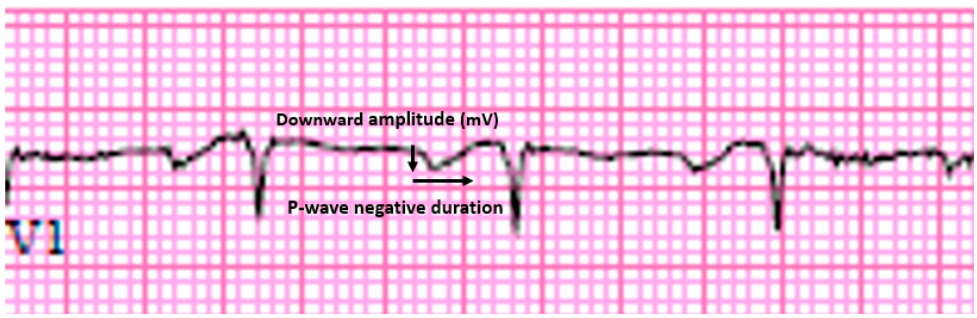

Figure 8: P-wave terminal force measurement (downward amplitude multiplied by P-wave negative duration (mVms).

Vectorcardiography and Atrial depolarization

The only previous studies to assess atrial arrhythmia burden based on the Pvm were conducted in patients with congenital heart disease including those with tetralogy of Fallot, and those patients with single ventricle physiologies (from hypoplastic left heart syndrome, tricuspid atresia, unbalanced atrioventricular canal or other single ventricle physiology) who underwent Fontan palliation (20, 21). The Pvm, however, did identify flutter and intra-atrial re-entrant tachycardia in those patients with right-sided congenital heart disease, tetralogy of Fallot, based on lower Pvm cut-off values (20). As a univariate predictor, the QRSVM outperformed the Pvm for identification of atrial flutter and intra-atrial re-entrant tachycardia in patients with single ventricle physiology (21). And although a low P-wave amplitude in lead I is associated with displaced conduction and clinical recurrence of paroxysmal AF post-radiofrequency ablation, the Pvm had not been assessed as a predictor of atrial fibrillation at the time we performed our first study, Paper I (22). Some importance from the studies with congenital heart disease patients was that the Pvm significantly correlated inversely with right atrial pressure, inversely with left ventricular volume and inversely with the QRS duration (QRSd) (20).

Ventricular arrhythmogenesis

Ventricular arrhythmias (VA) may occur for various reasons and can typically be considered as abnormal automaticity (warm and up and cool down from focal area), re-entry or triggered activity due to early after depolarizations (R on T phenomenon causes Torsades Des Pointes, premature ventricular beat on phase 3 of the action potential) or by late after depolarizations (premature beat which occurs in phase 4 of the action potential), as exemplified in Figures 6 and 9. VA's may be non-re-entrant (triggered or abnormal impulse initiation) or re-entrant (abnormal impulse propagation), with the latter typically due to acquired anatomic injury or structural heart disease (23). Although myocardial infarction and subsequent ischemic cardiomyopathy makes up a vast number of ventricular tachycardia cases in older individuals (23). In in young adults, however, who may otherwise appear healthy, there are other non-ischemic cardiomyopathies and ion-channelopathies which may cause VA and sudden death, including hypertrophic cardiomyopathy, arrhythmogenic right ventricular cardiomyopathy/dysplasia, and long QT syndrome.

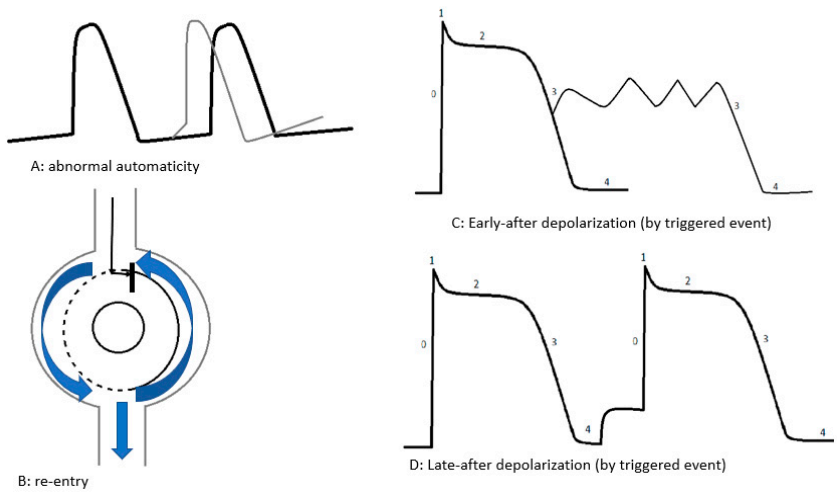

Figure 9: Mechanisms of ventricular tachycardia: A-abnormal automaticity, B-re-entry, C and D: triggered activity during early (C) and late (D) after depolarizations. 0-4 represent phases of the ventricular action potential mediated by the SCN5A (0), ITO (1), ICA (2), IKr (2,3) and IKs (3) cellular ion-channels.

Left ventricular abnormality: Hypertrophic cardiomyopathy

One example of left ventricular hypertrophy is hypertrophic cardiomyopathy (HCM), which has an estimated prevalence of up to 1 in 500 people, and it is the most common cause of cardiac death in those patients under 35 years of age in most countries (24). The phenotype of HCM can include thickened ventricular walls (at least 13-15mm absolute thickness) with or without obstruction to blood flow and diastolic dysfunction with asymmetric (85%), concentric (10%) and apical (5%) phenotypes (25-26). Patients with HCM can develop sudden death or progression towards New York Heart Association (NYHA) class III or IV functional class heart failure symptoms (24-26). One study demonstrated up to a 5% sudden death risk within a 5-year median follow-up (26). Increased sudden death/VA risk has been demonstrated to be associated with increased maximum left ventricular thickness, family history of sudden death, unexplained syncope and increased left atrial dimension (24-26). Abnormal markers of depolarization, such as QRS fragmentation and electrical left ventricular hypertrophy criteria have typically been used to identify HCM (27,28).

12-lead electrocardiogram and hypertrophic cardiomyopathy

Previous traditional 12-lead ECG markers demonstrating sudden death risk include prolongation of the corrected QT interval (QTc) as well as notching in 2-consecutive QRS lead complexes, called QRS-fragmentation (27).

The QRS fragmentation, which, if present in 3 of the following territories on the ECG, including inferior, lateral, septal and/or anterior regions, was associated with a hazard ratio of 3.4 (95% CI 1.54 to 14.9) for VA/sudden death (27). Although thought of as a way to identify small changes in QRS vector due to myocardial disorganization and scarring, the QRS fragmentation is still a qualitative parameter, which makes reproducibility difficult (27).

Additionally, other authors have assessed T-wave inversions in the lateral and inferior leads as well as sums of the R and S-wave voltages (or Q if larger) in the precordial leads, the bipolar leads, or all leads, as well as a dot product between those voltages and the QRS duration in patients with HCM (28). Out of 114 total patients with hypertrophic cardiomyopathy, age, limb-lead QRS voltage sum, precordial lead QRS voltage sum, 12-lead QRS voltage sum (all of them added together), the voltage sums multiplied by QRS duration as well as Sokolow-Lyon index all identified HCM patients with VA's (28). Regarding the QTc, if it was 440ms or longer, the hazard ratio for VA development was 2.4 (95% confidence interval (CI), 1.07 to 5.58), but this cut-off is limited as unfortunately in the general

population, 5% of normal males will have a QTc of 440ms or greater with a much larger number of females also having a QTc of 440ms or longer as normal (27).

A fairly complex risk score was made based on the study on QRS voltage sum, which took into account other risk factors as well, which at a cut-off of 6-points or more gave a sensitivity of 84%, specificity of 85%, positive predictive value of 67% and negative predictive value of 93% with odds ratio of 28.4 for a patient with HCM having VA/arrest (28). The score includes 1 point for QRS axis deviation, pathological T-wave inversions in limb leads, for limb-lead QRS amplitude sum of 7.7mV or more, for QTc of 440ms or more, and for 12-lead amplitude/duration product of 2.2mVms or more, whereas 2 points are given for pathological T-waves in precordial leads, ST-segment depression of 2 millimeters (mm) or more, dominant S in V4, limb-lead QRS sum of 10mV or greater, 12-lead amplitude/duration product of 3mVms or more, and 3 points for limb-lead QRS amplitude of 12mV or more or 12-lead amplitude/duration product of 3mVms or more (28).

Vectorcardiography and hypertrophic cardiomyopathy

In adults, since the inception of the vectorcardiogram, a large spatial QRS-T angle was identified as a parameter associated with left ventricular hypertrophy (typically larger than 100 degrees, Figure 3) (4). In paediatric and adult populations, the spatial peaks QRS-T angle has demonstrated ability to differentiate patients with HCM from controls with higher depolarization vector shifted towards the septum in those with asymmetric or severe HCM (5, 29, 30). In HCM patients, a higher spatial QRS-T angle identifies patients with higher absolute maximum left ventricular thickness and higher maximum left ventricular thickness Z-score in adult and paediatric patients, respectively (29,30). Thus, one might think that an increased spatial peaks QRS-T angle might also be associated with increased VA risk.

Right ventricular abnormality – Arrhythmogenic Right Ventricular Dysplasia/Cardiomyopathy

Another non-ischemic cardiomyopathy, which also causes cardiac death and which is the most common cause of cardiac death in young persons in Italy, is arrhythmogenic right ventricular dysplasia/cardiomyopathy (ARVD/C), which occurs in 1 in 5000 people (31). ARVD/C is characterized by fibro-fatty replacement of predominately the right ventricle, which predisposes patients to life-threatening ventricular arrhythmias and usually slowly progressive ventricular dysfunction (31). This disease is caused by many different mutations of either plakoglobin, plakophilin, Lamin A/C or others but typically follows an autosomal

dominant pattern with incomplete penetrance and higher variable expressivity (32). The diagnosis is made by combining multiple sources of diagnostic information as prescribed by the 2010 Taskforce criteria update (32). Although arrhythmogenicity of the disease is important, even diagnosis of the disease can be difficult and require multiple modalities of testing, and first-degree relatives may only have incomplete expression of the disease thus not meet the same criteria as their probands (33). Thus, clinical cascade screening of family members in genotype-negative ARVD/S can be complex and changes on the 2010 Taskforce criteria-ECG-changes, in particular may only be present in half of family members who would otherwise meet 2010 Taskforce criteria (34,35). However, the taskforce criteria does not include VCG, and although typically electrocardiographic changes may develop prior to histologic evidence of myocyte changes, this does not appear to be identifiable by the current 12-lead ECG changes prescribed by the 2010 Taskforce criteria (34,35).

12-lead ECG (2010 Taskforce criteria) and ARVD/C

Although the aim of the Taskforce criteria is meant to be broad enough to not miss cases, it was also revised in 2010 from its original 1994 version as specificity was also a concern, thus the ECG criteria by design have an error in sensitivity (32). Similar to the rest of the criteria, the 12-lead ECG criteria are composed of major and minor criteria. Signal-averaged ECG (SAECG) is a part of the diagnostic algorithm for ARVD/C, however, given the lack of signal-averaged ECG availability, it can be difficult clinically to obtain these measures, however, they are part of the minor depolarization criteria (below) and the concepts can likely be applied to a routine 12-lead ECG, but have thus far not yet been applied.

Table 2: Arrhythmogenic right ventricular dysplasia/cardiomyopathy Taskforce ECG criteria.

ARVD/C 2010 Taskforce ECG criteria
Repolarization criteria – major
• **T-wave inversions in V_1-V_3 or beyond in those over 14 years of age (no RBBB)**
Repolarization criteria – minor
• **T-wave inversions in V_1 and V_2 in those over 14 years old (no RBBB) or in V_4, V_5 or V_6**
• **T-wave inversions in V_1-V_4 (with RBBB)**
Depolarization criteria – major
• **Epsilon wave (reproducible low-amplitude signal between QRS and T-wave in V_1,V_2 or V_3**
Depolarization criteria – minor
• **Terminal activation delay (TAD) of QRS at least 55ms in duration from S-wave nadir to end of QRS (V_1,V_2 or V_3 no RBBB)**
• **Signal-averaged ECG (SAECG):** **Late potentials present if ⩾1 of the following with QRS⩽110 ms:**
1. Filtered QRS duration ⩾114ms
2. Duration of terminal QRS (<40 μV) ⩾38ms
3. Root mean square voltage of terminal 40 ms of QRS ⩽20 μV

Two vectorcardiographic parameters which had not been evaluated in ARVD/C patients were the spatial peaks QRS-T angle and the QRSVM. Given the QRSVM represents voltage magnitude, which is derived by the root mean square of the X, Y and Z voltage magnitudes, it seems very similar to the latter of the SAECG parameters. Furthermore, given ARVD/C is typically a right-ventricular disease, possibly assessing a right-precordial-directed angle and vector magnitude as a way to try to assess right-sided forces only, may be of benefit for detection of disease with only an ECG (derived-VCG) needed.

Vectorcardiography and prediction in right-sided heart disease and in the general population

How the structural heart disease effects the QRSVM has been demonstrated in congenital heart, including diseases of the right ventricle (tetralogy of Fallot) including arrhythmia prediction in cases with lower QRSVM predicting higher burden of VA's (36). The spatial QRS-T angle did not identify those with VA's in this same cohort of tetralogy of Fallot patients tested (36).

This spatial QRS-T angle, however, has demonstrated significant value for identification of cardiac death in the general population (37,38,39). Thus, its ability to identify VA's in patients with right-sided heart disease may be limited, but perhaps directing it towards right-sided forces only may be helpful in ARVD/C.

Ventricular repolarization abnormality: Long QT Syndrome

One classic example of a syndrome associated with repolarization abnormality is Long QT syndrome (LQTS), which is another cause of sudden cardiac death in children and young adults. LQTS in an inheritable arrhythmia syndrome which affects 1 in 2000 people (40). There are three main subtypes of LQTS including down regulations in KCNQ1 (Long QT1-LQT1, present in phase 3 of the ventricular action potential), down regulation of KCNH2 (Long QT 2-LQT2, phase 2 and 3 of the ventricular action potential), and upregulation of SCN5A (Long QT-3, LQT3, phase 0 of the ventricular action potential). Please see Figure 6C for diagram of the ventricular action potential.

12-lead ECG and LQTS

Each type of LQTS is associated with a particular arrhythmic trigger and T-wave morphology. LQT1 is associated with broad-based T-waves and sudden death

during exercise or swimming (during mammalian vagal reflex as one dives into the water) (41). LQT2 is associated with biphasic or flat T-waves and associated with sudden death due to being startled, for instance by an alarm clock (41). LQT3 is associated with delayed peak T-waves (prolonged ST segment) and sudden death while asleep (37).

Twenty to fifty percent of genotype positive LQTS patients have a normal QTc and may still be at sudden death risk (42,43). Given the qualitative changes identifiable in patients with LQTS and in particular with LQT2 (biphasic/flat T-waves), one can conclude that likely a global marker of T-wave maximum deviation from the origin (TwVM) may provide insight into cardiac event-risk in patients with LQT2 without corrected QT prolongation in lead II and V5. Thus far only prolongation of the QTc has been shown to demonstrate some predictive value for arrhythmic events with a QTc of 500ms demonstrating an absolute risk of VA of 40% (44). However, the 12-lead ECG quantitative parameters have not been able to identify those patients with normal QTc intervals at risk for sudden death (44). Recently, however, in Long QT 2 patients (LQT2), the morphology of the T-wave, qualitatively assessed by electrophysiologists, to risk stratify patients with LQT2 with normal QTc intervals was assessed (45). This study demonstrated for the first time that the 12-lead ECG may be able to help risk stratify LQTS patients with normal QTc intervals, but the qualitative methods, based on flattening and biphasic nature of the T-wave, have yet to be quantified, and thus may lack reproducibility for those not as comfortable with 12-lead analysis as the authors (45).

Vectorcardiography and Long QT syndrome

The only previous study to assess vectorcardiography and LQTS is a study assessing 610 patients with LQTS (46). In this study, T-wave eigenvector (vector associated with linear equation) values differentiated LQT1 from LQT2 and LQT3 with LQT2 patients having lower T-wave eigenvector values in the first 4 eigenvector values. In those with normal QTc intervals, the fourth T-wave eigenvector value (4^{th} largest if all maximum vector values lined up maximum to minimum) differentiated LQTS patients with cardiac events (symptomatic), from those without cardiac events (asymptomatic) (46). However, a special additional program is needed with complex calculations to derive the eigenvector values, thus this method is not very practical. Otherwise, one helpful aspect of the above-mentioned study was there was also assessment of a spatial QT peak, which did differentiate normal QTc interval LQTS patients from controls. The Spatial peaks QRS-T angle nor ventricular gradient aided in identification of LQTS from controls nor did those measures risk stratify LQTS patients with normal QTc intervals regarding cardiac event status (46).

Motives for studies

Overall, the above diseases lack reproducible quantitative parameters that may aid in the identification of those at risk for repeat cryptogenic stroke or for sudden death by ventricular arrhythmia. Thus, earlier identification of these higher risk patients may help prevent further stroke or sudden death by identifying those who should have early anticoagulation and those who may need implantable cardioverter defibrillators, respectively.

Only lead-specific ECG criteria have been assessed regarding voltage changes and duration of the P-wave seems to be inconsistent regarding prediction of atrial fibrillation or stroke (17-19). Thus, vectorcardiography may be able to help by assessing absolute voltage magnitude in the atrium as a measure of maximum deviation from the sinus node. Similar to findings in congenital heart disease and atrial flutter, the P-wave vector magnitude will likely still provide a basis for altered structure/atrial pressure/scar formation that would lend to development of atrial fibrillation.

Thus far, very lengthy and time-consuming calculations of all leads and multiple parameters (T-wave inversions, voltage dot products, voltage sums in all leads, etc) are all aiming at attempting to assess risk for VA's in patients with HCM (28). Given, the ability of the spatial QRS-T angle to identify HCM and even identify the degree of maximum left ventricular wall thickness, along with its ability to identify VA risk in other subpopulations, it would be reasonable the spatial peaks QRS-T angle may have prognostic use in the assessment of VA risk in patients with HCM.

Although, the 2010 Taskforce criteria has an 12-lead ECG sub-criteria, given the ability to only identify half of those with definite diagnosis of ARVD/C, clearly further criteria are needed for screening identification of possible ARVD/C patients, and thus VCG may be of help (32). Given the predominance of mostly right-sided disease in patients with ARVD/C, VCG with direction towards the right-precordium may add diagnostic or prognostic aid.

Risk assessment for LQTS patients with prolonged QTc intervals is important, however, thus far, ability to identify those at high risk for cardiac events in those with normal QTc intervals (family members identified by cascade screening, etc) has not been successful, aside from utilizing very complex derivation of eigenvector values or based on qualitative methods (45,46). Thus, there is room for identification of more easily calculated parameters for quantitative identification of LQTS patients, with normal QTc values, who are at risk for cardiac events. Given the morphology of the ECG of LQT2 patients (flat/biphasic T-waves), it would be prudent to assess this sub-population of patients with the T-wave vector magnitude first to determine prognostic value of the T-wave vector magnitude for cardiac event risk.

Aims:

Paper I: To assess the value of the three-dimensional P-wave vector magnitude (Pvm) and its relationship to P-wave duration for prediction of new-onset AF after ischemic stroke.

Paper II: To assess whether the SPQRS-T angle would differentiate HCM patients with sustained VAs (≥30seconds) from those without VAs with increased predictive values compared with the QTc interval. A secondary aim was to assess if those with HF (NYHA class III/IV) would also have higher SPQRS-Tangles.

Paper III: To assess whether right-precordial-directed vectorcardiographic parameters, particularly a right precordial-directed-orthogonal QRS-T angle (RPD angle) and right-sided depolarization magnitude (right root mean square of the QRS, RtRMS-QRS) improve detection of ARVD/C patients who have no depolarization or repolarization criteria by 2010 taskforce criteria.

Paper IV: To assess whether T-wave vector magnitude (TwVM), a quantifiable measure of T-wave flattening, is associated with risk for cardiac events in LQT2 patients without QTc prolongation.

Methods:

Study cohorts:

Ischemic stroke survivors (Lund Stroke Registry, Paper I):

The study population originated from the Lund Stroke Register (LSR) and comprised 336 consecutive first-ever ischemic stroke patients included in LSR between March 1, 2001 and February 28, 2002 as it had been described previously (47). At enrolment in the LSR, 109 ischemic stroke patients had AF detected by ECG screening, medical records review or record linkage with the Swedish National Patient Register as described previously and were excluded from this analysis (47). All patients enrolled signed written consents. The present study sample therefore comprised of 227 first-ever ischemic stroke patients (median age 73 years at stroke onset (interquartile range 25–75% (IQR 63–80), 92 females) without known AF at inclusion in the LSR. We followed up all study subjects until October 17, 2011, the date when the information from the Swedish National Patient Register was obtained. Informed consent was obtained from all participants included in the LSR. The study was approved by the Lund University Ethics Committee. Medical records of all study subjects were analysed for history of cardiac failure, hypertension, diabetes mellitus, transient ischemic attack (TIA) and ischemic heart disease at baseline. Cardiovascular risk profiles measured by $CHADS_2$ and CHA_2DS_2-VASc scales were evaluated for the time of inclusion in the LSR in the acute phase when the index ischemic stroke had just occurred (47).

Hypertrophic cardiomyopathy (Paper II):

A retrospective study of HCM patients from 2000 to 2013 at the University of Colorado Hospital and Children's Hospital of Colorado was performed. Internal review board permission was obtained, and written permission was waived. Patients with the diagnosis of HCM by evidence of diastolic dysfunction and 15mm absolute septal thickness by echocardiogram were identified by first author chart review without knowledge of VA or congestive HF history. The diagnosis of HCM was based on echocardiographic evidence of diastolic dysfunction and those with an absolute septal or posterior wall thickness of ≥15mm by echocardiographic M-mode

measurement during diastole from a parasternal short-axis view by the cardiologist seeing the particular patient. Conduction abnormalities did not preclude patient participation in this retrospective study. Congestive HF is defined as those HCM patients who meet criteria as governed by the NYHA for functional classifications for objective or subjective measures (class I–IV).

Arrhythmogenic right ventricular dysplasia/cardiomyopathy (Paper III):

A cross-sectional study of patients with ARVC/D from an international cohort from the University of Colorado (Denver, CO, USA), Skåne University Hospital (Lund, Sweden), Linköping University Hospital (Sweden) and the University of Trieste (Italy) undergoing routine follow-up, classified as definite ARVD/C by the 2010 Task Force criteria was performed. Normal variant ECGs from patients, who did not have signs of bundle branch block and not fitting 12-lead ECG major or minor depolarization or repolarization criteria by 2010 Task Force guidelines (electrocardiographically concealed were compared with ECGs recorded from 1:1 age- and gender-matched control subjects who were screened in cardiology clinic at the University of Colorado (Denver, CO) or at Skåne University Hospital (Lund, Sweden) for murmurs or chest pain without family history of ARVD/C and through ultrasound and clinical observations were deemed normal. None of the control subjects had other underlying cardiac disease (no cardiomyopathy or other notable cardiac disease) nor did they have obvious obstructive or restrictive lung disease or thromboembolisms. All ECG's were taken from the first time the patient had presented to the particular institution and no patients were on antiarrhythmic treatment at the time of their ECG. The study was approved by the Institutional Review Boards at each of the institutions noted above.

Patients with long QT syndrome (Rochester LQTS Registry, Paper IV):

Patients in this study were from the Rochester-based LQTS Registry; enrolment into the registry has been previously described (48,49). Patients were selected to the current analysis if they were shown to be carriers of the disease-causing mutation in KCNH2 (LQT2), had Bazette-corrected QT interval (QTc) of less than 470ms for female and less than 460 ms for male, and were 18 years or older to exclude variation of the T-wave morphology that may be observed in children and adolescents. The first recorded ECG at age 18 or older was used and the Bazette-corrected QTc was calculated based on digital calliper QT measurement by an electrophysiologist. Ten-second recordings were used. Patients were excluded from the study if they had more than one LQTS-associated mutation. The presence of LQTS-causing KCNH2 mutations was verified with the use of standard genetic tests performed in the academic molecular genetic laboratories reported previously (48). The study population also required the patients who met the above criteria to have ECGs (at

time of enrolment in the prospective registry) with flat baselines in leads I, II, and V1-V6 (<0.1mV movement), adequate for assessment of voltage parameters. Poor quality ECGs, with movement artifact, were excluded. Patients with LQT2 without QTc prolongation were compared with a control population of 1007 individuals who belonged to families with genotype-positive probands, but who were genetically tested and found to be negative for LQT-associated mutations and who also had normal QTc intervals (per above).

Electrocardiogram:

P-wave analysis (Paper I):

Sinus rhythm ECG recordings obtained at stroke admission with median time from stroke event to ECG registration 0 day (IQR 0–2 days) were extracted from the regional electronic database (GE MUSE, GE Healthcare, MegaCare) and processed offline. The measurements of Pd, QRSd, PQ interval were performed automatically using the University of Glasgow 12-lead ECG analysis algorithm (50). The Pvm was calculated automatically as the square root of the sum of the squared P-wave magnitudes in leads V6, II and one half of the P-wave amplitude in V2 ($\sqrt{PV6^2 + PII^2 + (0.5 * PV2)^2}$,) based on the P-wave magnitude as defined by the visually transformed Kors' Quasi-orthogonal method (51,52). The Pd/Pvm was defined as the Pduration/Pvm and was calculated from the data above automatically utilizing MATLAB R2013b (The MathWorks, Inc., Natick, MA, USA) for Linux.

P wave duration, QRS duration, corrected QT interval and PQ interval were measured in ms. Corrected QT was calculated using Bazett's formula: QTc = QT/√R-R interval. Pvm was calculated in microvolts. Negative P-wave terminal force in lead V_1 was also calculated as described previously (47).

QRST analysis (Paper II):

Electrocardiograms were taken at a 25-mm/s speed with 10mm/mV for the limb and precordial leads (Phillips, Best, Netherlands) and ECG recordings (General Electric, Menominee Falls, WI) in sinus rhythm. The spatial peaks QRS-T angle was calculated by the Kors' regression-related method as shown in Figure 2 and Table 1 (51). QRST analysis (Paper III):
The resting ECG closest to time of diagnostic echocardiogram or magnetic resonance imaging studies from ARVD/C patients at a speed of 25 mm/s and with voltages of 10 mm/mV were assessed (GE, WI, USA or Phillips Healthcare, MA, USA).

Digital recordings were changed to PDF files and assessed at up to 150% magnification and used for vectorcardiographic derivations. Approximations of the Kors' quasi-orthogonal spatial peaks QRS-T angle (normally based on V6 defined as the X-axis, lead II as the Y-axis and −0.5*V2 as the Z-axis) were used with direction particularly toward the R-wave in V1 (as the Z-axis QRS vector magnitude) and S-wave in V5 (as the X-axis QRS vector magnitude) while ignoring magnitudes of the S-wave in V1 and the R-wave in V5 (as an attempt to have right-precordial-directed vector magnitude and angle). Lead II measures maximum deviation from baseline (whether R or S) was used as the Y-axis QRS vector magnitude, similar to Kors' quasi-orthogonal method (51). Right-precordial-directed orthogonal QRS-T angles (RPD angle, degrees, Fig. 7), right-precordial-directed vector magnitudes (RtRMS-QRS, mV, Fig. 7), and spatial peaks QRS-Tangles (SPQRS-Tangle, degrees) were measured in ARVD/C and compared to the same parameters from control patients.

The Bazett corrected QT interval (QTc) and the QRS duration (QRSd) were measured in milliseconds (ms).

The spatial QRS-T angle was calculated based on the visual transform estimation based on using selected leads and multipliers of those leads to approximate an orthogonal system. This is based on the Kors' visual estimations regression-related method, which has been described previously (51,52).

The RPD angle is similar in calculation to the Kors' quasi-orthogonal angle, but is a right-side restrictive measure meaning only the QRS maximum deviation in the orthogonal planes according to the following principles:

- X-axis: the S-wave deviation only in V5 (ignoring the R-wave in V5, even if it has a greater deviation from baseline than the S-wave);

- Y-axis: the R or S maximum deviation from lead II;

- Z-axis: the negative one half of the deviation of the R in lead V1.

These measures are then applied in the equation (Figure 2 legend) and inverse cosine is taken between the QRS deviations and the T-wave deviations (positive or negative in leads V6 (X-axis), II (Y-axis) and negative one half of the deviation in V1 (Z-axis)). Please see Figure 10 for further detail. The RtRMS-QRS is the vector magnitude of the QRS complex based on right-precordial-directed measures (please see equation noted above and Figure 10). V5 also more consistently demonstrated an S-wave than V6, thus the S-wave in V5 was used. All parameters were assessed by the first author if not otherwise noted above, while 10% of the sample was assessed by the 5th author to calculate inter-observer variability (per below).

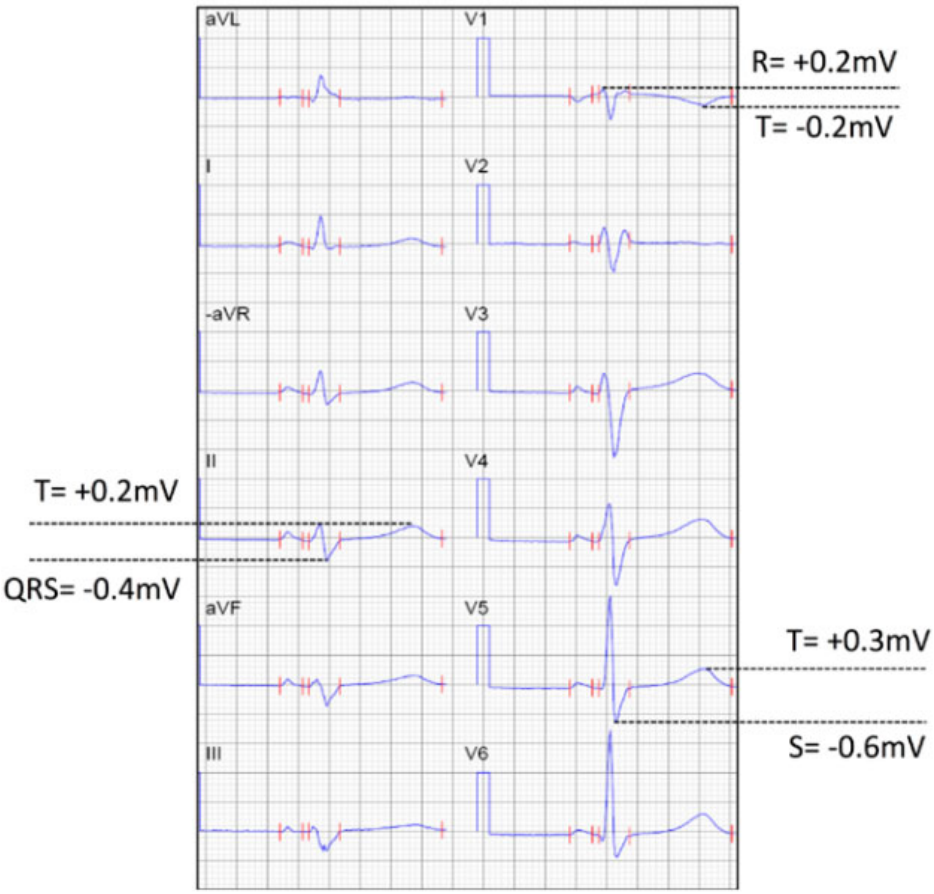

Figure 10: RtRMSQRS RPD angle calculations:
RtRMS-QRS=$\sqrt{(SV5^2+QRSmaxII^2+(-0.5*RV1)^2)}=\sqrt{((-0.6mV)^2+(-0.4mV)^2+(-0.5*0.2mV)^2)}$= **0.73mV**
RtRMST=$\sqrt{(TmaxV5^2+TmaxII^2+(-0.5*TmaxV1)^2)}=\sqrt{(0.3mV^2+0.2mV^2+(-0.5*-0.2mV)^2}$=**0.37mV**
RPD angle=$\cos^{-1}$([(SV5*TV5) + (QRSmaxII*TmaxII) + -0.5(RV1*TV1)]/(RtRMSQRS*RtRMST))=
$\cos^{-1}$([(-0.6mV*0.3mV)+(-0.4mV*0.2mV)-0.5(0.2mV*0.2mV)]/(0.73mV*0.37mV)=**172.4 degrees**

T-wave analysis (Paper IV):

ECG measurements were performed by the first author who was blinded to the clinical characteristics of the patients. ECG's were recorded at a speed of 25 mm/s with 10 mm/mV reference for limb and precordial leads. The corrected QT-intervals (QTc) from Bazette's formula, spatial QRS-T angles, and TwVM were assessed on all ECGs. The spatial QRS-T angle was calculated by the peaks method, utilizing the method of Kors' et al (51). TwVM was calculated as the square root of the sum of the squared T waves in leads V6, II and one half of the T wave amplitude in V2, given by the equation TwVM= $SQRT[(TwaveII)$^2 + (TwaveV6)^2 + (0.5*TwaveV2)^2], based on the T-wave magnitude as defined by the transformed Kors' Quasi-orthogonal method, utilizing the beat with a stable baseline (median when it met this standard) (51,52). Please see Figure 11 for example TwVM calculation.

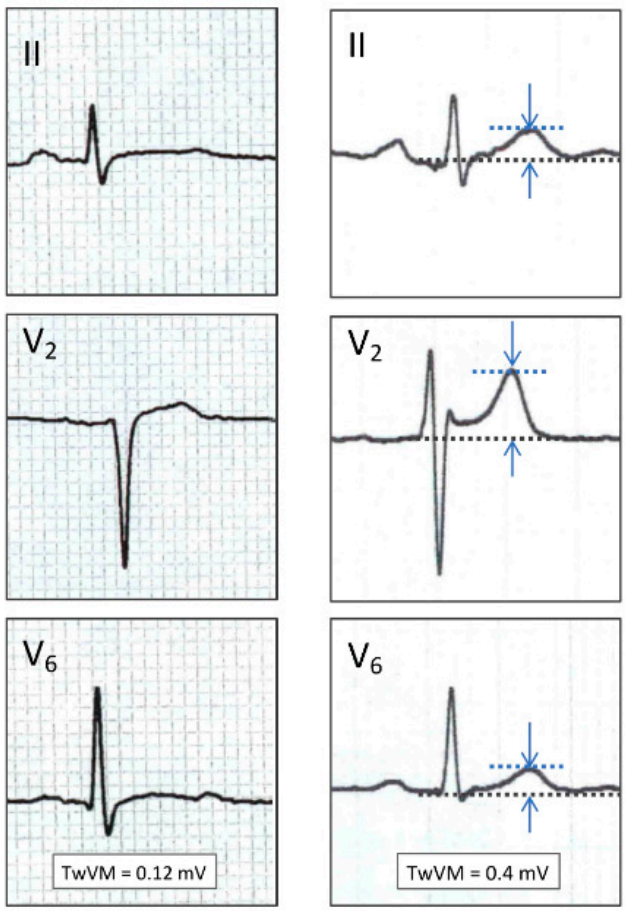

Figure 11: Example calculations for the T-wave vector magnitude (TwVM) including leads II, V2 and V6, which are used for the calculation. The example to the left is from a patient with low TwVM of 0.12mV and the example to the right is from an LQT2 mutation carrier with a higher TwVM of 0.40mV.

Endpoint definitions

Paper I:

New onset AF, study endpoint, was assessed during the follow-up period starting from the date of enrolment until the end of follow-up or date of death. AF documentation was based on information obtained from the regional electronic ECG archive which contains all ECG recordings taken in the hospital's local catchment area and also by linkage with national registers: the Swedish Patient Register and the Swedish Causes of Death Register. All available ECG recordings for all study subjects from the date of enrolment until the end of follow-up in 2011 were reviewed for the presen0ce of AF by a trained cardiologist (MB). On surface ECG, AF was defined as a rhythm disorder which lasted sufficiently long for a 12-lead ECG to be recorded, with irregular RR intervals, indistinct P waves and atrial cycle length of 200 milliseconds (ms) where distinct atrial activity was visible on surface ECG (47).

The Swedish Patient Register is administered by the Swedish National Board of Health and Welfare and includes data on main and secondary diagnoses at discharge from all public hospitals in Sweden starting in 1987. The register uses International Classification of Disease (ICD) codes with the 10th edition (ICD-10) used from 1997 and until today (15). The Cause of Death Register is also provided by the Swedish National Board of Health and Welfare and contains information (since 1961) from death records, including underlying causes of death and up to 20 contributory causes of death coded to the current edition (ICD-10). The presence of the ICD-10 code I48 in the Swedish national registers identified AF diagnosis with high specificity and modest sensitivity as we showed recently in a validation study on patients with ischemic stroke enrolled in the LSR (47).

Paper II:

The primary endpoint of this study was the diagnosis of sustained ventricular tachycardia of 30 seconds or of hemodynamic consequence as assessed by ECG, Holter or Event monitor, ICD or pacemaker identification of VA.

Paper III:

The primary endpoint of this study was diagnosis of arrhythmogenic right ventricular dysplasia/cardiomyopathy by the 2010 Taskforce criteria (32).

Paper IV:

The primary endpoint of the study was the occurrence of a first cardiac event that included syncope (transient loss of consciousness that was abrupt in onset/recovery), aborted cardiac arrest requiring defibrillation as part of resuscitation (ACA), LQTS-related sudden cardiac death (SCD, defined as abrupt in onset, if witnessed-not explained by other cause, if not witnessed-was not explained by any other cause) or implantable cardioverter-defibrillator (ICD) therapy including anti-tachycardia pacing (ATP) or shock therapy.

Statistics

Baseline clinical characteristics between compared groups using student T-testing versus

Data were assessed for normality using Shapiro–Wilk testing. Normally distributed continuous data are presented as mean and standard deviation. Student t-tests, χ^2, Fisher's exact testing and analysis of variance were used to identify significant differences between groups. Non-parametric data was presented as median with interquartile ranges. Sensitivity, specificity, positive and negative predictive values were performed. Receiver operating characteristic (ROC) curve analysis was performed to identify threshold values for VCG parameters associated with cardiac events. Logistic regression for univariate and multivariate odds rations was performed. The cumulative probability was assessed by the Kaplan–Meier method with significance testing by the log-rank statistic. The Cox proportional hazard model was used to evaluate the independent contribution of clinical and genetic factors to the first occurrence of time-dependent cardiac events for each study. For KCNH2 mutation patients, this was performed from the age of 18 years through the end of follow-up. In the same KCNH2 mutations cohort, the Cox regression model was adjusted for the time-dependent beta-blocker use (the age at which patients were on and off beta-blocker therapy) and stratified by sex. As preselected QTc inclusion overlapped with borderline QTc prolongation, the model was adjusted for QTc duration wit 440ms selected as a cut-off for normal vs borderline QTc values. The proportionality assumption was tested using time-dependent covariates created from interactions between survival time and various covariates.

Pearson and Spearman correlation coefficients were used as appropriate for parametric and non-parametric data. Intra-observer and interobserver variability were estimated by intraclass correlation coefficients based on a 10% sample of the population for each study when appropriate. All analyses were performed using SPSS Statistics 20 (SPSS Inc., Chicago, Illinois, USA) for most studies aside from study 2 (Left ventricular abnormality) for which GNUPSPP software was used (http://www.gnu.org/software/pspp/) .

Results:

Atrial depolarization indices of AF (Paper I):

Baseline characteristics of all study subjects at time of enrolment are presented in AF Table 3. At baseline 227 were fulfilled inclusion criteria and were included in the analysis**.** All patients had no evidence of AF in the immediate acute phase after stroke onset. Detection of new onset atrial fibrillation (10-year follow-up) The median time for follow-up was 9.4 years [IQR 6.1–9.9], 115 (51%) stroke patients died. Complete follow-up data were available for 112 (49%) of the stroke patients. In total, 2588 ECG's were reviewed with a median number of ECG recordings per person of four (IQR 1–9) (40). New onset atrial fibrillation was found in 39 (17%) of the stroke patients (Hazard ratio 1.49, 95% confidence interval 0.09– 2.35, p = 0.121). The median time to AF onset was 3.2 (IQR 1.3 to 5.9) years. ECG and clinical predictors of new onset atrial fibrillation after ischemic stroke On ECGs obtained in the acute phase after stroke onset, the median QRSd was 96 ms (IQR 88–108), the median duration of the P wave was 116 ms (IQR 106–124), and the median PQ interval was 169 ms (IQR 152–188). The median Pvm was 0.15 mV (IQR 0.13 to 0.20) and the median Pd/Pvm was 737 ms/mV (IQR 581 to 955).

Table 4 depicts univariate and multivariate predictors of new-onset atrial fibrillation in stroke patients. Significant univariate predictors of new-onset atrial fibrillation included age > 65 years, presence of hypertension, heart failure, QRSd, and Pd/Pvm (Table 4). No standard ECG characteristics including P-wave duration, QRS duration or negative P-wave terminal force in lead V1 or QRSd were significantly associated with new-onset AF during follow-up. Independent predictors of new-onset atrial fibrillation were Pvm/Pd and those parameters considered a moderator of Pvm/Pd including age > 65 years, hypertension, and heart failure (AF Table 4). The C-statistic for the model was 0.71 (95% CI 0.61 to 0.82).

The area under the ROC curve value for the Pd/Pvm was 0.63 (0.55 to 0.71, p = 0.013). At an optimal cut-off value of 870 ms/mV the sensitivity, specificity, positive and negative predictive values were 51, 79, 40 and 89%, respectively (optimized for highest negative predictive value given the ECG the screening value of the ECG). A Kaplan-Meier curve based on this cut-off value (Figure 12) provided a p-value of <0.001 for differentiation between survival curves for the risk of development AF during 10-year follow-up after first-ever ischemic stroke. Sub-

Table 3: Baseline clinical characteristics of stroke patients without or with subsequent development of atrial fibrillation (%).

Parameter	Stroke n=227	No AF n=188	AF n=39	P-value
Age, years	73 [63-80]	73 [61-80]	73 [69 to 80]	0.072
Male sex	135 (59%)	114 (61%)	21 (54%)	0.693
Heart Failure	7 (3%)	4 (2.1%)	3 (7.7%)	0.218
Hypertension	130 (57%)	101 (53.7%)	29 (74.4%)	0.012
Diabetes	35 (15%)	26 (13.8%)	9 (23.7%)	0.210
Vascular disease	95 (42%)	77 (41.0%)	18 (46.2%)	0.560
TIA	49 (22%)	45 (23.9%)	4 (10.3%)	<0.001
New-onset AF	39 (17%)	0 (0.0%)	39 (100.0%)	<0.001
Median time to AF/F/up (years)	3.2 [1.3-5.9])	9.7 [4.3-10.1]	2.9 [1.2-6.4]	<0.001
P duration	116 [106-126]	116 [106-122]	118 [111-131]	0.224
QRSd	78 [68-90]	86 [78-94]	88 [75-99]	0.880
Pvm	0.16 [0.13-0.20]	0.16[0.13-0.20]	0.13[0.11-0.19]	0.006
P duration/Pvm	711 [560-893]	694 [547-862]	801 [586-1046]	0.009

AF: atrial fibrillation, F/up: follow-up, Pvm: Pwave vector magnitude, QRSd:QRS duration, TIA: transient ischemic attack

Table 4: Clinical electrocardiographic predictors by Cox regression analyses of new-onset atrial fibrillation during 10-year follow-up of ischemic stroke patients without known atrial fibrillation at their index stroke.

	Univariate		Multivariate	
Parameter	HR (95% CI)	P-value	HR (95% CI)	P-value
Age>65 years	**2.88 (1.20-6.89)**	**0.018**	**1.04 (1.02-1.07)**	**0.001**
Hypertension	**3.45 (1.40-3.49)**	**0.007**	**3.21 (1.35-7.67)**	**0.008**
Heart failure	**4.04 (1.24-13.18)**	**0.020**	**2.72 (1.08-6.83)**	**0.033**
Diabetes	1.83 (0.87-3.87)	0.111		
Male gender	1.22 (0.50-1.59)	0.459		
Stroke group	1.391 (0.855-2.263)	0.184		
P duration	1.02 (0.96-1.05)	0.105		
QRS duration	1.02 (1.00-1.04)	0.025	1.01 (1.00-1.02)	0.354
PQ interval	1.00 (0.99-1.01)	0.966		
Pvm	1.001 (0.994-1.009)	0.751		
P duration/Pvm	**2.320 (1.367-3.938)**	**0.002**	**2.02 (1.18-3.46)**	**0.010**
P terminal force V1	1.00 (1.00-1.00)	0.142		

Pvm: p-wave vector magnitude, 95% CI: 95% confidence interval

analyses of patients who do not meet any of the independent predictors (ie. without hypertension, who were less than 65 years of age, did not have heart failure and had a Pd/Pvm of less than 870 ms/mV), did had a 93.2% chance of not developing atrial fibrillation. The positive predictive value for development of AF was 27.9% in a patient without hypertension, who were less than 65 years of age and did not have heart failure, but with a Pd/Pvm of less than 870 ms/mV.

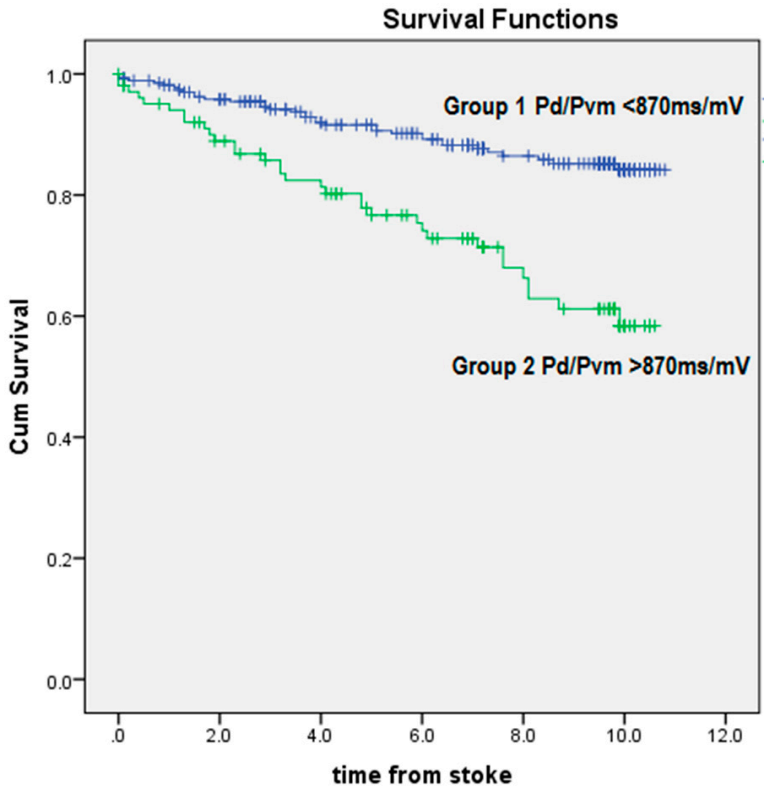

Figure 12: Kaplan-Meijer survival curve for p wave duration/ pwave vector magnitude (Pd/Pv) at a cut-off of 870 milliseconds/millivolt (ms/mV), p-value <0.001.

Left ventricular abnormality (Paper II)

Electrocardiographic results from 100 HCM patients (mean age, 32.7 ± 17.2 years) were assessed. Twenty patients with VAs were identified. Five patients with NYHA functional class III or IV HF were identified. Syncope differentiated those with vs those without VAs (Table 5). Four patients with VA had ICDs, and 1 patient without VA (but with atrial fibrillation) had an ICD. Holter monitoring identified 8 patients with VA; loop recording, exercise stress testing, and inpatient telemetry identified 3, 2, and 4 patients, respectively.

Corrected QT interval and QRS duration

The QTc interval differentiated those with VAs from those without VAs with values of 440.7 ± 48.1 ms and 472.0 ± 43.4 ms, respectively ($P = 0.013$; Table 3, Figure 12A). A QTc interval at a cutoff value of 460 ms gave PPV, NPV, and OR of 28.6%, 83.3%, and 2.0, respectively (95% confidence interval [CI]: 0.7-5.6). The QRSd did not differentiate HCM patients with VAs from those without VAs. Please see Figure 13A.

Spatial peaks QRS-T angle

The spatial peaks QRS-T angle differentiated those with sustained VAs from those without VAs (108.2 ± 45.9 degrees vs 144.0 ± 26.7 degrees; $P < 0.001$; HCM Table 5, Figure 12B). At an optimum cut-off value of 124.1 degrees, PPV and NPV were 36.7% and 96.1%, respectively, with an OR of 14.2 (95% CI: 3.1-65.6). Even in those without syncope, the SPQRS-T angle significantly differentiated those with vs those without VAs (109.3 ± 45.0 degrees vs 142.1 ± 28.6 degrees; $P < 0.001$). Please see Figure 13 B.

Heart failure

Only the SPQRS-T angle differentiated those with NYHA class III/IV HF from those without NYHA III/IV HF. There were 5 (5%) HCM patients with NYHA III/IV classification, all with systolic HF (1 with preserved ejection fraction), with a mean SPQRS-T angle of 150.3 ± 9.7 degrees vs 113.9 ± 45.3 degrees ($P < 0.001$). At an optimum cut-off value of 153.4 degrees, the PPV, NPV, and OR were 15.0%, 98.8%, and 13.9, respectively (95% CI: 1.4-142.3). When those with congestive HF or VAs were compared with HCM patients without congestive HF or VA, the PPV, NPV, and OR were 44.9%, 96.1%, and 20.0, respectively (95% CI: 4.4 to 91.5), at a cut-off value of 124.1 degrees.

Table 5: Patient demographics and results for hypertrophic cardiomyopathy patients with sustained ventricular arrhythmias (VA) and those without sustained ventricular arrhythmias (no VA). Parameters assessed include age, sex, history of syncope, atrial arrhythmias, New York Heart Association Heart Failure Class II or IV (NYHA class III/IV), maximum septal thickness, QRS duration (QRSd in milliseconds, ms), corrected QT interval (QTc in milliseconds, ms) and the spatial peaks QRS-T angle (SPQRS-T angle in degrees).

	VA (N=20)	No VA (N=80)	p-value
Age (years)	32.7±17.2	33.8±18.4	0.418
male (%)	13 (65%)	53 (66.3%)	0.833
Syncope (%)	7 (35%)	2 (2.50%)	**<0.001**
Atrial arrhythmias (%)	3 (15%)	8 (10%)	0.689
Nonsustained ventricular arrhythmias (%)	2 (10%)	3 (3.8%)	0.261
NYHA class III/IV	4 (5%)	4 (5%)	1.000
Maximum septal thickness (centimeter)	2.4±0.5	2.2±0.4	0.107
LVOT obstructions presence	2 (10%)	8 (10.0%)	1.000
Sokolow-Lion voltage criteria (%)	4 (20%)	27 (33.8%)	0.358
Cornell voltage criteria (%)	8 (40%)	18 (22.5%)	0.190
Inverted T-waves V4-V6 (%)	10 (50%)	33 (41.3%)	0.650
QRSd (ms)	116±36	99±22	0.137
QTc (ms)	472±43	440±48	**0.013**
SPQRS-T angle (degrees)	144±26	108±46	**<0.001**

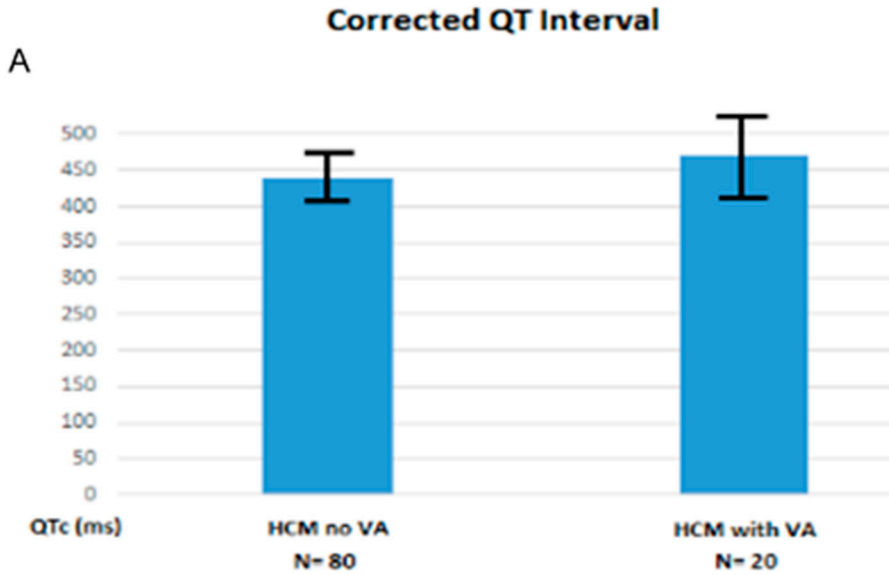

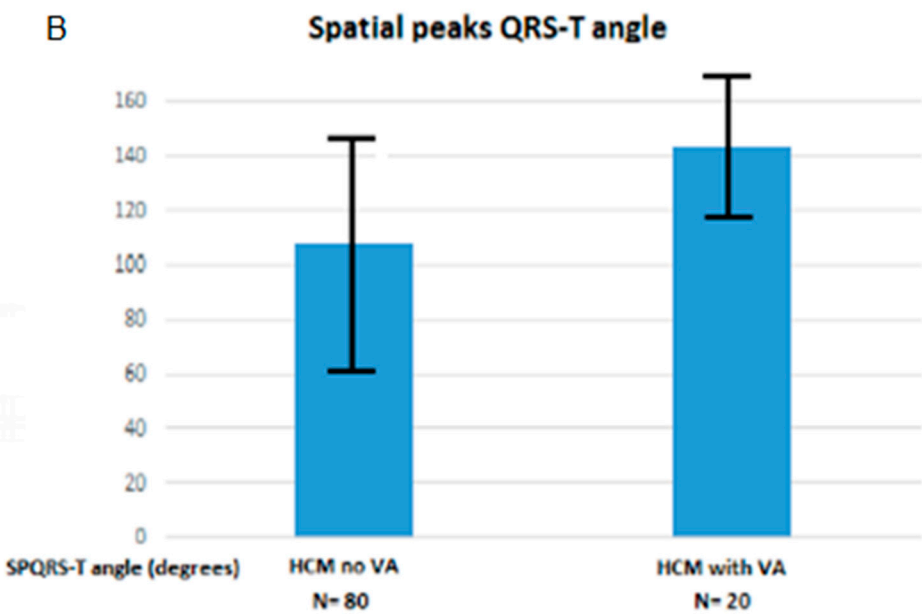

Figure 13 A-B:
A: Corrected QT interval (QTc) for HCM patients with versus without VA with bracket showing interquartile ranges (p=0.018).
B: Spatial peaks QRS-T angle for HCM patients with versus without VA with bracket showing interquartile ranges (p<0.001).

Multivariate Analysis

Logistic regression was used for multivariate analysis utilizing septal thickness, syncope, the QTc, and the SPQRST angle in the regression. Only syncope and the SPQRS-T angle both remained independent predictors of sustained

VAs (both $P < 0.001$). The OR for the SPQRS-T angle was

1.41 based on a cut-off of 121 degrees (95% CI: 1.20-1.65).

The R^2 value for spatial QRS-T angle vs septal thickness was 0.27. The R^2 for the QRSd and QTc compared with septal thickness were 0.63 and 0.26, respectively.

Right ventricular abnormality (Paper III):

Of a total of 155 patients with the diagnosis of definite ARVD/C by 2010 Task Force criteria, 66 patients did not have depolarization or repolarization changes consistent with either major or minor criteria (ECG-negative patients) who were compared with 1:1 age- and gender matched control patients. ARVD/C Tables 1 and 2 summarize patient demographic data. Apart from the ECG-related differences between ECG-positive and ECG-negative ARVD/C patients, on which group definitions were based, no other diagnostic criteria appeared to demonstrate significant difference between the groups (Table 6).

Borderline significant difference was observed in regard to the greater prevalence of patients fulfilling minor arrhythmia criterion in ECG-positive ARVD/C patients. However, we observed significant differences in regard to the major MRI volume criteria, which was twice as common in ARVD/C patients who met ECG criteria (ECG-positive ARVD/C) than in those who did not meet 12-lead ECG criteria (ECG-negative ARVD/C Figure 14a-d shows comparisons of various parameters for controls, ECG-negative and ECG-positive patients.

Five of our ECG-negative ARVD/C patients had right bundle branch blocks. While QRSd did not significantly differentiate ECG-negative ARVD/C patients from controls (ARVD/C Table 7), the QTc was significantly longer in ECG-negative ARVD/C than in control subjects (ARVD/C Table 8), with resultant optimum sensitivity, specificity, positive and negative predictive values shown in Table 9 with an odds ratio of 5.3 for QTc (95% confidence interval 0.6 to 46.6).

Table 6: All ARVD/C, ARVD/C with (+ECG) and without (-ECG) 2010 ECG taskforce criteria with major and minor criteria including arrhythmia (arrhyth).

	ARVC Total (N=155)	ECG-positive ARVC (N=89)	ECG-negative ARVC (N=66)	p-value
Age	42.1 ± 17.3	42.0 ± 17.4	41.7 ± 17.6	0.861
Sex (% male)	106 (68.4%)	63 (70.8%)	43 (65.2%)	0.488
Proband (%)	111 (71.6%)	71 (79.8%)	30 (45.5%)	0.012
Imaging, %	155 (100%)	89 (100%)	66 (100%)	1.000
major, %	111 (71.6%)	68 (76.4%)	43 (65.2%)	0.082
minor, %	89 (57.4%)	60 (67.4%)	29 (43.9%)	0.005
Tissue biopsies (%)	70 (45.2%)	39 (43.8%)	31 (47.0%)	0.745
major, %	53 (75.7%)	31 (79.1%)	22 (71.0%)	0.576
minor, %	63 (90.0%)	36 (92.3%)	27 (87.1%)	0.454
Repolarization abnl major	54 (34.8%)	54 (60.7%)	0 (0.0%)	<0.001
Repolarization abnl minor	20 (12.9%)	20 (22.5%)	0 (0.0%)	<0.001
Depolarization abnl major	13 (8.4%)	13 (14.6%)	0 (0.0%)	<0.001
Depolairzation abnl minor	17 (11.0%)	17 (19.1%)	0 (0.0%)	<0.001
Ventricular arrhyth major	44 (28.4%)	26 (29.2%)	18 (27.3%)	0.858
Ventricular arrhyth minor	64 (41.3%)	42 (47.2%)	22 (33.3%)	0.1000
Family History major	84 (54.2%)	48 (53.9%)	35 (53.0%)	1.000
VII. Genotype +	48 (31.0%)	29 (32.6%)	19 (28.8%)	0.726
PLN (% genotype +)	1 (2.1%)	0 (0.0%)	1 (5.3%)	0.396
TTN (% genotype +)	11 (22.9%)	8 (27.6%)	3 (15.8%)	0.488
PKP2 (% genotype +)	23 (47.9%)	17 (58.6%)	6 (31.2%)	0.083
DSC2 (% genotype +)	2 (4.2%)	1 (3.5%)	1 (5.3%)	1.000
DSG2 (%genotype +)	12 (25.0%)	6 (20.7%)	6 (31.5%)	0.501
DSG3 (%genotype +)	2 (4.2%)	1 (3.5%)	1 (5.30%)	1.000
DSP (%genotype +)	8 (16.7%)	6 (20.7%)	2 (10.56%)	0.4510

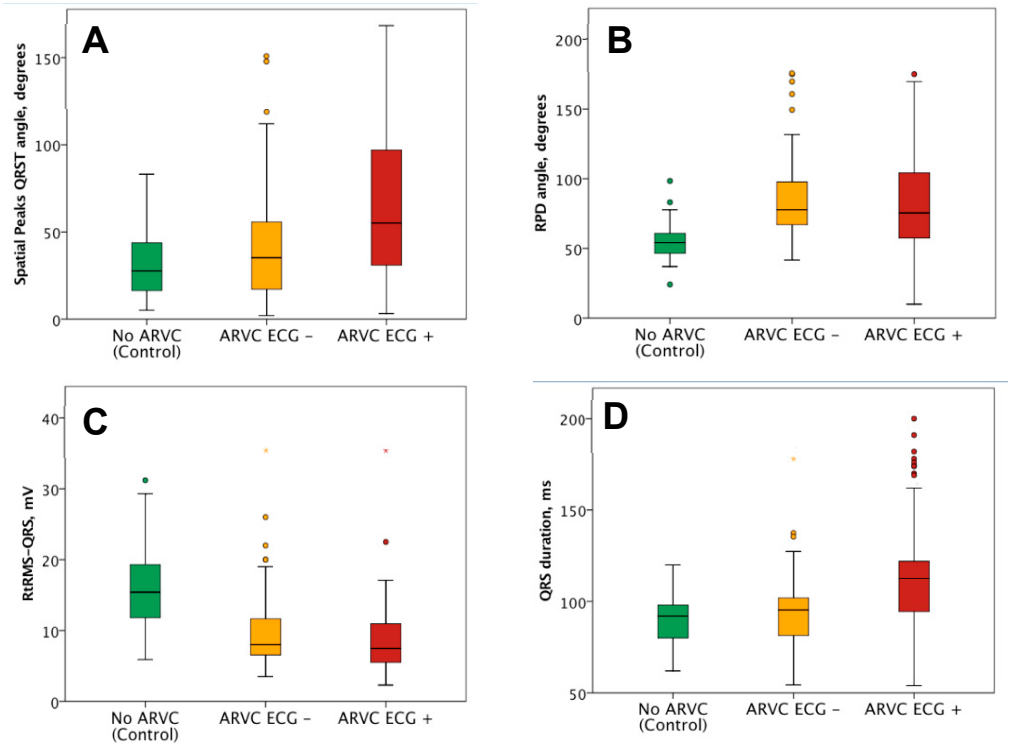

Figure 14 A-D:
A: Spatial peaks QRS-T angle angles for controls, ARVC without ECG changes (-) and ARVC with ECG changes (+)
B: Right precordial-directed angle (RPD angle) for controls, ARVC without ECG changes (-) and ARVC with ECG changes (+)
C: Right RMS-QRS (right QRSvm) for controls, ARVC without ECG changes (-) and ARVC with ECG changes (+)
D: QRS duration for controls, ARVC without ECG changes (-) and ARVC with ECG changes (+)

Table 7: Detailed electrocardiographical and imaging characteristics of ECG-positive and ECG-negative ARVC/D patients including Epsilon waves, upslope S-wave, Signal Average ECG measurements (SAECG) including fractional QRS duration (fqrsd), low amplitude signal under 40 microV in the latter part of QRS (LAS40) and root mean square amplitude in the last 40milliseconds (RMS40), repolarization abnormalities and echocardiogram/magnetic resonance imaging (MRI) including right ventricular end-diastolic volumes (RVEDV).

	ARVD/C (n=155)	**ARVD/C ECG-positive (N=84)**	**ARVD/C ECG-negative (N=66)**	**P-value**
ECG: Depolarization				
Epsilon waves	13 (8.4%)	13 (15.5%)	0 (0.0%)	**<0.001**
Upslope S-wave ≥55 ms V1,V2 or V3	17 (11.0%)	17 (20.2%)	0 (0.0%)	**<0.001**
Bundle branch blocks	22 (14.1%)	17 (20.2%)	0 (0.0%)	**0.035**
SAECG performed (% total)	63 (40.7%)	32 (38.1%)	31 (41.7%)	0.515
fQRSd ≥114ms (% of SAECG)	33 (52.4%)	17 (53.1%)	16 (51.6%)	1.000
LAS40 ≥38ms (% of SAECG)	31 (49.2%)	18 (56.3%)	13 (41.9%)	0.317
RMS40 ≤20μV (% of SAECG)	28 (44.4%)	13 (40.6%)	15 (48.4%)	0.616
ECG: Repolarization				
T-wave inversions V1-V3 >14years no RBBB	54 (34.8%)	54 (64.3%)	0 (0.0%)	**<0.001**
T-wave inversions V1-V4 with RBBB	12 (7.7%)	12 (14.3%)	0 (0.0%)	**<0.001**
- T-wave inversions V1 and V2 or in V4,V5,V6	8 (5.2%)	8 (9.5%)	0 (0.0%)	**0.008**
Imaging				
Echocardiograms performed (% total)	155 (100.0%)	84 (100.0%)	66 (100.0%)	1.000
Akinesia/dyskinesia/aneurysm echo	111 (71.6%)	65 (77.4%)	43 (65.2%)	0.108
MRI's performed (% total)	124 (80.0%)	72 (85.7%)	52 (73.2%)	0.070
Akinesia/dyskinesia/aneurysm	89 (71.8%)	58(80.6%)	31 (59.6%)	0.272
RVEDV ≥110ml/m^2(M), 100ml/m^2(F)	65 (52.4%)	49 (68.1%)	16 (30.8%)	**<0.001**
RVEDV ≥100ml/m^2 but <110 ml/m^2 (M), ≥90ml/m^2 but <100ml/m^2(F)	24 (19.4%)	10 (11.9%)	14 (26.9%)	0.106

Table 8: Vector and protractor measured angles and their respective p-values for the QRS duration (QRSd, milliseconds), corrected QT interval (QTc, milliseconds), the right precordial directed angle (RPD angle), and right root mean square QRS (RtRMS-QRS)respectively for different subsets of patients including controls, arrhythmogenic right ventricular dysplasia/cardiomyopathy patients who meet 12-lead 2010 Taskforce criteria (ECG-positive), who don't meet 12-lead 2010 Taskforce criteria (ECG-negative), who are ECG-negative without bundle branch blocks (BBB) and who are ECG-negative who have signal average ECG's do not have any late potentials (SAECG-). P-values as compared to controls.

Parameter	QRSd (ms), [p-value]	QTc (ms), [p-value]	SPQRS-T angle	RPD angle	RtRMS-QRS
Controls (N=66)	92 (86-99)	405 (387-430)	24.1 (13.5 to 42.1)	54.4 (48.9 to 61.5)	1.54 (1.17 to 1.90)
ARVD/C ECG-positive (N=89)	104.0 (94.0-122.0), [<0.001]*	425.0 (403.0 to 449.0), [0.022]*	43.8 (23.6 to 72.9), [0.228]	74.8 (58.4 to 94.7), [0.971]	0.81 (0.63 to 1.13), [0.371]
ARVD/C ECG- and no BBB (N=66)	98.0 (86.0-104.0), [0.052]	412.0 (399.0 to 430.0), [0.061]	33.6 (16.7 to 54.2), [0.004]	76.2 (62.3 to 92.9), [<0.001]	0.81 (0.64 to 1.15), [<0.001]
ARVD/C ECG-, no BBB, SAECG-negative (N=20)	93.0 (85.5-100.0), [0.947]	420.5 (397.5-430.0), [0.057]	40.9 (22.3-55.7), [0.081]	71.2 (60.4-84.7) [<0.001]	0.77 (0.67-1.18), [<0.001]

Table 9: Sensitivities, specificities, positive/negative predictive values and odds ratios (95% CI) for cut-off values based on ROC curve analysis for corrected QT interval, spatial peaks QRS-T angle, right precordial directed angle, right root mean square QRS, and both right parameters for ECG-negative ARVD/C versus controls.

Parameter	Cut-off	AUC	p-value	Sn (%)	Sp (%)	PPV (%)	NPV (%)	Odds ratio
QRSd	99.0ms	0.64	0.026	48.5	83.3	74.4	61.8	4.7 (2.1-10.6)
QTc	451ms	0.56	0.289	12.1	100.0	100.0	53.2	19.3 (1.1-342.1)
SPQRS-T angle	50.8°	0.68	<0.001	30.0	94.0	53.6	50.9	1.2 (0.5-2.7)
RPD angle	70.2°	0.86	<0.001	72.7	94.0	91.7	80.5	41.3 (13.1-130.2)
RtRMS-QRS	0.81 mV	0.85	<0.001	51.5	92.4	92.3	77.5	13.0 (4.6-36.4)
Both right parameters	N/A	N/A	N/A	81.8	90.9	90.0	83.3	45.0 (15.8-128.2)

The QRSd and the QTc significantly differentiated the ECG-positive versus ECG-negative ARVD/C patients (p-values of <0.001 and 0.002, respectively).

Spatial peaks QRS-T angles Both the SPQRS-T angle and the RPD angle demonstrated significant differences between ECG-negative ARVD/C patients and control subjects (p-value < 0.001, ARVD/C Table 8). The RPD angle showed much better sensitivity and specificity than the spatial QRS-T angle (Table 9) and with an odds ratio 34 times higher than that for the SPQRS-T angle at 41.3 (95% CI 13.1 to 130.2). The SPQRS-T angle demonstrated stepwise increase from the lowest value in the control group to ECG-negative ARVD/C and the highest value observed in the ECG-positive ARVD/C patients.

Right root mean square QRS voltage The right root mean square QRS (RtRMS-QRS) progressively and significantly decreased stepwise from the highest mean value observed in the control group to the lowest among the ECG-positive ARVD/C. Regarding discrimination between control subjects and ECG-negative ARVD/C patients, the ROC curve gave an optimum cut-off value of 0.81 mV giving an odds ratio of 13.0 (95% CI 4.6 to 36.4). Please see ARVD/C Tables 8 and 9.

Combined right-precordial directed parameters Based on combined right-precordial-directed-sided parameters including the RPD angle and RtRMS-QRS, at the above noted cut-off values, the sensitivity, specificity and odds ratios were 90.9%, 83.3%, and 45.0 (95% CI 15.8 to 128.2), respectively. Figure 14 (a-d) shows depolarization parameter box plots.

ECG-negative proband versus ECG-negative non-proband Thirty patients without abnormalities on the 12-lead ECG were probands (45.5%). At the cut-off values above (70.2 degrees for RPD angle and 0.81 mV for the RtRMS-QRS, respectively), the sensitivity for probands was 86.7% and for non-probands 72.5% for identification of those without 12-lead ECG abnormalities otherwise, while of course maintaining specificity 92.4% and 94.0% respectively.

ECG-based 2010 taskforce criteria and their relationship to the right-precordial ECG parameters When the whole ARVD/C cohort was assessed (N = 155), the RtRMS-QRS significantly differentiated those with TAD (terminal activation delay, ie. The upslope of the S-wave ≥55 ms, minor depolarization criterion) versus those ARVD/C patients with upslope of the S-wave <55 ms (p = 0.006). Patients with and without epsilon waves did not demonstrate significant difference in regard to the novel right-precordial parameters (Table 7). Patients with different extent of repolarization abnormalities, such as no T-wave inversion/T-wave inversion in V1 (repolarization criterion is not present), T-wave inversion in V1 and V2 only (minor repolarization criterion) or T-wave inversions in V1-V3 or beyond (major repolarization criterion) were not differentiated by the right-precordial parameters (Table 10). The spatial QRS-T angle was lower for those with only T-wave inversions in V1 and V2, versus those with more precordial T-wave inversions or those without T-wave inversions in the precordial leads (ARVD/C Table 10).

Table 10: Novel right-precordial and vectorcardiographic values compared to ARVD/C patients and 2010 Taskforce criteria values currently used.

	SPQRS-T angle (degrees)	RPD angle (degrees)	RtRMS-QRS (millivolts)
Epsilon-wave +, n=13	54.4 ± 31.3	100.5 ± 42.5	1.0 ± 0.8
Epsilon-wave -, n=142	54.6 ± 42.0	81.2 ± 31.2	0.9 ± 0.4
TAD >= 55 ms, n=17	67.0 ± 41.1	92.9 ± 40.7	**0.7 ± 0.3***
TAD< 55 ms, n=138	53.1 ± 41.1	81.7 ± 31.4	**0.9 ± 0.5***
No T-wave inversion/only in V1, n=26	56.7 ± 31.0	83.8 ± 33.8	1.0 ± 0.6
T-wave inversion V1-V2, n=56	**35.0 ± 28.0***	87.5 ± 31.8	0.9 ± 0.4
T-wave inversion V1-V3 or beyond, n=73	67.7 ± 46.8	78.1 ± 32.4	0.8 ± 0.4

Left ventricular involvement and clinical parameters Twelve total ARVD/C patients had left-sided disease (7.7%). Eleven had decreased left ventricular ejection fraction (median 52.5%, IQR 50.5 to 54.0%) and three had LVEDVi >100 ml/m^2 (median 30.8 ml/m^2, IQR 26.5 to 97.0 ml/m^2). Three patients were ECG-negative and one had no late potentials. There was only a significant difference in the QRSd with those without LV changes at median 100 ms (IQR 90-113 ms) versus those with left sided changes at a median of 97 ms (IQR 91.5 to 101 ms). The median values for ARVD/C patients with left-sided changes for the QTc, SPQRS-T angle, RPD angle and RtRMS-QRS were 417 ms (IQR 401 to 457 ms), 23.0 degrees (IQR 15.6 to 51.5 degrees), 79.4 degrees (IQR 70.0 to 99.8 degrees), and 0.91 mV (IQR 0.54 to 1.21 mV), respectively.

Intra-observer and inter-observer variability Intra-class correlation coefficients for the intra−/interobserver variability for the RPD angle were 0.93 and 0.92, for the RtRMS-QRS were 0.94 and 0.92. For the SPQRS-T angle, intra−/inter-observer variability has previously been described (8,17,26). Variability between automated analyses and 1st author calculations gave intra-class correlation coefficients of 0.971 and 0.917 for RtRMS-QRS and RPD angle.

Magnetic resonance imaging correlates MRI indexed volumes and ejection fractions were compared to the VCG/ECG parameters above. The highest

R-squared value for a VCG or ECG parameter was 0.24 for the SPQRS-T angle correlating to left ventricular ejection fraction (EF). Otherwise the RPD angle and RtRMS-QRS correlated poorly to RV indexed volume (indexed RVEDV) with R-squared values at 0.15 and 0.07, respectively and with RV EF R-squared values of 0.06 and 0.19, respectively, all without significant p-values. QRSd also correlated poorly with indexed RVEDV and RVEF with R-squared values of 0.10 and 0.11, respectively without significant p-values.

Ventricular repolarization abnormality (Paper IV):

One hundred and fifty-four patients met clinical inclusion criteria, of whom 113 patients had ECG's suitable for assessment. These 113 patients with LQT2 with normal QTc values (mean age 42±16 years, 43% male) comprised the study group and were compared with 1007 normal QTc control patients (mean age 41±15 years, 41% male). LQT2 mutation carriers did not differ from the control group in regard to the age at enrolment or gender distribution, however, they had significantly lower heart rate, longer QTc (even though still within normal range), QTpeak and Tpeak-Tend intervals in comparison with the genotype-negative subjects (LQT2 Tables 11 and 12). As previously reported, the proportion of subjects demonstrating visually abnormal T wave morphology at inclusion in the registry was nearly five times higher among LQT2 mutation-positive patients than in the control group. The proportion of individuals experiencing syncopal episodes was significantly higher among LQT2 mutation carriers, however, very few were treated with beta-blockers or had more serious events by the age of 18 (baseline), as shown in LQT2 Table 11.

Among patients carrying LQT2 mutation who had ECG available for TwVM assessment, median TwVM was 0.30mV, which was used as a cut-off for analyses of associations between TwVM and clinical characteristics and study endpoints. TwWM was significantly higher in LQT2 men than women:3.8±1.8vs3.0±1.3mV, respectively(P=0.020). Intraclass correlation coefficients for the TwVM measurements for a 10% sample of the population gave interobserver variability of 0.94. LQT2 mutation carriers with TwVM≤0.30mV were more likely to be female, have lower heart rates, have syncope and receive betablocker treatment (LQT2 Table 2). Low TwVM was strongly associated with the visually assessed abnormal T-wave morphology: of 35 LQT2 mutation carriers demonstrating abnormal T-wave morphology, 26 (75%) had low TwVM (P<.001). There was a trend indicating greater proportion of LQT2 pore-mutation carriers among patients with low TwVM, though the difference was not significant (21% vs 11%, P=.144).

Clinical course in LQT2 patients with normal QTc values

During follow up, 27 LQT2 mutation carriers had CE, of which 5 were ACA and 22 syncopal episodes (compared with 62 syncopal episodes and 1 ACA in the control group), which were assessed using Kaplan–Meier curve analysis and Cox regression analysis as outlined in the Methods. Four ACA events were observed among female LQT2 carriers who had low TwVM and one ACA event occurred to a male patient with high TwVM.

Figure 15A shows Kaplan–Meier curve analysis of the risk of cardiac events in normal QTc LQT2 mutation carriers dichotomized by the median TwVM and

compared with the genotype-negative controls shown for the entire study cohort and separately for men (Figure 15B) and women (Figure 15C).

Table 11: Clinical characteristics for genotype negative LQTS family members with normal QTc values and genotype positive LQT2 patients with normal QTc values at baseline (18 years).

Clinical characteristics	Normal QTc Genotype- negative family n=1007	Normal QTc LQT2 Carriers N=113	P Value
Male, #(%)	414 (41)	49 (43)	0.645
Age at ECG, yr	41±15	42±16	0.242
Pore Mutation	N/A	18 (16)	N/A
ECG characteristics			
RR, msec	893±166	951±176	**0.001**
PR, msec	161±28	163±23	0.807
QRS, msec	85±14	85±14	0.919
QTp, msec	305±31	326±42	**<0.001**
QT, msec	391±34	421±38	**<.0001**
QTc, msec	417±26	434±25	**<0.001**
TpTe, msec	86±21	95±30	**0.004**
Abnormal T-wave in V5/L2	64 (7)	35 (34)	**<0.001**
Treatment, #(%)			
Beta-blockers	3 (0)	2 (2)	**<0.001**
LCTSD	0 (0)	0 (0)	N/A
Pacemaker	1 (0)	0 (0)	1.000
ICD	1 (0)	1 (1)	0.192
Cardiac Events, # (%)			
Syncope	62 (6)	15 (13)	**0.009**
ACA	1 (0)	0 (0)	1.000
Appropriate Shock	0 (0)	0 (0)	N/A

Table 12: Characteristics of electrocardiographically concealed LQT2 patients (genotype positive KCNH2 with normal QTc values), based on cut-offs of the median product of the T wave vector magnitude (TwVM) at baseline (18 years).

Clinical Characteristics	TwVM ≤ median	TwVM > median	P-value
# of LQT2 Carriers	57	56	
Male, # (%)	17 (30)	32 (57)	**0.003**
Age at ECG, yr	44±16	40±15	0.230
Pore Mutation	12 (21)	6 (11)	0.144
ECG characteristics			
RR, sec	912±168	991±177	**0.017**
PR, sec	163±22	162±24	0.850
QRS, sec	83±12	87±15	0.102
QTp, sec	326±45	327±39	0.885
QT, sec	417±43	425±33	0.202
QTc, sec	438±22	430±27	**0.091**
TpTe, sec	92±33	98±27	0.404
Abnormal T-wave in V5/L2	26 (50)	9 (17)	**<0.001**
TwVM	0.22±0.05	0.45±0.14	**<0.001**
Treatment, # (%)			
Beta-blockers	1 (2)	1 (2)	**1.000**
LQTSD	0	0	N/A
Pacemaker	0	0	N/A
ICD	0	1(2)	0.495
Cardiac Events, # (%)			
Syncope	10 (18)	5 (9)	0.269
ACA	3 (5)	0	0.243
Sudden cardiac death	1 (2)	1 (2)	1.000
Appropriate Shock	0	0	N/A
Retroactive ACA/sudden death events (<18 years)	2 (4)	0 (0)	0.496

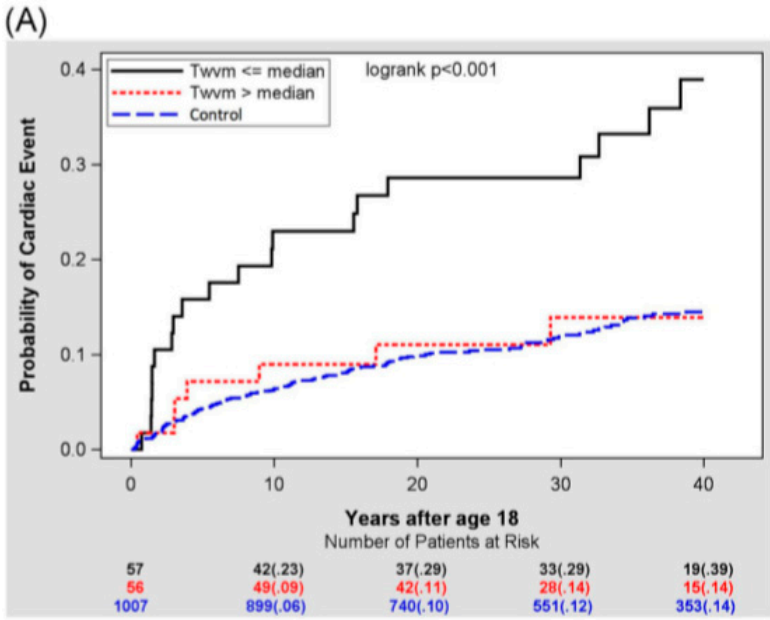

Figure 15 A:
Probability of cardiac event genotype positive KCNH2with normal QTc values based on T-wave vector magnitude (Twvm) cut-off value of 0.30mV compared to genotype negative controls for all patients.

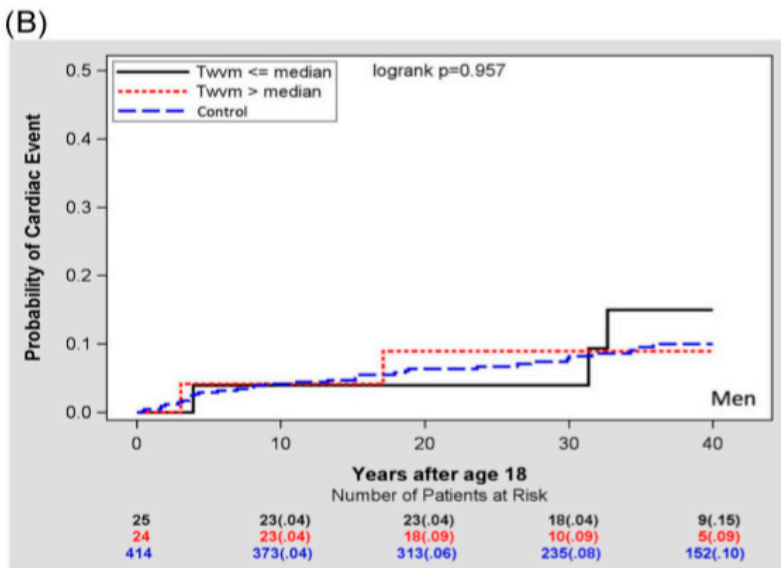

Figure 15 B:
Probability of cardiac event genotype positive KCNH2 with normal QTc values based on T-wave vector magnitude (Twvm) cut-off value of 0.30mV compared to genotype negative controls for men only.

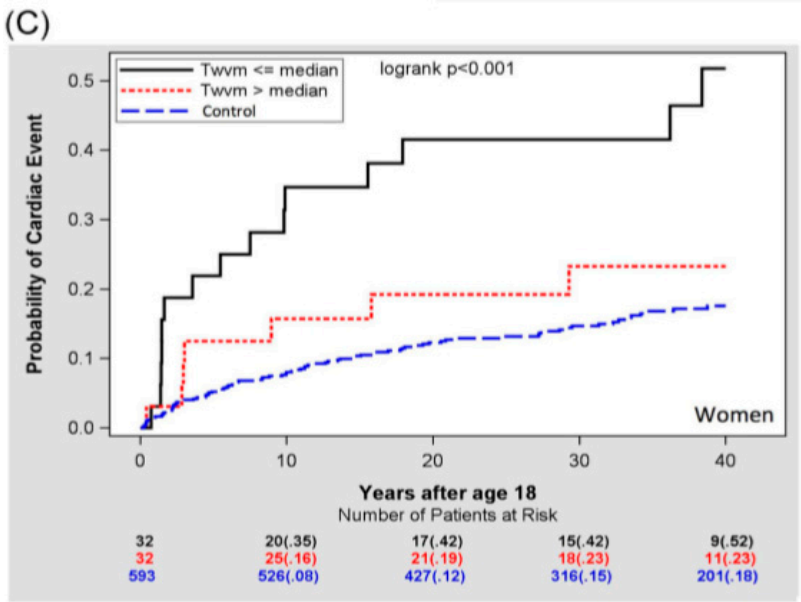

Figure 15 C:
Probability of cardiac event genotype positive KCNH2with normal QTc values based on T-wave vector magnitude (Twvm) cut-off value of 0.30mV compared to genotype negative controls for women only.

In the entire cohort, low TwVM was associated with a high risk of cardiac events among the LQT2 patients with normal QTc values, while the curve indicating the cumulative risk of cardiac events among these same patients with high TwVM was overlapping with the one corresponding to the genotype-negative controls. In the univariate Cox regression analysis, TwVM≤0.30mV was associated with the increased risk of cardiac events (HR=2.95, 95% CI, 1.25-6.98, P=0.014) compared to LQT2 patients (with normal QTc values) with TwVM>0.30mV. After including sex and time-dependent beta-blockade use in the multivariate Cox regression analysis, low TwVM remained a significant predictor of cardiac event risk (HR=2.55, 95% CI, 1.07-6.04, P=0.034). This difference was primarily due to the differences observed among women (HRfemale = 3.18, 95% CI, 1.91-5.98, P=<.001; HRmale =1.05, 95% CI, 0.25-4.37, P=0.947, Table 13).

After including sex and time-dependent betablockade use in the Cox regression analysis, low TwVM remained a significant predictor of cardiac event risk within the LQT2 cohort (HR=2.55, 95% CI, 1.07-6.04, P=.034). There were no differences in LQT2 patients with TwVM>0.30mV compared to controls in respect to survival to CE, and whether men and women, just women, or just men were evaluated (LQT2 Table 13). It is worth stressing that these associations were present in women but not in men who presented with low risk of cardiac events. As sensitivity analysis we repeated the above Cox analyses while using sex-specific median TwVM values as cut-offs in

males (≤0.37 mV) and females (≤0.27 mV) and the results were very similar: hazard ratio of 3.30 (P < .001) in females and 0.78 (P = .732) in males when comparing risk of events in individuals with lower vs higher than median TmVM values. TwVM demonstrated a significant association with the risk of ACA/SCD (HR=2.64, 95% CI, 1.64-4.24, P<.001) compared to genotype-negative family members (Figure 16).

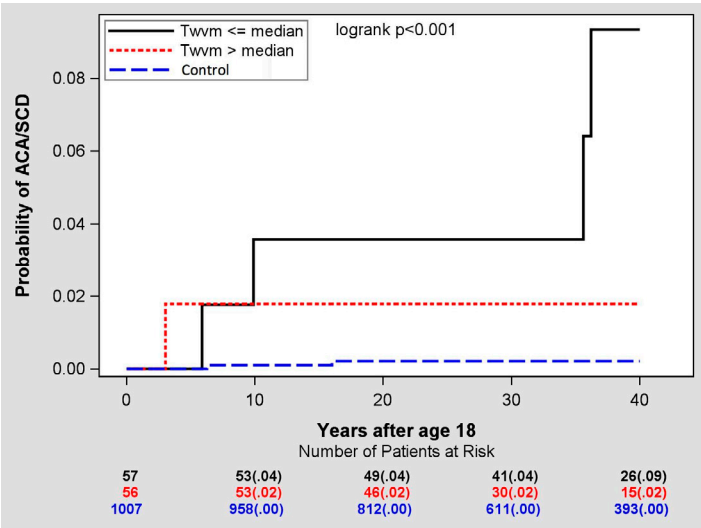

Figure 16: Probability of sudden cardiac death or aborted cardiac arrest in genotype positive KCNH2with normal QTc values based on T-wave vector magnitude (Twvm) cut-off value of 0.30mV compared to genotype negative controls .

Table 13: Probability of cardiac events in the Cox regression analysis in the ECG concealed LQT2 patients with adjustment for time-dependent beta blocker usage based on T-wave vector magnitude cut-off of 0.3mV with female and male cohorts also presented separately. The hazard ratio for the genotype-negative control population versus the entire genotype negative cohort is also presented.

	All			**Females**			**Males**		
	HR	95%CI	p-value	HR	95%CI	p-value	HR	95%CI	p-value
ecLQT2 TwVM ≤0.30 mV vs. ecLQT2 TwVM >0.30mV	2.55	1.07-6.04	0.034	3.18	1.08-9.40	0.036	0.99	0.17-5.95	0.993
ecLQT2 TwVM ≤0.30mV vs. Genotype-negative control	2.64	1.64-4.24	<0.001	3.18	1.91-5.28	<0.001	1.05	0.25-4.37	0.947
ecLQT2 TwVM >0.30mV vs. Genotype-negative control	1.38	0.72-2.62	0.333	1.37	0.64-2.95	0.422	1.39	0.43-4.52	0.589

Discussion:

Derived-vectorcardiography including right precordial-directed parameters, demonstrate improved prognostic and diagnostic capability over traditional 12-lead ECG parameters. Global atrial depolarization vector magnitude, when multiplied by the P-wave duration, gives the most predictive ECG measure for predicting atrial fibrillation, in a prospective cohort of ischemic stroke patients. Assessing the angle difference between the maximum vector of depolarization compared to the maximum vector of repolarization, the spatial peaks QRS-T angle, predicts ventricular tachycardia in a population of patients with hypertrophic cardiomyopathy. Another cardiomyopathy, arrhythmogenic right ventricular cardiomyopathy, can be identified with improved diagnostic accuracy by right precordial-directed vectorcardiography compared to the ECG or signal averaged ECG parameters that are currently part of the 2010 Taskforce criteria. Lastly, patients with KCNH2 mutations but normal QTc intervals, have risk of cardiac events, and can be risk stratified based on a lower TwVM. Thus, derived-vectorcardiography involving atrial depolarization, ventricular depolarization, and ventricular repolarization appear to have clinical usefulness in the subpopulations we assessed, and likely have value in other subpopulations.

Atrial fibrillation prediction

Our study demonstrates that a measure of P-wave dispersion by duration and voltage assessment from the standard 12-lead ECG, taken during hospital admission for ischemic stroke, in the form of Pd/Pvm can predict new-onset AF during follow-up while neither P-wave duration nor P-wave terminal force in lead V1 were significantly associated with subsequent AF occurrence. The relation of Pd/Pvm to new-onset AF remained independent after adjustment for other clinical parameters.

Presence of AF as previously reported, by the end of the 10-year follow-up AF was detected in 15% of our initially AF-free subjects, which corresponds to the reported AF incidence for an aging population of 18% in those older than 85 years by the end of a 7-year follow-up and 17% of those 65– 74 years by the end of a 6-year follow-up (14,15,47, 53). Compared with studies based on only ECG screening, studies that employed implantable devices generally have shown higher AF detection rates - of

up to 28–30% in patients with ischemic stroke or TIA, as well as in those with risk factors for ischemic stroke (54,55,56,57).

We previously reported that in the same cohort age > 65 years, presence of hypertension or heart failure showed a univariate as well as multivariate predictive relation to subsequent AF onset during a 10-year follow-up period (47). Clinical parameters we found significant in previous analyses were used in the Cox modelling in the current analysis (47).

P-wave duration divided by 3-dimensional p-wave vector magnitude (Pd/Pvm)

Previous literature mostly has focused on P-wave duration as a predictive tool for new-onset atrial fibrillation with some success in non-ischemic stroke populations (17,58). Although in the subgroup of those <60 years of age, the overall P-wave duration yielded a nonsignificant HR (1.15, 95% CI 0.90 to 1.47). It has also been shown that maximum P wave duration at the upper fifth percentile was associated with long-term AF risk in an elderly community-based cohort (17). In hypertensive patients the P-wave duration independently predicted the development of new-onset atrial fibrillation (58). However, in a recent publication of our cohort, no significant predictive value was found for the P-wave duration as a predictor for new-onset AF (47). In another study, prolonged P-wave duration and advanced interatrial block in particular have shown an association with AF (18). Furthermore, PTFV1 was not found to be a reproducibly significant predictor of AF (47). In patients with recurrent atrial fibrillation after catheter ablation, low voltage in lead I (<0.01 mV) was associated with recurrence of AF (22). Our results demonstrate that atrial voltage dispersion, as measured by Pvm is not in itself alone associated with the development of AF. However, our study is the first to show that atrial time duration versus voltage dispersion (Pd/Pvm) is a potentially clinically useful predictive measure which can be obtained by the ECG alone.

After our study was published a subsequent study by Nakatani et al, which referenced our method, assessed the value of lower Pvm in predicting left atrial low-voltage areas which found to be the only significant independent predictor (59). This provides further pathophysiologic changes, ie. scar formation leading to lower absolute vector magnitude in one particular direction, which is quantified by the Pvm (59). Another study published subsequent to ours (referenced in our methods section), was a study performed to assess the ability of Pvm to identify those patients with recurrence of atrial fibrillation after pulmonary vein isolation (ablation) procedure (60). This study assessed post-operative ECG and derived the Pvm by our same method and found that in 126 consecutive patients with persistent atrial fibrillation who underwent catheter ablation, only the Pvm could independently predict recurrence of atrial fibrillation based on a cut-off value of 0.13mV, with

lower values identifying those with recurrence of atrial fibrillation with freedom from atrial fibrillation of 93% if Pwm was above 0.13mV after ablation (60).

Pvm has also shown predictive value for atrial arrhythmias in patients with congenital heart disease, and in particular tetralogy of Fallot patients undergoing pulmonary valve replacements (20). In this same study Pvm inversely correlated with higher right atrial pressure, left and right ventricular ejection fractions, QRSd, and older age (20). In the above publication Pvm was predictive of organized right atrial arrhythmias (intra-atrial re-entrant tachycardia and typical flutter), thus in the more disorganized left atrial arrhythmia (AF), it appears time dispersion across the left atrium must also be taken into account. A risk score based on the above parameters might be helpful in ruling out those at risk for atrial fibrillation, and furthermore can be automatically calculated, however further reproducibility with other ECG systems and automated methods would be required. Our study also demonstrated a high specificity and negative predictive value for identification of AF in ischemic stroke patients but with low sensitivity and positive predictive values. This demonstrates that in our cohort although those who develop AF cannot necessarily all be identified (sensitivity 51%) and the value of a Pd/Pvm > 870 ms/mV does not necessarily identify all of those who may develop AF (positive predictive value 30%). Those who do not develop AF, however, are going to be those who have a Pd/Pvm <870 ms/mV. Thus, if effectively reproduced independently, this may be a reasonable and cost-effective screening test for those at risk for developing AF.

The duration of the P-wave when assessed (divided) by its vector magnitude predicted atrial fibrillation in cryptogenic stroke patients, whereas no 12-lead parameter by itself had atrial fibrillation predictive value.

Left ventricular abnormality (Paper II):

Ventricular tachycardia prediction **in hypertrophic cardiomyopathy**

Corrected QT Interval and QRS Duration

Corrected QT interval prolongation has been previously described in HCM patients, with 13% having values >480ms (26). However, the association between a prolonged QTc interval, specifically >460ms, and VAs, as well as sudden cardiac death in HCM, has been described (26). In our study, the QTc interval had too low of a predictive value (positive or negative) for any clinical usefulness.

Spatial Peaks QRS-T Angle The SPQRS-T angle has been previously been shown to identify patients with HCM and to predict VA's in adults with myocardial

ischemia; thus, it seems logical that it would predict VA's in patients with HCM (39,61). Hypertrophic cardiomyopathy, however, can involve subendocardial ischemia; thus, the SPQRS-T angle is not as robust a predictor as one might have thought. Given its positive correlation with worsening HF, it is likely that the SPQRS-T angle, given a larger population size, would identify HF in patients with HCM (62,63,64). However, identification of significant morbidity from either HF or VAs is obtained by utilizing the SPQRS-T angle with improved ORs at the same VA optimum cut-off value for the SPQRS-T angle. Thus, arrhythmia and HF risk are both conferred by an increase in the SPQRS-T angle. The spatial QRS-T angle correlates with reduced left ventricular ejection fraction, left ventricular dilation, and increased left ventricular mass and is associated with ischemic scar, which are known risk factors for VA's (65). Furthermore, the derived spatial QRS-T angle from the 12-lead ECG, which was the method used in this study, shows similar diagnostic ability to the vectorcardiographically measured spatial QRS-T angle with tight Bland-Altman 95% limits of agreement; thus, is a reasonable and clinically available tool for risk assessment in HCM patients (30,52).

In hypertrophic cardiomyopathy patients, an increased spatial QRS-T angle identified those patients with sustained ventricular arrhythmias better than any 12-lead EKG predictor and also had predictive value for those HCM patients with late-stage systolic heart failure.

Right ventricular abnormality (Paper III):

Identification of ARVC in electrocardiographically concealed patients

We found that patients with ARVD/C, diagnosed using the 2010 revised Task Force criteria, exhibit subtle electrocardiographic abnormalities, which do not fit in the frame of the depolarization and repolarization criteria outlined in the Task Force 2010 document. By comparing with a cohort of healthy controls we found that ostensibly normal ECG pattern in patients with ECG-negative ARVD/C contain signs of abnormal ventricular depolarization and repolarization that can be quantified using novel right precordial-adjusted VCG markers. RPD angle, SPQRS-T angle, and the RtRMSQRS demonstrated significant ability to differentiate patients with electrocardiographically concealed ARVD/C from healthy controls. In addition, SPQRS-T angle exhibited stepwise increase and RtRMSQRS a decrease when control cohort was compared with ECG-negative and ECG-positive ARVD/C patients thus suggesting novel markers potential for quantification of electrocardiographic ARVD/C phenotype. These may aid in early detection in clinical cascade screening.

QRSd and QTc

The QRSd was not a specific marker for -ECG ARVC/D, which is not surprising, given the patients don't meet 2010 taskforce criteria including epsilon waves or delayed S-wave upstroke. It does significantly differentiate ECG-positive ARVD/C from ECG-negative ARVD/C. The QTc did significantly differentiate patients with ECG-negative ARVD/C with minimal diagnostic assistance. The QTc also prolongs significantly as the ARVD/ C patients develop Taskforce 2010 ECG criteria, which may or may not assist in diagnosis.

Spatial angles

Although conventional VCG markers have shown use in left sided heart disease (5,29,30,62-65), they have shown limited use in right heart disease (32). For instance, in hypertrophic cardiomyopathy, the spatial QRS-T angle improves diagnostic ability for detection of hypertrophic cardiomyopathy over conventional 12-lead ECG parameters, however only detected part of our ECG-negative ARVD/C cohort (5,29,30). This same angle, however showed limited prognostic ability in other right-ventricle disease patients, namely those with tetralology of Fallot and with single ventricle physiology (36,66). The RPD angle had the highest identification ability out of all parameters tested and gave the highest odds ratio for identification of ECG-negative ARVD/C. Although the SPQRS-T angle significantly differentiates controls from ECG-negative ARVD/C, it did not prove as clinically useful with less sensitivity and less specificity than the RPD angle. Although some cases of ARVD/C include left sided disease (12 patients in our cohort), more often than not a right-sided only phenotype is present (32). Thus, even though the SPQRS-T angle has prognostic and diagnostic use, and specifically for a generally left sided cardiomyopathy, it is not surprising that a right-sided specific marker is more helpful in identification of disease in those without other depolarization/repolarization abnormalities in ARVD/C as suggested by our findings (5,29,30,62-65). This also seemed to be particularly a good marker for those family members detected by cascade screening, who likely represent an early ARVC/D phenotype. This may be a useful marker for screening and can be programmed in most ECG software.

The RtRMS-QRS or right precordial-directed QRS vector magnitude is simply a measure of depolarization dispersion in the right ventricle which should become smaller as more fibrosis occurs. The lower the RtRMSQRS, the more dispersion of depolarization in the right ventricle would likely occur. The RtRMS-QRS had significant identification ability in those with ECG-negative ARVD/C compared to control patients with a high specificity. This is useful as it is a simple parameter to calculate (Figure 11). Similar to other right side-specific voltage parameters, it has low sensitivity for detection of right heart disease in this study, however as a non-

invasive and cost-effective test, this simple method still detected over one half of patients who were not initially detected by ECG (35). Given the fibro-fatty infiltration of right ventricular myocardium often observed in ARVD/C, it seems logical that dispersion of depolarization (ie. lower RtRMS-QRS) would be affected, and furthermore, this has already been identified by the low amplitude of the last 40ms of the QRS when SAECG has been evaluated (32). Again, this would also particularly be helpful in identification of those with early ARVC/D disease, as it was able to detect those non-proband family members who represent an early stage of ARVC/D and meet 1 of their major criteria by family association alone.

Combined, the diagnostic value of these parameters demonstrated superior identification power than each parameter alone. Combined, without compromising specificity, these parameters identified 65/71 (91.6%) of patients who would not have otherwise been identified with ECG screening. A high odds ratio was determined. These right-sided specific parameters, although not perfectly sensitive, combined have an additive identification ability without compromising specificity for patients who might otherwise fit 2010 taskforce criteria for definite ARVD/C based on genetic testing or further imaging (35).

Novel right-precordial parameters and the degree of ARVD/C phenotype manifestation In the case of the RtRMS-QRS, there appears to be a significant step-wise progression from control patients to ECG-negative and further on to the ECG-positive ARVD/C patients, which suggests that these novel VCG/ECG markers may be considered as electrocardiographic equivalent of the disease substrate in ARVC/D. RtRMS-QRS appears to be related to the conventional electrocardiographic disease markers such as terminal activation delay in the right precordial leads, however they perform well in differentiating patients with ARVC/D from controls also in the “normal” TAD range. This demonstrates the ability of the novel VCG/ ECG markers to detect ARVC/D manifesting with subtle depolarization abnormalities only and indicate their potential in identification of affected family members, which requires additional studies.

The RPD angle did not have a stepwise progression, however, was similar in number between those ARVD/C patients with and those without other depolarization or repolarization abnormalities. Also, this parameter did not differentiate the degree of T-wave inversion (Table 5), thus must be more affected by depolarization versus repolarization abnormalities. Even though not a significant difference, the RPD angle (as well as the other right precordial parameters) demonstrated trends with Epsilon wave differentiation, which seem to indicate dependence on dispersion of depolarization. Regardless, all three parameters detect ARVD/C patients with electrographically concealed changes. Further studies are warranted to define these changes over time as well as genotype differences.

Right-precordial directed vectorcardiography can identify ARVD/C patients not otherwise identified by 2010 Taskforce 12-lead EKG or signal average EKG parameters.

Prediction of cardiac events in patients with genotype-positive long QT 2 syndrome and normal QT intervals

Our study demonstrates the ability of an easily calculated, quantifiable parameter, the TwVM, to identify LQT2 patients with normal QTc values at risk for cardiac events with increased cardiac events risk being associated with reduced TwVM. While an earlier study by our group suggested abnormal T wave morphology, which included qualitatively assessed flat, broad or notched T waves, as an indicator of mutation penetrance associated with cardiac event risk, the current analysis has demonstrated the value of a quantitative (versus recently reported quantitative) measure of three-dimensional T-wave magnitude for risk stratification of LQT2 patients with unaffected QTc (45). To our knowledge, this is the first study to demonstrate this particular risk factor in the LQTS context.

Earlier attempts to quantify T-wave morphology in patients with LQTS involved VCG studies and standard 12-lead ECG based measures such as measured T-wave slope or T-wave center of gravity (67,68). An advantage of VCG is its ability to address three-dimensional T wave morphology while other T wave measures are bound to specific surface ECG leads. For example, the significant association with cardiac events in LQTS patients with prolonged QTc values was shown regarding the slope of the T-wave in lead V6 (68). The earlier reported VCG measures, however, have been limited to computed eigenvector values. More complicated compared to TwVM, the eigenvector values appeared to be able to differentiate symptomatic from asymptomatic LQTS patients but are difficult to conceptualize and most of the commonly used ECG systems are not able to calculate them (68). On the other hand, not all T wave morphology markers have performed as significant risk indicators in the context of LQTS with normal QTc values. The center of gravity x-axis (last 25% of T-wave) in lead I, for example, was an independent predictor of cardiac events in LQTS patients with prolonged QTc but not in unaffected mutation carriers (68). Our study demonstrated that cardiac event risk stratification was similarly determined for female patients with LQT2 (with normal QTc values) by our quantitative parameter as by the T-wave morphology as read by electrophysiologist (45). As noted in Table 2, there were more patients of female sex with TwVM of less than or equal to 0.3mV. Similar to our earlier report, the T-wave changes noted were not significant for risk stratification in males, although the number of male patients with cardiac events were generally low (45).

In LQT2 patients with normal QTc values, male sex male was associated with higher TwVM values. Lower T-wave amplitudes have been demonstrated in females after

oophorectomy with improvement once estrogen replacement was given, thus, likely sex hormonal variation affects the TwVM to some degree as well (69). Differences in corrected QT interval have also been demonstrated in healthy males and females, including menstrual cycle phase-dependent for females (69-70). However, in a population of LQTS patients with normal QTc values, it is difficult to know if subtle prolongation would have any significant effect. Otherwise, utilizing the control group of genotype negative family members allows a true risk of events within families of patients with LQT2 based on their genotype status and ECG findings. Given a similar effect on Ikr, implications for risk stratification of patients with QTc prolongation on particular medications may be of significance. The TwVM may help identify those at risk for torsades, who take QTc prolonging agents given similar T-wave morphologies and effect on Ikr. Future studies should consider this approach for risk assessment.

The TwVM predicted cardiac events in KCNH2 carriers with normal QTc values. Please see Table 14 for summary of studies.

Table 14: Diagnosis and arrhythmia prediction (or diagnostic utility) for ECG usefulness, VCG advantage and page reference within dissertation.

Diagnosis **Arrhythmia (or diagnostic utility)**	ECG usefulness	VCG advantage	Page reference
Cryptogenic stroke **Atrial fibrillation prediction**	None	**Pd/Pvm predicted atrial fibrillation develoment.**	Table 4, Figure 12, **pages 43-44.**
Hypertrophic Cardiomyopathy **Sustained VA prediction**	Complex algorith including multiple voltages in every lead give some use, but no parameter alone useful.	**Spatial peaks QRS-T angle alone predicted VA.**	Table 5, Figure 13B, **pages 46-47.**
ARVD/C **Diagnostic utility only**	50% diagnosis rate by ECG alone	**RPD angle and RtRMSQRS idenfity ARVD/C in those with normal EKG/SAECG's**	Tables 8,9, Figure 14B/C, **pages 50-52.**
KCNH2 (LQT2) with normal QTc **Cardiac Event prediction**	Qualitative morphology changes only (question reproducibility).	**Lower TwVM predicts cardiac events in female KCNH2 carriers.**	Tables 12-13, Figures 15A-C, **Pages 57-59, 61**.

Conclusion

Vectorcardiography has prognostic and significance for identifying atrial and ventricular arrhythmias in patients with cryptogenic stroke, hypertrophic cardiomyopathy and long QT syndrome, respectively. Right-precordial-directed vectorcardiography may help identify more patients with arrhythmogenic right ventricular cardiomyopathy/dysplasia than traditional ECG alone and thus if independently reproduces, may be a reasonable/cost-effective screening test**.**

Future Perspectives

We have demonstrated that atrial and ventricular depolarization, as well as ventricular repolarization measures with inclusion of the Z-axis can be helpful diagnostically and prognostically in out subpopulations. Further studies (although one already performed) may find the P-wave vector magnitude helpful for follow-up of patients after atrial fibrillation ablation procedures in patients without structural heart disease. In patients with structural heart disease, further prospective study should attempt to validate the Pwvm as a predictor of postoperative arrhythmias as well as after ablation of complex flutter.

The QRSVM and TWVM may be helpful in subpopulation of structural heart disease not mentioned in these manuscripts. The idea of a baseline quadrant for each subpopulation prior to measurable changes (including single ventricle patients) along with a narrow spatial QRS-T angle may help give an additional measure that heart failure treatment may or may not be working. Furthermore, when discussing risk of cardiomyopathy with ventricular pacing as well as optimum pacing vector during cardiac resynchronization therapy, a smaller spatial QRS-T angle as well as higher QRSVM and TWVM in a physiologic quadrant in space may also be helpful to assess in future studies.

Lastly, atrial repolarization is always a difficult measure in patients without complete heart block and thus the idea of quantifying the Tau wave in these patients to assess atrial abnormality (Tau wave vector magnitude) and direction of the Tau wave may helpful to identify recurrent atrial arrhythmias or as a non-invasive measure of atrial scar.

Financial Support

Two separate travel grants from the Swedish Heart Lung Foundation were used for international travel for conference presentation.

This work was supported by the Swedish National Health Service, Donation funds at Skåne University Hospital, Lund, Sweden, the Swedish Heart-Lung Foundation (20140734 and 20150574), the Swedish Research Council (K2010-61X-20,378-043), Region Skåne, the Freemasons Lodge of Instruction EOS in Lund, King Gustaf V and Queen Victoria's Foundation, Lund University, Sparbanksstiftelsen Färs & Frosta, the Swedish Stroke Association, and the Swedish Institute, scholarship grants from the Fulbright Commission, Maggie Stephens Foundation, and the Swedish Society of Medicine (SLS-551761)..

Acknowledgements

My PhD journey has been an awe-inspiring, at times frustrating, intellectually stimulating challenge filled with supported ambition, tough timelines, and many, many rewards. It has been my most enjoyable professional challenge.

To my advisor, **Pyotr Platonov,** I thank you for always supporting me, being an amazing mentor, and making sure I practice good scientific method for testing my theories, always. I could not have asked for better mentorship. When I met you I was looking for a mentor who not only knew vectorcardiography, who not only could fill the shoes of recently-retired mentor, but who also knew the clinical application to guide my spur of thoughts and intrigue into a formulated direction and eventual PhD defense. You are the most enthusiastic, supportive, productive (I still have no idea how you are so productive) and kind advisor I could have asked for. I have learned so much about research, electrophysiology and good mentorship from you. Thank you truly for everything.

To **Jonas Carlson**, my co-advisor. Thank you for your endless support of my equally as endless inquiries and computation assistance. You do so with such poise and are always pleasant to deal with no matter what.

To **Maria Baturova**, thank you for helping the atrial fibrillation manuscript along so much and allowing me to test a parameter on your thoroughly described subpopulation and it's been a pleasure to see your research career blossom including having the chance to catch up at international meetings.

In the same vein, thank you **Arne Lindgren, Yuri Shubik and Bertil Olsson** for supporting the atrial fibrillation manuscript and for your wonderful insights and manuscript revisions.

To **Luisa Mestroni and Sharon Graw**, thank you for allowing me as a student to come work with your team and for being so supportive and helpful with the HCM and ARVD/C projects.

To **Francesca. Brun and Anita Spezzacatene**, thank you for supporting the ARVD/C project.

To **Anneli Svensson,** my co-conspirator in all things ECG as related to ARVD/C. I can't thank you enough for allowing my co-travel along the ARVD/C train down the electrocardiographic tracks around the world to different conferences. It is

always a pleasure to see your research presented around the world and to catch-up my friend.

To **Wojciech Zareba**, thank you for allowing me to work with your amazing group and for all of your excellent and timely points in the revisions.

To **Scott McNitt**, thank you for your excellent statistical analyses and for being so available.

To **Slava Polonsky, and Spencer Rosero**, thank you for your wonderful revisions.

To **Monica and Lena**, thank you for your excellent responsiveness and keeping us all on track, even when we may have deviated far off.

To **Todd Schlegel,** thank you for your mentorship and introduction to the world of vectorcardiography. Without your support I would have never visited Sweden, presented in Lund, or kept coming back, which allowed my introduction to Dr. Platonov, and you were instrumental to my applications for cardiology fellowship.

To **Elizabeth Braunlin** and **Edward Kaplan**, thank you for the insightful reviews of this dissertation and continued cardiology mentorship.

To my beautiful wife, **Nandita,** for always supporting such intellectual undertakings and for putting up with late nights of writing and planning vacations around my PhD courses and research. Team Dr. Buggu, always.

To our amazing child, **Natalia**, way your wonderment and amazement with life always persist and may you always be as curious in life.

To my wonderful **mother**, thank you for always supporting higher education and doing everything in your power to support it, always.

To my deceased **father**, thank you for being such a wonderful support in my life academically and otherwise, we were lucky to have you while we did. I'm so glad you got to meet Natalia.

References:

1. Wilson FN, MacLeod AG, Barker PS, Johnston FD. The determination and significance of the areas of the ventricular deflections of the electrocardiogram. Am Heart J 1934; 10:46-61.
2. Grant RP. In: Grant RP, Clinical Electrocardiography: The Spatial Vector Approach, New York, McGraw-Hill Inc. 1957; 1-225.
3. Draisma HH, Schalij MJ, van der Wall EE, Swenne CA. Elucidation of the spatial ventricular gradient and its link with dispersion of repolarization. Heart Rhythm 2006; 3:1092-9.
4. Chou TC, Helm RA. Clinical Vectorcardiography. 1st edition. New York and London: Grune and Stratton;1967.
5. Cortez D, Schlegel TT, Ackerman MJ, Bos JM. ECG-derived spatial QRS-T angle is strongly associated with hypertrophic cardiomyopathy. J Electrocardiology. 2017;50:195-202.
6. Cortez D, Schlegel TT, When deriving the spatial QRS-T angle from the 12-lead electrocardiogram, which transform is more Frank: regression or inverse Dower? J Electrocardiol. 2010;43:302-309.
7. Tasic J, Zupan I. T-wave variability as a risk stratifier in patients with dilated cardiomyopathy. Pacing Clin Electrophysiol. 2009;32:S155-7.
8. Cortez D, Patell SS, Sharma N, Landeck BF, McCanta AC, Jone PN. Repolarization vector magnitude differentiates Kawasaki disease from normal children. Ann Noninvasive Electrocardiol. 2016;21:493-499.
9. Hewlett AW, Wilson FN. Course auricular fibrillation in man. Arch Intern Med; 1915;15:786-793.
10. Garrey WE. The nature of fibrillary contraction of the heart-its relation to tissue mass and form. Am J Physiol. 1914;33:397-414.
11. Moe GK, Rheinboldt WC, et al. A computer model of atrial fibrillation. Am Heart J. 1964;67:200.
12. Moe GH, Abildskov JA. Experimental and laboratory reports: atrial fibrillation as a self-sustaining arrhythmia independent of focal discharge. 1959;58:59-70.
13. Voigt N, Heijman J, Wang Q, Chiang DY, Li N, Karck M, Wehrens XHT, Nattel S, Dobrev D. Cellular and molecular mechanisms of atrial arrhythmogenesis in patients with paroxysmal atrial fibrillation. Circulation. 2014;129:145-156.
14. Friberg L, Hammar N, Pettersson H, Rosenqvist M. Increased mortality in paroxysmal atrial fibrillation: report from the Stockholm cohort-study of atrial fibrillation (SCAF). Eur Heart J. 2007;28:2346-2353.

15. Baturova MA, Lindgren A, Shubik YV, Olsson SB, Platonov PG. Atrial fibrillation in patients with ischaemic stroke in the Swedish national patient registers: how much do we miss? Europace. 2014;16:1714-1719.
16. Sanna T, Diener HC, Passman RS, Di Lazzaro V, Berstein RA, Morillo CA, et al. Cryptogenic stroke and underlying atrial fibrillation. N Engl J Med. 2014;370:2478-2486.
17. Magnani JW, Johnson VM, Sullivan LM, Gorodeski EZ, Schnabel RB, Lubitz SA, et al. Wave duration and risk of longitudinal atrial fibrillation in persons >/= 60 years old (from the Framingham heart study). Am J Cardiol. 20122;107:917-921.
18. Martinez-Selles M, Baranchuk A, Elosua R, Bayes de Luna A, O'Neal WT, Kamel H, et al. Advanced interatrial block and ischemic stroke: the atherosclerosis risk in communities study. Neurology. 2016;87:352-356.
19. Kamel H, Soliman EZ, Heckbert SR, Kronmal RA, Longstreth WT Jr, Nazarian S, Okin PM. P-wave morphology and the risk of incident ischemic stroke in the Multi-Ehtnic Study of Atherosclerosis. Stroke. 2014;45:2786-2788.
20. Cortez D, Barham W, Ruckdeschel E, Sharma N, McCanta AC, von Alvensleben J, Sauer WH, Collings KK, Kay J, Patel SS, Nguyen DT. Noninvasive predictors of perioperative atrial arrhythmias in patients with tetralogy of Fallot undergoing pulmonary valve replacement. Clin Cardiol. 2017;40:591-596.
21. Cortez D, Sharma N, Imundo JR, Cohen M. Non-invasive electrocardiographic predictors of atrial arrhythmias in patients with the Fontan palliation. J Electrocardiol. 2017;50:576-583.
22. Park JK, Park J, Uhm JS, Joung B, Lee MH, Pak HN. Low P-wave amplitude (<0.1mV) in lead I is associated with displaced inter-atrial conduction and clinical recurrence of paroxysmal atrial fibrillation after radiofrequency catheter ablation. Europace. 2016;18:384-391.
23. Almendral J, Caulier-Cisterna R, Rojo-Alvarez JL. Resetting and entrainment of reentrant arrhythmias: part I: concepts, recognition, and protocol for evaluation: surface ECG versus intracardiac recordings. Pacing Clin Electrophysiol. 2013;36:508-532.
24. Olivotto I, Girolami F, Ackerman MJ, et al. Myofilament protein gene mutation screening and outcome of patients with hypertrophic cardiomyopathy. Mayo Clin Proc. 2008;83:630-638.
25. Spirito P, Autore C, Rapezzi C, et al. Syncope and risk of sudden death in hypertrophic cardiomyopathy. Circulation. 2009;119:1703-1710. HCM2
26. Elliott PM, Poloniecki J, Dickie S, et al. Sudden death in hypertrophic cardiomyopathy: identification of high risk patients. J Am Coll Cardiol. 2000;36:2212-2218.
27. Debonnaire P, Katsanos S, Joyce E, et al. QRS fragmentation and QTc duration relate to malignant ventricular tachyarrhythmias and sudden cardiac death in patients with hypertrophic cardiomyopathy. J Cardiovasc Electrophysiol. 2015;26:547-555.

28. Ostman-Smith Ingegerd, Wisten Aase, Nylander Eva, Bratt Ewa-Lena, Granelli Anne de-Wahl, Oulhaj Abderrahim, Ljungstrom Erik. Electrocardiographic amplitudes: a new risk factor for sudden death in hypertrophic cardiomyopathy. 2010;31:439-449.
29. Potter SI, Holmqvist F, Platonov PG, et al. Detection of hypertrophic cardiomyopathy is improved when using advanced rather than strictly conventional 12-lead electrocardiogram. J Electrocardiol. 2010;43:713-718.
30. Cortez D, Sharma N, Cavanaugh J, et al. The spatial QRS-T angle outperforms the Italian and Seattle ECG-based criteria for detection of hypertrophic cardiomyopathy in pediatric patients. J Electrocardiol. 2015;48:826-833.
31. Basso C, Corrado D, FI M, Nava A, Thiene G. Arrhythmogenic right ventricular cardiomyopathy. Lancet. 2009;373:289-300.
32. FI M, McKenna WI, Shemil D, Basso C, Bauce B, Bluemke DA, Calkins H, Corrado D, Cox MG, Daubert JP, Fontaine G, Gear K, Hauer R, Nava A, Picard MH, Progonotarios N, Saffitz JE, Sanborn DM, Steinberg JS, Tandri H, Thiene G, Towbin JA, Tsatsopoulou A, Wichter T, Zareba W,. Diagnosis of right ventricular cardiomyopathy/dysplasia proposed modification of the task force criteria. Circulation. 2010;121:1533-1541.
33. Hamid MS, Normal JM, Quraishi A, Firoozi S, Thaman R, Gimeno JR, Sachdev B, Rowland E, Elliott PM, McKenna WJ: Prospective evaluation of relative for familial arrhythmogenic right ventricular cardiomyopathy/dysplasia reveals a need to broaden diagnostic criteri. J Am Coll Cardiol. 2002;40:1445-1450.
34. Kaplan SR, Gard JJ, Protonotarios N, Tsatsopoulou A, Spiliopoulou C, Anastasakis A, Squarcioni CP, McKenna WJ, Thiene G, Basso C, Brousse N, Fontaine G, Saffitz JE. Remodeling of myocyte gap junctions in arrhythmogenic right ventricular cardiomyopathy due to deletion in plakoglobin. Heart Rhythm. 2004;1:3-11.
35. Te Riele AS, James CA, Rastegar N, Bhonsale A, Murray B, Tichnell C, Jude DP, Bluemke DA, Zimmerman SL, Kamel IR, Calkins H, Tandri H. Yield of serial evaluation in at-risk family members of patients with ARVD/C. J Am Coll Cardiol. 2014;64:293-301.
36. Cortez D, Barham W, Ruckdechel E, Sharma N, McCanta AC, von Alvensleben J, Sauer WH, Collins KK, Kay J, Patel S, Nguyen DT. Noninvasive predictors of ventricular arrhythmias in patients with tetralogy of Fallot undergoing pulmonary valve replacement. JACC Clin Electrophysiol. 2017;3:162-170.
37. Kardys I, Kors JA, van der Meer IM, Hofman A, van der Kuip DA, Witteman JC. Spatial QRS-T angle predicts cardiac death in a general population. Eur Heart J. 2003;24:1357–64. 9.
38. Kors JA, Kardys I, van der Meer IM, van Herpen G, Hofman A, van der Kuip DA, Witteman JC. Spatial QRS-T angle as a risk indicator of cardiac death in an elderly population. J Electrocardiol. 2003;36(Suppl):113–4. 10.
39. Yamazaki T, Froelicher VF, Myers J, Chun S. Wang pl: spatial QRS-T angle predicts cardiac death in a clinical population. Heart Rhythm. 2005;2:73–78.16.

40. Schwartz PJ, Stamba-Badiale M, Crotti L, et al. Prevalence of the congenital long-QT syndrome. Circulation. 2009;120:1761-1767.
41. El-Sherif N, Turitto G, Boutjdir M. Congenital Long QT syndrome and torsades de pointes. Ann Noninvasive Electrocardiol. 2017;22:e12481.
42. Vincent GM, Timothy KW, Leppert M, Keating M. The spectrum of symptoms and QT intervals in carriers of the gene for the long-QT syndrome. N Engl J Med. 1992;327:846-852.
43. Vink AS, Neumann B, Lieve KVV, et al. Determination and interpretation of the QT Interval: comprehensive analysis of a large cohort of long QT syndrome patients and controls. Circulation. 2018;138:2345-2358.
44. Monnig G, Eckardt L, Wedekind H, Haverkamp W, Gerss J, Milberg P, Wasmer K, Kirchhof P, Assmann G, Gunter B, Schulze-Bahr E. Electrocardiographic risk stratification in families with congenital long QT syndrome. Eur Heart J. 2006;27:2074-2080.
45. Platonov PG, McNitt S, Polonsky B, et al. Risk stratification of type 2 long-QT syndrome mutation carriers with normal QTc interval: the value of sex, T-wave morphology and mutation type. Circ Arrhythm Electrophysiol. 2018;11e005918.
46. Cortez D, Bos JM, Ackerman MJ. Vectorcardiography identifies patients with electrocardiographically concealed long QT syndrome. J Heart Rhythm. 2017;14:894-899.
47. Baturova MA, Lindgren A, Carlson J, Shubik YV, Olsson SB, Platonov PG. Predictors of new onset atrial fibrillation during 10-year follow-up after first-ever ischemic stroke. Int J Cardiol. 2015;199:48-52.
48. Zareba W, Moss AJ, Locati EH, et al. International Long QT syndrome Registry. Modulating effects of age and gender on the clinical course of long QT syndrome by genotype. J Am Coll Cardiol. 2003;43:103-109.
49. Kutylfa V, Dalmoe UA, McNitt S, et al. Clinical aspects of the three major genetic forms of long QT syndrome (LQT1, LQT2,LQT3). Ann Noninvasive Electrocardiol. 2018;23e12537
50. Macfarlane PW, Device B, Clark E. The University of Glasgow (Uni-G) ECG analysis program. Comput Cardiol. 2005;32:451-454.
51. Kors JA, van Herpen C, Sitig AC, van Bemmel JH. Reconstruction of the Frank vectorcardiogram from standard electrocardiographic leads. Eur Heart J. 1990;11:1083-1092.
52. Cortez D, Sharma N, Devers C, Devers E, Schlegel TT. Visual transform applications for estimating the spatial QRS-T angle from the conventional 12-lead ECG's: Kors is still most Frank. J Electrocardiol. 2014;47:12-19.
53. Camm AJ, Kirchhof P, Lip P, Lip GY, Schotten U, Savelieva I, Ernst S, et al. Guidelines for the management of atrial fibrillation of the European Society of Cardiology (ESC). Eur Heart J. 2010;31:2369-2429
54. Zuo ML, Liu S, Chan KH, Lau KK, Chong BH, Lam KF, et al. The CHADS2 and CHA2DS2-VAsc scores predict new occurrence of atrial fibrillation and ischemic stroke. J Interv Card Electrophysiol. 2013;37:47-54.

55. Heeringa J, van der Kuip DA, Hofman A, Kors JA, van Herpen G, Stricker BH, et al. Prevalence, incidence and lifetime risk of atrial fibrillation: the Rotterdam study. Eur Heart J. 2006;27:949-953.
56. Ziegler PD, Glotzer TV, Daoud EG, Singer MD, Ezekowitz MD, Hoyt RH, et al. Incidence of newly detected atrial arrhythmias via implantable devices in patients with history of thromboembolic events. Stroke. 2010;41:256-260.
57. Ziegler PD, Glotzer TV, Daoud EG, Singer MD, Ezekowitz MD, Hoyt RH, et al. Detection of previously undiagnosed atrial fibrillation in patients with stroke risk factors and usefulness of continuous monitoring in primary stroke prevention. Am J Cardiol. 2012;110:309-314.
58. Giaroni S, Cuenoud I, Bloch A. Clinical study to investigate the predictive parameters for the onset of atrial fibrillation in patients with essential hypertension. Am Heart J. 2000;139:814-819.
59. Nakatani Y, Sakamoto T, Yamaguchi Y, Tsujino Y, Kataoka N, Kinugawa K. P-wave vector magnitude predicts left atrial low-voltage area in patients with paroxysmal atrial fibrillation. J Electrocardiology. 2020;59:35-40.
60. Nakatani Y, Sakamoto T, Yamaguchi Y, Tsujino Y, Kataoka N, Kinugawa K. P-wave vector magnitude predicts recurrence of atrial fibrillation after catheter ablation in patients with persistent atrial fibrillation. Ann Noninvasive Electrocardiol. 2019;24:e12646.
61. Triola B, Olson MB, Reis SE, et al. Electrocardiographic predictors of cardiovascular outcome in women: the National Heart, Lung, and Blood Institute-sponsored Women's Ischemia Syndrome Evaluation study. J Am Coll Cardiol. 2005;46:51-56.
62. Voulgari C, Tentolouris N, Moyssakis I, et al. Spatial QRS-T angle: association with diabetes and left ventricular performance. Eur J Clin Invest. 2006;36:608-613.
63. Rautaharju PM, Kooperberg C, Larson JC et al. Electrocardiographic predictors of incident congestive heart failure and all-cause mortality in postmenopausal women: the Women's Health Initiative. Circulation. 2006;113:481-489.
64. Rautaharju PM, Princas RJ, Wood J. Electrocardiographic predictors of new-onset heart failure in men and women free of coronary heart disease (from the Atherosclerosis in Communities [ARIC] Study). Am J Cardiol. 2007;100:1437-1441.
65. Shi B, Ferrier KA, Sasse A, et al. Correlation between vectorcardiographic measures and cardiac magnetic resonance imaging of the left ventricle in implantable cardioverter defibrillator population. J Electrocardiol. 2014;47:52-58.
66. Tran TV, Cortez D. Clinical application of the QRS-T angle for the prediction of ventricular arrhythmias in patients with the Fontan palliation. Pediatr Cardiol. 2017;38:1049-1056.
67. Priori SG, Mortara DW, Napolitano C, et al. Evaluation of the spatial aspects of the T-wave complexity in the Long-QT syndrome. Circulation. 1997;96:3006-3012.

68. Sugrue A, Noseworthy PA, Kremen V, et al. Identification of concealed and manifest long QT syndrome using a novel T wave analysis program. Circ Arrhythm Electrophysiol. 2016;9:e003830.
69. De Leo V, la Marca A, Agricola E, Morgante G, Mondillo S, Setacci C. Resting ECG is modified after oophorectomy and regresses with estrogen replacement therapy in premenopausal women. Maturitas. 2000;36:43-47.
70. Burke JH, Ehlert FA, Kruse JT, Parker MA, Goldberger JJ. Gender-specific differences in QT interval and the effect of the autonomic tone and menstrual cycle in healthy adults. Am J Cardiol. 1997;79:178-181.

Paper I

Cortez et al. BMC Cardiovascular Disorders (2017) 17:200
DOI 10.1186/s12872-017-0631-1

BMC Cardiovascular Disorders

RESEARCH ARTICLE Open Access

Atrial time and voltage dispersion are both needed to predict new-onset atrial fibrillation in ischemic stroke patients

Daniel Cortez[1,2*†], Maria Baturova[1,3,4†], Arne Lindgren[5,6], Jonas Carlson[1], Yuri V. Shubik[4], Bertil Olsson[1] and Pyotr G. Platonov[1,7]

Abstract

Background: Atrial fibrillation (AF) is a known risk factor for ischemic stroke. Electrocardiographic predictors of AF in population studies such as the Framingham Heart Study, as well as in hypertensive patients have demonstrated a predictive value of the P-wave duration for development of AF. QRS vector magnitude has had a predictive value in ventricular arrhythmia development. We aimed to assess the value of the three-dimensional P-wave vector magnitude and its relationship to P-wave duration for prediction of new-onset AF after ischemic stroke.

Methods: First-ever ischemic stroke patients without AF at inclusion in the Lund Stroke Register were included. Measurements of P wave duration (Pd), QRS duration, corrected QT interval, and PQ interval were performed automatically using the University of Glasgow 12-lead ECG analysis algorithm. The P-wave vector magnitude (Pvm) was calculated automatically as the square root of the sum of the squared P-wave magnitudes in leads V6, II and one half of the P-wave amplitude in V2 ($\sqrt{PV6^2 + PII^2 + (0.5*PV2)^2}$), based on the P-wave magnitude (Pvm) as defined by the visually transformed Kors' Quasi-orthogonal method.

Results: The median age was 73 (IQR 63–80) years at stroke onset (135 males, 92 females). Multivariate predictors of new-onset atrial fibrillation included age > 65 years, hypertension, and Pd/Pvm. A cut-off value of 870 ms/mV gave sensitivity, specificity, positive and negative predictive values of 51, 79, 30 and 87%, respectively. The Pd/Pvm was the only ECG predictor of AF with a significant multivariate hazard ratio of 2.02 (95% CI 1.18 to 3.46, $p = 0.010$).

Conclusion: P-wave dispersion as measured by the Pd/Pvm was the only ECG parameter measured which independently predicted subsequent AF identification in a cohort of stroke patients. Further prospective studies in larger cohorts are needed to validate its clinical usefulness.

Keywords: Atrial fibrillation, Ischemic stroke, P-wave vector magnitude, P-wave duration

Background

Atrial fibrillation (AF) is a known risk factor for ischemic stroke [1]. A high prevalence of AF is noted in ischemic stroke patients [1]. The impact of ischemic stroke on the risk of subsequent development of AF is only beginning to become clear [2, 3]. Information on development of new AF in ischemic stroke patients using ECG monitoring has been seldom reported until recently [4–6]. Clinical cardiovascular risk scoring tools such as the $CHADS_2$ and CHA_2DS_2-VASc have demonstrated association with development of first-ever AF during 2-year and 10-year follow-up time frames in recent studies [7–9].

Electrocardiographic predictors of AF in populations such as the Framingham Heart Study, as well as in hypertensive patients have demonstrated a predictive value of the p-wave duration for development of AF [10, 11]. This parameter, however, was not predictive in ischemic stroke patients during a 10-year follow-up [9]. However P-wave axis change has not been assessed nor has P-wave vector

* Correspondence: dr.danielcortez@gmail.com
†Equal contributors
[1]Department of Cardiology, Clinical Sciences, Lund University, Lund, Sweden
[2]Electrophysiology Department, Penn State Milton S. Hershey Medical Center, Hershey, USA
Full list of author information is available at the end of the article

magnitude in this population, as the P-wave axis normally corresponds to 60 degrees with similar variability in the frontal plane to the QRS axis with more variability in the transverse and sagittal planes [12]. In regards to voltage assessment, the P-wave terminal force in V_1 of >0.04 mm/s (PTFV1) has also not reliably been predictive of AF in this same population [8]. Recently, another P-wave time measure, the prolongation of the P-wave duration (Pd) >120 ms along with biphasic morphology in the inferior leads or in aVF and III along with notched p-wave in II, known as advanced inter-atrial block, has been shown to have predictive value for development of atrial fibrillation in ischemic stroke patients [13]. In a 10-year follow-up in ischemic stroke patients, the QRS duration (QRSd) has only had very modest results for predicting AF in ischemic stroke patients [8]. Thus, to date only one useful time-dependent independent 12-lead electrocardiographic predictor for AF in ischemic stroke patients has shown its value (advanced inter-atrial block), whereas no voltage-dependent measures have been tested.

Vectorcardiographic (VCG) principles (3-dimensional parameters, derived from a 12-lead electrocardiogram) have provided additional diagnostic [14, 15] and prognostic [16–20] information, building upon the traditional 12-lead ECG. Dispersion of ventricular depolarization, as measured by the QRS vector magnitude has had predictive value in ventricular arrhythmia development pre-operatively and peri-operatively in patients with congenital heart disease, independent of QRSd [21, 22]. Furthermore, a low P-wave amplitude in lead I is associated with displaced conduction and clinical recurrence of paroxysmal AF post-radiofrequency ablation [23]. A low 3-dimensional P-wave vector magnitude (Pvm), however, has not been assessed in any known cohorts based on the 12-lead ECG or otherwise. Also, this potentially useful tool, which gives the magnitude of the p-wave in 3-dimensional space has yet to be employed for the prediction of AF. Given the relationship between P-wave amplitude and ventricular depolarization duration, further assessment into time-duration and amplitude interrelationship is warranted. To date no relationship of atrial voltage to time duration have been assessed for prediction of AF. Furthermore, P-wave time duration per voltage assessment has therefore also not been assessed in predicting AF in ischemic stroke patients or otherwise.

We aimed to assess the value of the three-dimensional P-wave vector magnitude (Pvm) and its relationship to P-wave duration for prediction of new-onset AF after ischemic stroke.

Methods

Study cohort

The original study population originated from the Lund Stroke Register (LSR) and comprised 336 consecutive first-ever ischemic stroke patients included in LSR between March 1, 2001 and February 28, 2002 as it had been described previously [8]. At enrollment in the LSR, 109 ischemic stroke patients had AF detected by ECG screening, medical records review or record linkage with the Swedish National Patient Register as described previously [8] and were excluded from this analysis. All patients enrolled signed written consents. The present study sample therefore comprised of 227 first-ever ischemic stroke patients (median age 73 years at stroke onset (interquartile range 25–75% (IQR 63–80), 92 females) without known AF at inclusion in the LSR. We followed up all study subjects until October 17, 2011, the date when the information from the Swedish National Patient Register was obtained. Informed consent was obtained from all participants included in the LSR. The study was approved by the Lund University Ethics Committee.

Baseline ECG and clinical assessment

Medical records of all study subjects were analyzed for history of cardiac failure, hypertension, diabetes mellitus, transient ischemic attack (TIA) and ischemic heart disease at baseline. Cardiovascular risk profiles measured by $CHADS_2$ and CHA_2DS_2-VASc scales [8] were evaluated for the time of inclusion in the LSR in the acute phase when the index ischemic stroke had just occurred.

Sinus rhythm ECG recordings obtained at stroke admission with median time from stroke event to ECG registration 0 day (IQR 0–2 days) were extracted from the regional electronic database (GE MUSE, GE Healthcare, MegaCare) and processed offline. The measurements of Pd, QRSd, corrected QT interval (QTc), PQ interval were performed automatically using the University of Glasgow 12-lead ECG analysis algorithm [24]. The Pvm was calculated automatically as the square root of the sum of the squared P-wave magnitudes in leads V6, II and one half of the P-wave amplitude in V2 ($\sqrt{PV6^2 + PII^2 + (0.5^*PV2)^2}$), based on the P-wave magnitude as defined by the visually transformed Kors' Quasi-orthogonal method [25, 26]. Please see Figs. 1 and 2. The Pd/Pvm was defined as the Pduration/Pvm and was calculated from the data above automatically utilizing MATLAB R2013b (The MathWorks, Inc., Natick, MA, USA) for Linux.

P wave duration, QRS duration, corrected QT interval and PQ interval were measured in ms. Corrected QT was calculated using Bazett's formula: QTc = QT/√R-R interval. Pvm was calculated in microvolts. Negative P-wave terminal force in lead V_1 was also calculated as described previously [8].

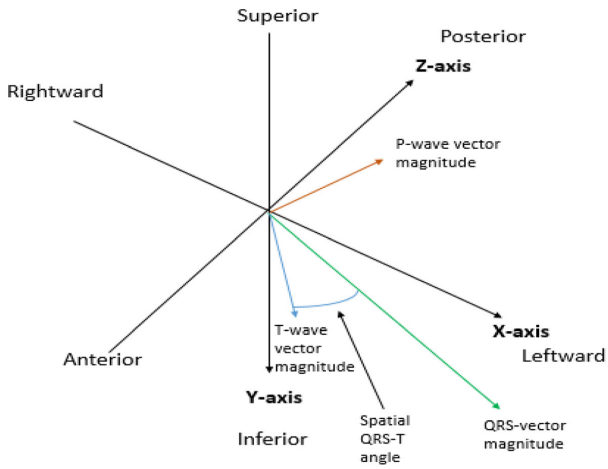

Fig. 1 Example of determining the P wave vector magnitude (Pvm) along with QRS and T wave vector magnitudes

Ascertainment of new-onset AF during follow-up

New onset AF was assessed during the follow-up period starting from the date of enrollment until the end of follow-up or date of death. AF documentation was based on information obtained from the regional electronic ECG archive which contains all ECG recordings taken in the hospital's local catchment area and also by linkage with national registers: the Swedish Patient Register and the Swedish Causes of Death Register. All available ECG recordings for all study subjects from the date of enrollment until the end of follow-up in 2011 were reviewed for the presence of AF by a trained cardiologist (MB). On surface ECG, AF was defined as a rhythm disorder which lasted sufficiently long for a 12-lead ECG to be recorded, with irregular RR intervals, indistinct P waves and atrial cycle length of 200 ms where distinct atrial activity was visible on surface ECG [27].

The Swedish Patient Register is administered by the Swedish National Board of Health and Welfare and includes data on main and secondary diagnoses at

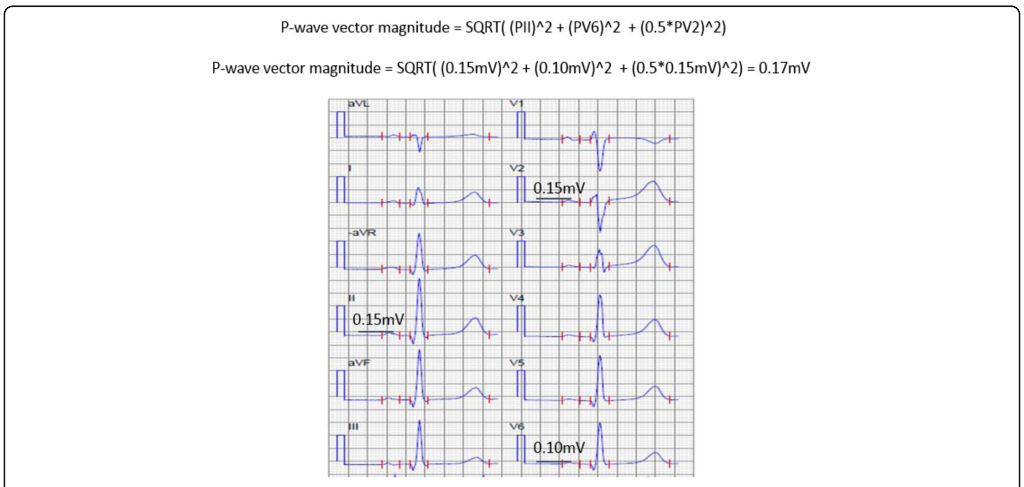

Fig. 2 Example of calculation of the P wave vector magnitude (Pvm)

discharge from all public hospitals in Sweden starting in 1987. The register uses International Classification of Disease (ICD) codes with the 10th edition (ICD-10) used from 1997 and until today. The Cause of Death Register is also provided by the Swedish National Board of Health and Welfare and contains information (since 1961) from death records, including underlying causes of death and up to 20 contributory causes of death coded to the current edition (ICD-10). The presence of the ICD-10 code I48 in the Swedish national registers identified AF diagnosis with high specificity and modest sensitivity as we showed recently in a validation study on patients with ischemic stroke enrolled in the LSR [2].

Statistical methods

Baseline clinical characteristics were compared between stroke patients who developed AF during follow-up and those who remained AF-free using chi-square or Fisher's exact test for categorical variables and Student's t-test versus Mann–Whitney U-testing, as appropriate, for continuous variables with an approximately normal distribution or alternatively non-parametric tests, as appropriate. Parametric data are presented as mean ± standard deviation, whereas non-parametric data are presented as median (interquartile range). For log linearity, each variable was categorized into quartiles where applicable and plotted to assess linearity of the quartiles. The primary outcome in this study was defined as occurrence of AF. Subjects who did not develop AF during the 10-year follow-up were censored at time of death or at end of follow-up.

Cox proportional hazard regression models were used to estimate the adjusted hazard ratios (HR) and their 95% confidence intervals (CI) of new onset AF associated with clinical and ECG covariates. Univariate Cox regression analyses were performed separately for each component of CHA_2DS_2-VASc score and for each ECG parameter. Clinical factors and ECG parameters significantly associated with new onset AF in the univariate analyses were included in a stepwise regression analysis with backward elimination. Our Cox model was adjusted for known significant clinical covariates (known to predispose to AF or known to have a relationship to the Pd/Pvm). The Kaplan-Meier product-limit method was used to generate a survival curve indicating new onset AF during 10-year follow-up after enrollment in LSR. A Kaplan-Meier curve was also used to demonstrate discernible differences at an optimum cut-off for the Pd/Pvm in identifying incidence of new-onset atrial fibrillation. Optimum cut-off was assessed by the receiver operating characteristic (ROC) curve. Cut-off *p*-values at 0.10 or less were used as entry cut-off values for multivariate analyses. *P* values of 0.05 were considered significant. All analyses were performed using SPSS Statistics 20 (SPSS Inc., Chicago, Illinois, USA). No reproducibility testing was performed given our fully automatic data processing.

Results

Baseline characteristics of all study subjects at time of enrollment are presented in Table 1. At baseline 227 were fulfilled inclusion criteria and were included in the analysis.

Table 1 Baseline clinical characteristics of stroke patients without or with subsequent development of atrial fibrillation

Parameter	Stroke (N=227)	No AF (n=188)	AF (n=39)	*P*-value
Age, years	73 [63 to 80]	73 [61 to 80]	73 [69 to 80]	0.072
Male sex (%)	135 (59%)	114 (61%)	21 (54%)	0.693
Heart Failure	7 (3%)	4 (2.1%)	3 (7.7%)	0.218
Hypertension (%)	130 (57%)	101 (53.7%)	29 (74.4%)	0.012
Diabetes (%)	35 (15%)	26 (13.8%)	9 (23.7%)	0.210
Vascular disease (%)	95 (42%)	77 (41.0%)	18 (46.2%)	0.560
TIA (%)	49 (22%)	45 (23.9%)	4 (10.3%)	<0.001
New-onset atrial fibrillation	39 (17%)	0 (0.0%)	39 (100.0%)	<0.001
Median time to AF onset/end follow-up	3.2 [1.3 to 5.9])	9.7 [4.3 to 10.1]	2.9 [1.2 to 6.4]	<0.001
P duration	116 [106 to 126]	116 [106 to 122]	118 [111 to 131]	0.224
QRSd	78 [68 to 90]	86 [78 to 94]	88 [75 to 99]	0.880
Pvm	0.16 [0.13 to 0.20]	0.16 [0.13 to 0.20]	0.13 [0.11 to 0.19]	0.006
P duration/Pvm	711 [560 to 893]	694 [547 to 862]	801 [586 to 1046]	0.009

Data presented as Median [Interquartile range]
All patients had no evidence of AF in the immediate acute phase after stroke onset
AF atrial fibrillation, *TIA* transient ischemic attack, *QRSd* QRS duration, *Pvm* P-wave vector magnitude

Detection of new onset atrial fibrillation (10-year follow-up)

The median time for follow-up was 9.4 years [IQR 6.1–9.9], 115 (51%) stroke patients died. Complete follow-up data were available for 112 (49%) of the stroke patients. In total, 2588 ECG's were reviewed with a median number of ECG recordings per person of four (IQR 1–9) [8]. New onset atrial fibrillation was found in 39 (17%) of the stroke patients (Hazard ratio 1.49, 95% confidence interval 0.09–2.35, p = 0.121) as previously reported [2, 8]. The median time to AF onset was 3.2 (IQR 1.3 to 5.9) years.

ECG and clinical predictors of new onset atrial fibrillation after ischemic stroke

On ECGs obtained in the acute phase after stroke onset, the median QRSd was 96 ms (IQR 88–108), the median duration of the P wave was 116 ms (IQR 106–124), and the median PQ interval was 169 ms (IQR 152–188). The median Pvm was 0.15 mV (IQR 0.13 to 0.20) and the median Pd/Pvm was 737 ms/mV (IQR 581 to 955).

Table 2 depicts univariate and multivariate predictors of new-onset atrial fibrillation in stroke patients. Significant univariate predictors of new-onset atrial fibrillation included age > 65 years, presence of hypertension, heart failure, QRSd, and Pd/Pvm (Table 2). No standard ECG characteristics including P-wave duration, QRS duration or negative P-wave terminal force in lead V1 or QRSd were significantly associated with new-onset AF during follow-up. Independent predictors of new-onset atrial fibrillation were instead Pvm/Pd and those parameters considered a moderator of Pvm/Pd including age > 65 years, hypertension, and heart failure (Table 2) [28]. The C-statistic for the model was 0.71 (95% CI 0.61 to 0.82).

The area under the ROC curve value for the Pd/Pvm was 0.63 (0.55 to 0.71, p = 0.013). At an optimal cut-off value of 870 ms/mV the sensitivity, specificity, positive and negative predictive values were 51, 79, 40 and 89%, respectively (optimized for highest negative predictive value given the ECG the screening value of the ECG). A Kaplan-Meier curve based on this cut-off value (Fig. 3) provided a p-value of <0.001 for differentiation between survival curves for the risk of development AF during 10-year follow-up after first-ever ischemic stroke. Subanalyses of patients who do not meet any of the independent predictors (ie. without hypertension, who were less than 65 years of age, did not have heart failure and had a Pd/Pvm of less than 870 ms/mV), did had a 93.2% chance of not developing atrial fibrillation. The positive predictive value for development of AF was 27.9% in a patient without hypertension, who were less than 65 years of age and did not have heart failure, but with a Pd/Pvm of less than 870 ms/mV.

Discussion

Our study demonstrates that a measure of P-wave dispersion by duration and voltage assessment from the standard 12-lead ECG, taken during hospital admission for ischemic stroke, in the form of Pd/Pvm can predict new-onset AF during follow-up while neither P-wave duration nor P-wave terminal force in lead V_1 were significantly associated with subsequent AF occurrence. The relation of Pd/Pvm to new-onset AF remained independent after adjustment for other clinical parameters.

Presence of AF

As previously reported, by the end of the 10-year follow-up AF was detected in 15% of our initially AF-free

Table 2 Clinical electrocardiographic predictors of new-onset atrial fibrillation during 10-year follow-up of ischemic stroke patients without known atrial fibrillation at their index stroke

Univariate Cox regression analysis			Multivariate Cox regression analysis	
Parameter	Hazard ratio (95% CI)	*P*-value	Hazard ratio (95% CI)	*P*-value
Age > 65 years	2.88 (1.20 to 6.89)	0.018	1.04 (1.02 to 1.07)	0.001
Hypertension	3.45 (1.40 to 3.49)	0.007	3.21 (1.35 to 7.67)	0.008
Heart failure	4.04 (1.24–13.18)	0.020	2.72 (1.08 to 6.83)	0.033
Diabetes	1.83 (0.87 to 3.87)	0.111		
Male gender	1.22 (0.50 to 1.59)	0.459		
Stroke group	1.391 (0.855 to 2.263)	0.184		
P duration	1.02 (0.96 to 1.05)	0.105		
QRS duration	1.02 (1.00 to 1.04)	0.025	1.01 (1.00 to 1.02)	0.354
PQ interval	1.00 (0.99 to 1.01)	0.966		
Pvm	1.001 (0.994 to 1.009)	0.751		
P duration/Pvm	2.320 (1.367 to 3.938)	0.002	2.02 (1.18 to 3.46)	0.010
P terminal force V1	1.00 (95% CI 1.00–1.00)	0.142		

Pvm p-wave vector magnitude, *95% CI* 95% confidence interval

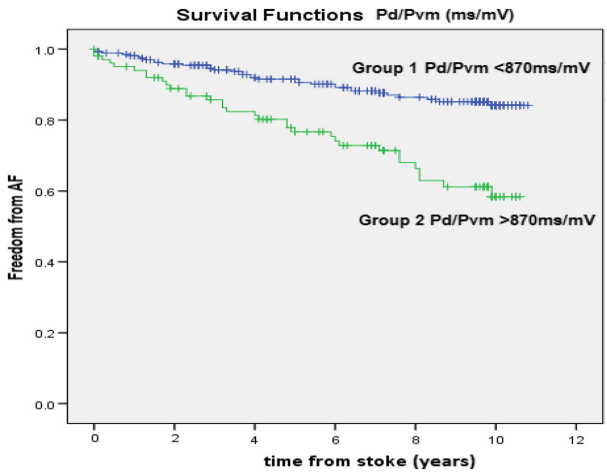

Fig. 3 Kaplan-Meijer survival curve from stroke onset to atrial fibrillation detection for p wave duration/p-wave vector magnitude (Pd/Pvm) at a cut-off of 870 milliseconds/millivolt (ms/mV), log rank *p*-value <0.001

subjects, which corresponds to the reported AF incidence for an aging population of 18% in those older than 85 years by the end of a 7-year follow-up and 17% of those 65–74 years by the end of a 6-year follow-up [9, 29]. Compared with studies based on only ECG screening, studies that employed implantable devices generally have shown higher AF detection rates - of up to 28–30% in patients with ischemic stroke or TIA, as well as in those with risk factors for ischemic stroke [30–32].

Clinical parameters

We previously reported that in the same cohort age > 65 years, presence of hypertension or heart failure showed a univariate as well as multivariate predictive relation to subsequent AF onset during a 10-year follow-up period [8]. Clinical parameters we found significant in previous analyses were used in the Cox modeling in the current analysis [8, 28].

P-wave duration divided by 3-dimensional p-wave vector magnitude (Pd/Pvm)

Previous literature mostly has focused on P-wave duration as a predictive tool for new-onset atrial fibrillation with some success in non-ischemic stroke populations [10, 11]. Although in the subgroup of those <60 years of age, the overall P-wave duration yielded a non-significant HR (1.15, 95% CI 0.90 to 1.47). It has also been shown that maximum P wave duration at the upper fifth percentile was associated with long-term AF risk in an elderly community-based cohort [11]. In hypertensive patients the P-wave duration independently predicted the development of new-onset atrial fibrillation [11]. However, in a recent publication of our cohort, no significant predictive value was found for the P-wave duration as a predictor for new-onset AF [8]. In another study, prolonged P-wave duration and advanced interatrial block in particular have shown an association with AF [13]. Furthermore, PTFV1 was not found to be a reproducibly significant predictor of AF [9]. In patients with recurrent atrial fibrillation after catheter ablation, low voltage in lead I (<0.01 mV) was associated with recurrence of AF [21]. Our results demonstrate that atrial voltage dispersion, as measured by Pvm is not in itself alone associated with the development of AF. However, our study is the first to show that atrial time duration versus voltage dispersion (Pd/Pvm) is a potentially clinically useful predictive measure which can be obtained by the ECG alone. Pvm has also shown predictive value for atrial arrhythmias in patients with congenital heart disease, and in particular tetralogy of Fallot patients undergoing pulmonary valve replacements [28]. In this same study Pvm inversely correlated with higher right atrial pressure, left and right ventricular ejection fractions, QRSd, and older age [28]. In the above publication Pvm was predictive of organized right atrial arrhythmias (intra-atrial re-entrant tachycardia and typical flutter), thus in the more disorganized left atrial arrhythmia (AF), it appears time dispersion across the left atrium must also be taken into account. A risk score based on the above parameters might be helpful in ruling out those at risk for atrial fibrillation, and furthermore can be automatically calculated, however further reproducibility with

other ECG systems and automated methods would be required. Our study also demonstrated a high specificity and negative predictive value for identification of AF in ischemic stroke patients but with low sensitivity and positive predictive values. This demonstrates that in our cohort although those who develop AF cannot necessarily all be identified (sensitivity 51%) and the value of a Pd/Pvm > 870 ms/mV does not necessarily identify all of those who may develop AF (positive predictive value 30%). Those who do not develop AF, however, are going to be those who have a Pd/Pvm <870 ms/mV. Thus if effectively reproduced independently, this may be a reasonable and cost-effective screening test for those at risk for developing AF.

Limitations

This study was retrospective and did not use a prespecified AF screening protocol, thus the number of ECG's available during follow-up analysis was lower in subjects without detected AF. This may represent an underestimation of AF in patients with asymptomatic AF, given their lack of need to contact health care providers. Also, the ECG search utilized in this study was limited to Southern Sweden's Skania region, thus other ECG's possibly performed outside of the Skania region were unavailable for review. Therefore, if a patient was mobile and sought healthcare elsewhere, these ECG's would not be included. Other prolonged data monitoring such as via implantable devices (e.g. loop recorders) were not available for data analysis. Our data was, however obtained via linkage with the Swedish Patient Register, which for each specific treatment occasion contains up to 20 contributory diagnoses per patient, suggesting that if observed, AF would have been registered in the Patient register. Also, during a 10-year follow-up after stroke a number of confounders such as inability to detect all episodes of AF and lack of reported events such as transient ischemic attacks or other parameters in the CHA_2DS_2-VASc score calculation as well as degree of heart failure, which may not have been taken into account. This is also inherently a limitation of Registry data along with lack of atrial size/volume data, which have been shown to be predictors of atrial fibrillation [32, 33]. Furthermore, the Cox model assumes constant effect over time, which may not be complete accurate for every single parameter. Our results need to be viewed in light of these possible confounders. Also the analysis was a post-hoc analysis performed on a prospectively this prospectively enrolled cohort, thus limitations exist regarding assessment of Pd/Pvm compared to other parameters.

Conclusion

Atrial time dispersion over voltage magnitude, as measured by the Pd/Pvm, appears to have some usefulness in risk stratifying stroke patients for risk of subsequent AF in the post-hoc analysis of an observational study on ischemic stroke survivors. It was the only ECG parameter measured which predicted new-onset AF independently from the clinical covariates. Further prospective studies in larger cohorts, including investigation regarding non-invasive imaging parameter directly compared, are needed to validate its clinical usefulness, however, Pd/Pvm may be worth further investigation for potential usefulness as a relatively simple and easily available clinical tool for AF prediction after ischemic stroke.

Abbreviations

AF: Atrial fibrillation; ECG: Electrocardiogram; ICD: Internal cardiac defibrillator; LSR: Lund Stroke Register; ms: millisecond; mV: millivolt; Pd: P-wave duration (milliseconds); PTFV1: P-wave terminal force in V_1 of >0.04 mm/s; Pvm: P-wave vector magnitude (millivolts); QRSd: QRS duration; ROC: Receiver operating characteristic curve; TIA: Transient ischemic attack

Acknowledgements

Not applicable.

Funding

This work was supported by the Swedish National Health Service, Donation funds at Skåne University Hospital, Lund, Sweden, the Swedish Heart-Lung Foundation (20140734), the Swedish Research Council (K2010-61X-20,378-04-3), Region Skåne, the Freemasons Lodge of Instruction EOS in Lund, King Gustaf V and Queen Victoria's Foundation, Lund University, Sparbanksstiftelsen Färs & Frosta, the Swedish Stroke Association, and the Swedish Institute.

Availability of data and materials

The data supporting the results and conclusions of the survey might be available from the corresponding author on reasonable request.

Authors' contributions

DC made substantial contributions to data conception, design, analysis and interpretation; he wrote the manuscript. MB was responsible for the data collection, and was thoroughly involved in drafting the manuscript. JC was responsible for the data, analysis and interpretation; he was involved in drafting the manuscript. AL made substantial contributions to conception, design, analysis and interpretation of data; was responsible for manuscript revision. YS was responsible for manuscript revision. BO made substantial contributions to conception, design, and manuscript revision. PP made substantial contributions to conception, design, data acquisition, analysis and interpretation; he was involved in drafting and revising the manuscript; agreed to be accountable for all aspects of work in ensuring that any questions related to accuracy or integrity are appropriately investigated and resolved. All authors read and approved the final manuscript.

Ethics approval and consent to participate

This study was part of the Lund Stroke Register and thus all patients were consented and the study was approved by the Internal Review Board of Lund University and Skane Hospital and conformed to the Declaration of Helsinki and which included analysis of ECG variables.

Consent for publication

Not applicable.

Competing interests

The authors declare that they have no competing interests.

Publisher's Note

Author details
[1]Department of Cardiology, Clinical Sciences, Lund University, Lund, Sweden. [2]Electrophysiology Department, Penn State Milton S. Hershey Medical Center, Hershey, USA. [3]St. Petersburg University Clinic, St. Petersburg, Russia. [4]Cardiology Research, Clinical and Educational Center, St. Petersburg State University, St. Petersburg, Russia. [5]Department of Neurology and Rehabilitation Medicine, Skane University Hospital, Lund, Sweden. [6]Department of Clinical Sciences Lund, Neurology, Lund University, Lund, Sweden. [7]Arrhythmia Clinic, Skåne University Hospital, Lund, Sweden.

Received: 20 April 2017 Accepted: 14 July 2017
Published online: 24 July 2017

References

1. Friberg L, Hammar N, Pettersson H, Rosenqvist M. Increased mortality in paroxysmal atrial fibrillation: report from the Stockholm cohort-study of atrial fibrillation (SCAF). Eur Heart J. 2007;28:2346–53.
2. Baturova MA, Lindgren A, Shubik YV, Olsson SB, Platonov PG. Atrial fibrillation in patients with ischaemic stroke in the Swedish national patient registers: how much do we miss? Europace. 2014;16:1714–9.
3. Sanna T, Diener HC, Passman RS, Di Lazzaro V, Berstein RA, Morillo CA, et al. Cryptogenic stroke and underlying atrial fibrillation. N Engl J Med. 2014;370:2478–86.
4. Jabaudon D, Sztajzel J, Sievert K, Landis T, Sztajzel R. Usefulness of ambulatory 7-day ECG monitoring for the detection of atrial fibrillation and flutter after acute stroke and transient ischemic attack. Stroke. 2004;35(7):1647–51.
5. Stahrenberg R, Weber-Kruger M, Seegers J, Edelmann F, Lahno R, Haase B, et al. Enhanced detection of paroxysmal atrial fibrillation by early and prolonged continuous Holter monitoring in patients with cerebral ischemia presenting in sinus rhythm. Stroke. 2010;41:2884–8.
6. Brachmann J, Morillo CA, Sanna T, Di Lazzaro V, Diener HC, Bernstein RA, et al. Uncovering atrial fibrillation beyond short-term monitoring in cryptogenic stroke patients: three-year results from the cryptogenic stroke and underlying atrial fibrillation trial. Circ Arrhythm Electrophysiol. 2016;9:1.
7. Henriksson KM, Farahmand B, Asberg S, Terent A, Edvardsson N. First-ever atrial fibrillation documented after hemorrhagic or ischemic stroke: the role of the CHADS(2) score at the time of stroke. Clin Cardiol. 2011;34:309–16.
8. Baturova MA, Lindgren A, Calrson J, Shubik YV, Olsson SB, Platonov PG. Predictors of new onset atrial fibrillation during 10-year follow-up after first-ever ischemic stroke. Int J Cardiol. 2015;199:248–52.
9. Zuo ML, Liu S, Chan KH, Lau KK, Chong BH, Lam KF, et al. The CHADS2 and CHA2DS2-VASc scores predict new occurrence of atrial fibrillation and ischemic stroke. J Interv Card Electrophysiol. 2013;37:47–54.
10. Magnani JW, Johnson VM, Sullivan LM, Gorodeski EZ, Schnabel RB, Lubitz SA, et al. Wave duration and risk of longitudinal atrial fibrillation in persons ≥ 60 years old (from the Framingham heart study). Am J Cardiol. 2011;107:917–21.
11. Ciaroni S, Cuenoud L, Bloch A. Clinical study to investigate the predictive parameters for the onset of atrial fibrillation in patients with essential hypertension. Am Heart J. 2000;139:814–9.
12. Bonow RO, Mann DL, Zipes DP, Libby P. Braunwald's heart disease. A textbook of cardiovascular medicine. 9th ed. New York: W.B. Saunders Company; 2011.
13. Martinez-Selles M, Baranchuk A, Elosua R, Bayes de Luna A, O'Neal WT, Kamel H, et al. Advanced interatrial block and ischemic stroke: the atherosclerosis risk in communities study. Neurology. 2016;87:352–6.
14. Triola B, Olson MB, Reis SE, Rautaharju P, Merz CN, Kelsey SF, et al. Electrocardiographic predictors of cardiovascular outcome in women: the National Heart, Lung, and Blood Institute-sponsored women's ischemia syndrome evaluation (WISE) study. J Am Coll Cardiol. 2005;46:51–6.
15. Voulgari C, Tentolouris N, Moyssakis I, Dilaveris P, Gialafos E, Papadogiannis D, et al. Spatial QRS-T angle: association with diabetes and left ventricular performance. Eur J Clin Investig. 2006;36:608–13.
16. Borleffs CJ, Scherptong RW, Man SC, van Welsenes GH, Bax JJ, van Erven L, et al. Predicting ventricular arrhythmias in patients with ischemic heart disease: clinical application of the ECG-derived QRS-T angle. Circ Arrhythm Electrophysiol. 2009;2:548–54.
17. de Torbal A, Kors JA, van Herpen G, Meij S, Nelwan S, Simoons ML, et al. The electrical T-axis and the spatial QRS-T angle are independent predictors of long-term mortality in patients admitted with acute ischemic chest pain. Cardiology. 2004;101:199–207.
18. Kardys I, Kors JA, van der Meer IM, Hofman A, van der Kuip DA, Witteman JC. Spatial QRS-T angle predicts cardiac death in a general population. Eur Heart J. 2003;24:1357–64.
19. Rautaharju PM, Ge S, Nelson JC, Marino Larsen EK, Psaty BM, Furberg CD, Zhang ZM, et al. Comparison of mortality risk for electrocardiographic abnormalities in men and women with and without coronary heart disease (from the cardiovascular health study). Am J Cardiol. 2006;97:309–15.
20. Yamazaki T, Froelicher VF, Myers J, Chun S, Wang P. Spatial QRS-T angle predicts cardiac death in a clinical population. Heart Rhythm. 2005;2:73–8.
21. Cortez D, Ruckdeschel E, McCanta A, Collins K, Sauer W, Kay J, et al. Vectorcardiographic predictors of ventricular arrhythmia inducibility in patients with tetralogy of Fallot. J Electrocardiol. 2015;48:141–4.
22. Cortez D, Barham W, Ruckdeschel E, Sharma N, McCanta AC, von Alvensleben J, et al. Non-invasive predictors of ventricular arrhythmias in patients with tetralogy of Fallot undergoing pulmonary valve replacement. JACC Electrophys. 2017;3:162–70.
23. Park J-K, Park J, Uhm J-S, Joung B, Lee M-H, Pak H-N. Low P-wave amplitude (<0.1mV) in lead I is associated with displaced inter-atrial conduction and clinical recurrence of paroxysmal atrial fibrillation after radiofrequency catheter ablation. Europace. 2016;18:384–91.
24. Macfarlane PW, Devine B, Clark E. The University of Glasgow (Uni-G) ECG analysis program. Comput Cardiol. 2005;32:451–4.
25. Kors JA, van Herpen G, Sitig AC, van Bemmel JH. Reconstruction of the Frank vectorcardiogram from standard electrocardiographic leads. Eur Heart J. 1990;11:1083–92.
26. Cortez D, Sharma N, Devers C, Devers E, Schlegel TT. Visual transform applications for estimating the spatial QRS-T angle from the conventional 12-lead ECG: Kors is still most frank. J Electrocardiol. 2014;47:12–9.
27. Camm AJ, Kirchhof P, Lip GY, Schotten U, Savelieva I, Ernst S, et al. Guidelines for the Management of Atrial Fibrillation: the task force for the management of Atrial fibrillation of the European Society of Cardiology (ESC). Eur Heart J. 2010;31:2369–429.
28. Cortez D, Barham W, Ruckdeschel E, Sharma N, McCanta AC, von Alvensleben J, et al. Noninvasive predictors of perioperative atrial arrhythmias in patients with tetralogy of Fallot undergoing pulmonary valve replacement. Clin Cardiol. 2017; [Epub ahead of print]
29. Heeringa J, van der Kuip DA, Hofman A, Kors JA, van Herpen G, Stricker BH, et al. Prevalence, incidence and lifetime risk of atrial fibrillation: the Rotterdam study. Eur Heart J. 2006;27(8):949–53.
30. Ziegler PD, Glotzer TV, Daoud EG, Wyse DG, Singer DE, Ezekowitz MD, et al. Incidence of newly detected atrial arrhythmias via implantable devices in patients with history of thromboembolic events. Stroke. 2010;41:256–60.
31. Ziegler PD, Glotzer TV, Daoud EG, Singer MD, Ezekowitz MD, Hoyt RH, et al. Detection of previously undiagnosed atrial fibrillation in patients with stroke risk factors and usefulness of continuous monitoring in primary stroke prevention. Am J Cardiol. 2012;110:1309–14.
32. Kim D, Shim CY, Cho IJ, Kim YD, Nam HS, Chang HJ, et al. Incremental value of left atrial global longitudinal strain for prediction of post stroke atrial fibrillation in patients with acute ischemic stroke. J Cardiovasc Ultrasound. 2016;24:20–7.
33. Baturova MA, Sheldon SH, Carlson J, Brady PA, Lin G, Rabinstein AA, et al. Electrocardiographic and echocardiographic predictors of paroxysmal atrial fibrillation detected after ischemic stroke. BMC Cardiovasc Disord. 2016;16:209.

Paper II

In Hypertrophic Cardiomyopathy, the Spatial Peaks QRS-T Angle Identifies Those With Sustained Ventricular Arrhythmias

Address for correspondence:
Daniel Cortez, MD
13123 E. 16th Avenue, Box 100
Aurora, CO 80045
dr.danielcortez@gmail.com

Daniel Cortez, MD; Sharon Graw, PhD; Luisa Mestroni, MD
Department of Pediatric Cardiology (Cortez), Children's Hospital of Colorado/University of Colorado, Aurora, Colorado; Department of Cardiology, Clinical Sciences (Cortez), Lund University, Lund, Sweden; Cardiovascular Institute and Adult Medical Genetics Program (Graw, Mestroni), University of Colorado Denver Anschutz Medical Campus, Aurora, Colorado

ABSTRACT

Background: The spatial peaks QRS-T (SPQRS-T) angle differentiates hypertrophic cardiomyopathy (HCM) patients from controls. Increased angle confers arrhythmia risk in other populations.
Hypothesis: We predict that the SPQRS-T angle will identify HCM patients with sustained ventricular arrhythmias (VAs) and those with New York Heart Association class III/IV heart failure.
Methods: Corrected QT interval, QRS duration, and SPQRS-T angle were assessed in HCM patients with VAs (>30 seconds) and those without VAs.
Results: One hundred HCM patients (mean age, 32.7 ± 17.2 years) were assessed. Twenty patients had VAs. The corrected QT interval identified VA ($P = 0.018$) and at 460 ms gave positive and negative predictive values of 28.6% and 83.3%, respectively, and an odds ratio of 2.0 (95% confidence interval: 0.7-5.6). The SPQRS-T angle differentiated VA from no VA ($P < 0.001$) and at 124.1 degrees gave positive and negative predictive values and an odds ratio of 36.7%, 96.1%, and 14.2 (95% confidence interval: 3.1-65.6), respectively.
Conclusions: The SPQRS-T angle best differentiated patients with VAs.

Introduction

Hypertrophic cardiomyopathy (HCM) has an estimated prevalence of 1 in 500 individuals and its phenotype can include thickened ventricular walls (with or without obstruction of blood flow at the left ventricular outflow tract), increased risk of progression to New York Heart Association (NYHA) III/IV functional class, and increased risk of arrhythmia-induced sudden cardiac death.[1–3] An increase in the corrected QT interval (QTc) has been associated with increased ventricular arrhythmia (VA) risk in patients with HCM.[4]

Recent advances in electrocardiographic (ECG) technology, including the ability to automatically transform digital 12-lead ECG data into orthogonal vectorcardiographic data,[5] can add further diagnostic[6–8] and prognostic[9–17] utility to traditional 12-lead ECGs. Among the derived vectorcardiographic parameters obtainable after such transformations, the spatial peaks QRS-T (SPQRS-T) angle has notable diagnostic utility for conditions in which sudden death may be an outcome,[10–12,15,17] as well as for identification of HCM in adult[18] and pediatric patients.[19] The SPQRS-T angle has also been positively correlated with VA risk in patients with ischemic heart disease,[9] whereas an increased angle also correlates with increasing severity of heart failure (HF).[7,8,14,16]

We hypothesized that the SPQRS-T angle would differentiate HCM patients with sustained VAs (≥30 seconds) from those without VAs with increased predictive values compared with the QTc interval. A secondary aim was to assess if those with HF (NYHA class III/IV) would also have higher SPQRS-T angles.

Methods

A retrospective study of HCM patients from 2000 to 2013 at the University of Colorado Hospital and Children's Hospital of Colorado was performed. Internal review board permission was obtained and written permission was waivered. Patients with the diagnosis of HCM by evidence of diastolic dysfunction and 15 mm absolute septal thickness by echocardiogram were identified by first author chart review without knowledge of VA or congestive HF history.

Electrocardiogram, Echocardiogram, and Heart Failure Measures

Electrocardiograms were taken at a 25-mm/s speed with 10 mm/mV for the limb and precordial leads (Phillips, Best, Netherlands) and ECG recordings (General Electric, Menominee Falls, WI) in sinus rhythm. The diagnosis of HCM was based on echocardiographic evidence of diastolic dysfunction and those with an absolute septal or

The authors have no funding, financial relationships, or conflicts of interest to disclose.

Received: February 8, 2016
Accepted with revision: March 24, 2016

Published online in Wiley Online Library (wileyonlinelibrary.com)
DOI:10.1002/clc.22549

posterior wall thickness of ≥15 mm by echocardiographic M-mode measurement during diastole from a parasternal short-axis view by the cardiologist seeing the particular patient. Conduction abnormalities did not preclude patient participation in this retrospective study.

Congestive HF is defined as those HCM patients who meet criteria as governed by the NYHA for functional classifications for objective or subjective measures (class I–IV).

Sustained Ventricular Arrhythmias

Ventricular arrhythmias were documented by Holter monitoring, exercise stress test, or by implantable cardioverter-defibrillator (ICD)/pacemaker devices in patients with history of sustained VAs (≥30 seconds) and compared with those HCM patients without sustained VAs. Given the retrospective nature of the study, routine screening was variable dependent on the cardiologist seen by each patient.

Parameters

Electrocardiograms within 3 months prior to VA documentation were assessed. The QTc interval, QRS duration (QRSd), and SPQRS-T angles were assessed. The vectorcardiographic SPQRS-T angle was visually derived from conventional 12-lead ECG recordings based on the method recently described by Cortez et al, utilizing the method described by Kors by the first author, as shown in Figure 1A–C.[6,20] The QRSd and QTc interval were automatically calculated, whereas the Sokolow-Lion (S-wave in V_1 + R-wave in $V_5 \geq 3.5$ mV) and Cornell (R-wave in aVL + S-wave in $V_4 \geq 2.5$ mV) left ventricular hypertrophy voltage criteria and inverted T-waves in the lateral leads were also assessed. All parameters were assessed under blinded conditions (blinded to outcome).

Statistical Analysis

Normality was tested and *t* testing was used to evaluate differences between parameters tested between the HCM patients with VAs and the HCM patients without VAs. A *P* value ≤0.05 was deemed significant. Odds ratios (ORs) were also calculated for each of the criteria, as well as positive and negative predictive values (PPV, NPV) based on receiver operating characteristic curve analysis optimum cutoff values. All statistics were performed using GNU PSPP software (http://www.gnu.org/software/pspp/). Logistic regression was used to assess for independent predictors of VA with a *P* value cutoff of 0.05. Intra- and interobserver variability for the SPQRS-T angle has been previously presented in a cohort that included a subset of the patients presented here in this manuscript.[20]

Results

Patient Population

Electrocardiographic results from 100 HCM patients (mean age, 32.7 ± 17.2 years) were assessed. Twenty patients with VAs were identified. Five patients with NYHA functional class III or IV HF were identified. Syncope differentiated those with vs those without VAs (Table 1). Four patients with VA had ICDs, and 1 patient without VA (but with atrial fibrillation) had an ICD. Holter monitoring identified 8 patients with VA; loop recording, exercise stress testing, and inpatient telemetry identified 3, 2, and 4 patients, respectively.

Corrected QT Interval and QRS Duration

The QTc interval differentiated those with VAs from those without VAs with values of 440.7 ± 48.1 ms and 472.0 ± 43.4 ms, respectively ($P = 0.013$; Table 1, Figure 2). A QTc interval at a cutoff value of 460 ms gave PPV, NPV, and OR of 28.6%, 83.3%, and 2.0, respectively (95% confidence interval [CI]: 0.7-5.6). The QRSd did not differentiate HCM patients with VAs from those without VAs.

Spatial QRS-T Angle

The SPQRS-T angle differentiated those with sustained VAs from those without VAs (108.2 ± 45.9 degrees vs 144.0 ± 26.7 degrees; $P < 0.001$; Table 1, Figure 2). At an optimum cutoff value of 124.1 degrees, PPV and NPV were 36.7% and 96.1%, respectively, with an OR of 14.2 (95% CI: 3.1-65.6; Figure 3). Even in those without syncope, the SPQRS-T angle significantly differentiated those with vs those without VAs (109.3 ± 45.0 degrees vs 142.1 ± 28.6 degrees; $P < 0.001$).

Heart Failure

Only the SPQRS-T angle differentiated those with NYHA class III/IV HF from those without NYHA III/IV HF. There were 5 (5%) HCM patients with NYHA III/IV classification, all with systolic HF (1 with preserved ejection fraction), with a mean SPQRS-T angle of 150.3 ± 9.7 degrees vs 113.9 ± 45.3 degrees ($P < 0.001$). At an optimum cutoff value of 153.4 degrees, the PPV, NPV, and OR were 15.0%, 98.8%, and 13.9, respectively (95% CI: 1.4-142.3). When those with congestive HF or VAs were compared with HCM patients without congestive HF or VA, the PPV, NPV, and OR were 44.9%, 96.1%, and 20.0, respectively (95% CI: 4.4 to 91.5), at a cutoff value of 124.1 degrees.

Multivariate Analysis

Logistic regression was used for multivariate analysis utilizing septal thickness, syncope, the QTc, and the SPQRS-T angle in the regression. Only syncope and the SPQRS-T angle both remained independent predictors of sustained VAs (both $P < 0.001$). The OR for the SPQRS-T angle was 1.41 (95% CI: 1.20-1.65).

The R^2 value for spatial QRS-T angle vs septal thickness was 0.27. The R^2 for the QRSd and QTc compared with septal thickness were 0.63 and 0.26, respectively.

Discussion

Corrected QT Interval and QRS Duration

Corrected QT interval prolongation has been previously described in HCM patients, with 13% having values >480 ms.[21] However, the association between a prolonged QTc interval, specifically >460 ms, and VAs, as well as sudden cardiac death in HCM, has been described.[4] In this

Published online in Wiley Online Library (wileyonlinelibrary.com)
DOI:10.1002/clc.22549

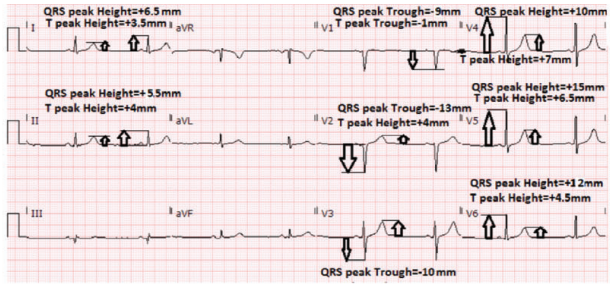

(A)

QRSx= QRSI*0.38-QRSII*0.07-QRSV1*0.13+QRSV2*0.05-QRSV3*0.01+QRSV4*0.14+QRSV5*0.06+QRSV6*0.54
QRSy=-QRSI*0.07+QRSII*0.93+QRSV1*0.06-QRSV2*0.02-QRSV3*0.05+QRSV4*0.06-QRSV5*0.17+QRSV6*0.13
QRSz= QRSI*0.11-QRSII*0.23-QRSV1*0.43+QRSV2*0.06-QRSV3*0.14-QRSV4*0.20-QRSV5*0.11+QRSV6*0.31
Tx=TI*0.38-TII*0.07-TV1*0.13+TV2*0.05-TV3*0.01+TV4*0.14+TV5*0.06+TV6*0.54
Ty=-TI*0.07+TII*0.93+TV1*0.06-TV2*0.02-TV3*0.05+TV4*0.06-TV5*0.17+TV6*0.13
Tz=TI*0.11-TII*0.23-TV1*0.43+TV2*0.06-TV3*0.14-TV4*0.20-TV5*0.11+TV6*0.31
RMSQRS=SQRT(QRSx^2+QRSy^2+QRSz^2)=13.5 mm
RMST=SQRT(Tx^2+Ty^2+Tz^2)= 6.2mm
SPQRS-T=cos^-1((QRSx*Tx+QRSy*Ty+QRSz*Tz)/RMSQRS*RMST]=44.8 degrees

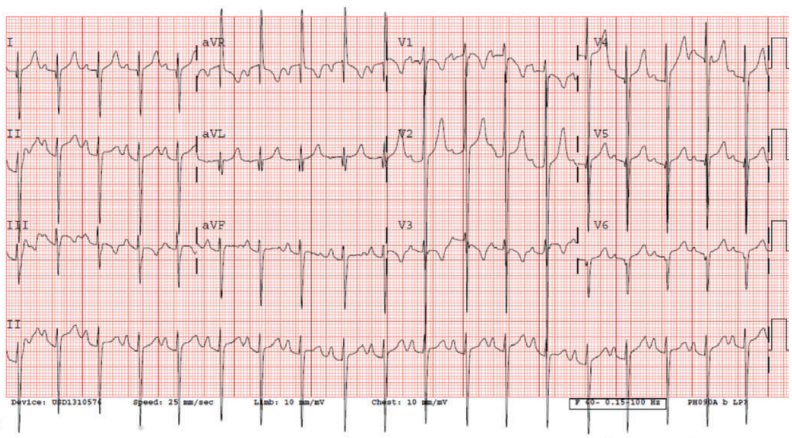

(B)

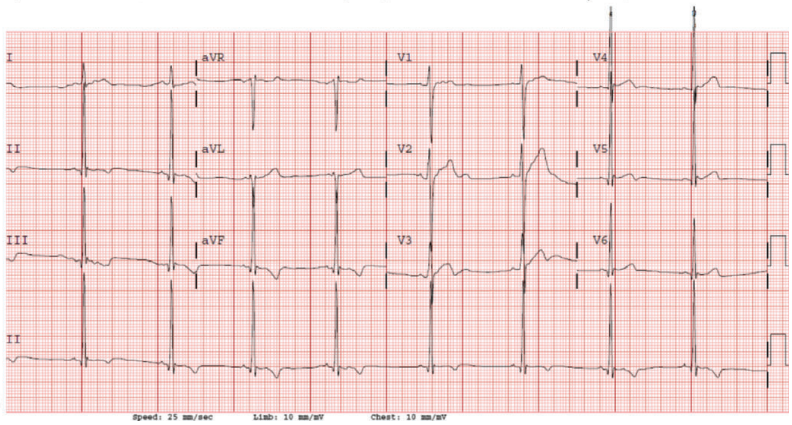

(C)

Figure 1. (A) Spatial QRS-T angle calculation for a patient with mild hypertrophy (maximum thickness, 15 mm). (B) A spatial QRS-T angle for a patient with HCM with sustained VAs (spatial QRS-T angle, 141.6 degrees). (C) Sample ECG of an HCM patient without sustained VAs (spatial QRS-T angle, 83.3 degrees). Abbreviations: ECG, electrocardiogram; HCM, hypertrophic cardiomyopathy; VA, ventricular arrhythmia.

Published online in Wiley Online Library (wileyonlinelibrary.com)
DOI:10.1002/clc.22549

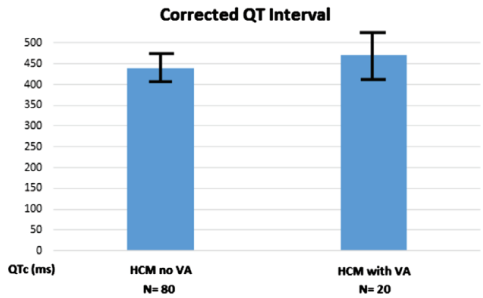

Figure 2. Corrected QT interval for HCM patients with sustained VAs and those without VAs ($P = 0.018$, which gives a significant difference between the patients). Abbreviations: HCM, hypertrophic cardiomyopathy; VA, ventricular arrhythmia.

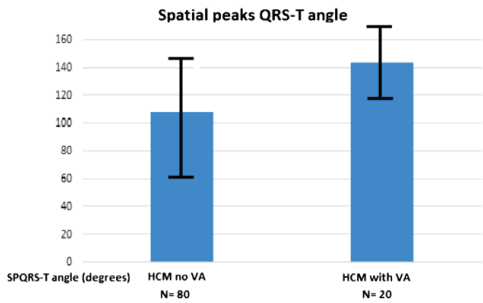

Figure 3. Spatial peaks QRS-T angle (angles) for HCM patients with sustained VAs and those without Vas ($P < 0.001$, which gives a significant difference between the patients). Abbreviations: HCM, hypertrophic cardiomyopathy; VA, ventricular arrhythmia.

case, the QTc interval had too low of a predictive value (positive or negative) for any clinical usefulness.

Spatial Peaks QRS-T Angle

The SPQRS-T angle has been previously been shown to identify patients with HCM[18,19] and to predict VAs in adults with myocardial ischemia[9]; thus, it seems logical that it would predict VAs in patients with HCM. Hypertrophic cardiomyopathy, however, can involve subendocardial ischemia; thus, the SPQRS-T angle is not as robust a predictor as one might have thought. Given its positive correlation with worsening HF, it is likely that the SPQRS-T angle, given a larger population size, would identify HF in patients with HCM.[7,8,14,16] However, identification of significant morbidity from either HF or VAs is obtained by utilizing the SPQRS-T angle with improved ORs at the same VA optimum cutoff value for the SPQRS-T angle. Thus, arrhythmia and HF risk are both conferred by an increase in the SPQRS-T angle. The spatial QRS-T angle correlates with reduced left ventricular ejection fraction, left ventricular dilation, and increased left ventricular mass and is associated with ischemic scar, which are known risk factors for VAs.[22] Furthermore, the derived spatial QRS-T angle from the 12-lead ECG, which was the method used in this study, shows similar diagnostic ability to the vectorcardiographically measured spatial QRS-T angle with tight Bland-Altman 95% limits of agreement; thus, is a reasonable and clinically available tool for risk assessment in HCM patients.[19,20]

Table 1. Patient Demographics and Results for HCM Patients With Sustained VAs and Those Without Sustained VAs

	VAs, n = 20	No VAs, n = 80	*P* Value
Age, years	32.7 ± 17.2	33.8 ± 18.4	0.418
Male sex	13 (65)	53 (66.3)	0.833
History of syncope	7 (35.0)	2 (2.50)	<0.001
Atrial arrhythmias	3 (15.0)	8 (10)	0.689
Nonsustained VAs	2 (10)	3 (3.8)	0.261
NYHA class III/IV	4 (5.0)	4 (5.0)	1.000
Maximum septal thickness, cm	2.4 ± 0.5	2.17 ± 0.4	0.107
LVOT obstructions presence	2 (10.0)	8 (10.0)	1.000
Sokolow-Lion voltage criteria	4 (20.0)	27 (33.8)	0.358
Cornell voltage criteria	8 (40.0)	18 (22.5)	0.190
Inverted T-waves V_4 through V_6	10 (50.0)	33 (41.3)	0.650
QRSd, ms	116.8 ± 36.1	98.8 ± 22.0	0.137
QTc, ms	472.0 ± 43.4	440.7 ± 48.1	0.013
SPQRS-T, degrees	144.0 ± 26.7	108.2 ± 45.9	<0.001

Abbreviations: HCM, hypertrophic cardiomyopathy; HF, heart failure; LVOT, left ventricular outflow tract; NYHA, New York Heart Association; QRSd, QRS duration; QTc, corrected QT interval; SD, standard deviation; SPQRS-T, spatial peaks QRS-T angle; VA, ventricular arrhythmia.
Data are presented as n (%) or mean ± SD.

Study Limitations

This study had limitations, including the size of the HCM group. This was also a retrospective study, and thus not prospective in nature, as would be needed to validate this method. New York Heart Association class III/IV HF patients were in limited number, so comparisons of these patients with others may not represent true population comparisons. Also, although by definition all HCM patients had some component of diastolic dysfunction, specific evaluation for diastolic HF was not performed due to limited numbers of patients. Another limitation in any study assessing VAs includes identification of VAs in patients without ICDs, as all VAs might not be documented. The last ECG prior to arrhythmia diagnosis was used to calculate the parameters assessed; all patients in the study happened to have an ECG within 3 months of diagnosis, so these were the ones used; and, unfortunately, given the retrospective nature of the study, further time assessment (closer to VA timing) was not available in all patients, thus this is viewed as a limitation of the study, regarding optimal timing for spatial QRS-T angle assessment.

Published online in Wiley Online Library (wileyonlinelibrary.com)
DOI:10.1002/clc.22549

Conclusion

In our HCM cohort, the SPQRS-T angle and the QTc interval differentiated HCM patients with VAs from those without VAs. The SPQRS-T angle best differentiated patients with VAs with highest predictive values and ORs. The spatial QRS-T angle had the best predictive values for either VA or NYHA class III or IV HF identification in HCM patients. Prospective studies are needed to validate this method.

Acknowledgments

No disclosures.

References

1. Olivotto I, Girolami F, Ackerman MJ, et al. Myofilament protein gene mutation screening and outcome of patients with hypertrophic cardiomyopathy. *Mayo Clin Proc.* 2008;83:630–638.
2. Spirito P, Autore C, Rapezzi C, et al. Syncope and risk of sudden death in hypertrophic cardiomyopathy. *Circulation.* 2009;119:1703–1710.
3. Elliott PM, Poloniecki J, Dickie S, et al. Sudden death in hypertrophic cardiomyopathy: identification of high risk patients. *J Am Coll Cardiol.* 2000;36:2212–2218.
4. Debonnaire P, Katsanos S, Joyce E, et al. QRS fragmentation and QTc duration relate to malignant ventricular tachycarrhythmias and sudden cardiac death in patients with hypertrophic cardiomyopathy. *J Cardiovasc Electrophysiol.* 2015;26:547–555.
5. Kors JA, van Herpen G, Sittig AC, et al. Reconstruction of the Frank vectorcardiogram from standard electrocardiographic leads: diagnostic comparison of different methods. *Eur Heart J.* 1990;11:1083–1092.
6. Dilaveris P, Gialafos E, Pantazis A, et al. The spatial QRS-T angle as a marker of ventricular repolarisation in hypertension. *J Hum Hypertens.* 2001;15:63–70.
7. Triola B, Olson MB, Reis SE, et al. Electrocardiographic predictors of cardiovascular outcome in women: the National Heart, Lung, and Blood Institute–sponsored Women's Ischemia Syndrome Evaluation (WISE) study. *J Am Coll Cardiol.* 2005;46:51–56.
8. Voulgari C, Tentolouris N, Moyssakis I, et al. Spatial QRS-T angle: association with diabetes and left ventricular performance. *Eur J Clin Invest.* 2006;36:608–613.
9. Borleffs CJ, Scherptong RW, Man SC, et al. Predicting ventricular arrhythmias in patients with ischemic heart disease: clinical application of the ECG-derived QRS-T angle. *Circ Arrhythm Electrophysiol.* 2009;2:548–554.
10. de Torbal A, Kors JA, van Herpen G, et al. The electrical T-axis and the spatial QRS-T angle are independent predictors of long-term mortality in patients admitted with acute ischemic chest pain. *Cardiology.* 2004;101:199–207.
11. Kardys I, Kors JA, van der Meer IM, et al. Spatial QRS-T angle predicts cardiac death in a general population. *Eur Heart J.* 2003;24:1357–1364.
12. Kors JA, Kardys I, van der Meer IM, et al. Spatial QRS-T angle as a risk indicator of cardiac death in an elderly population. *J Electrocardiol.* 2003;(36 suppl):113–114.
13. Rautaharju PM, Ge S, Nelson JC, et al. Comparison of mortality risk for electrocardiographic abnormalities in men and women with and without coronary heart disease (from the Cardiovascular Health Study). *Am J Cardiol.* 2006;97:309–315.
14. Rautaharju PM, Kooperberg C, Larson JC, et al. Electrocardiographic predictors of incident congestive heart failure and all-cause mortality in postmenopausal women: the Women's Health Initiative. *Circulation.* 2006;113:481–489.
15. Rautaharju PM, Kooperberg C, Larson JC, et al. Electrocardiographic abnormalities that predict coronary heart disease events and mortality in postmenopausal women: the Women's Health Initiative. *Circulation.* 2006;113:473–480.
16. Rautaharju PM, Prineas RJ, Wood J, et al. Electrocardiographic predictors of new-onset heart failure in men and in women free of coronary heart disease (from the Atherosclerosis in Communities [ARIC] Study). *Am J Cardiol.* 2007;100:1437–1441.
17. Yamazaki T, Froelicher VF, Myers J, et al. Spatial QRS-T angle predicts cardiac death in a clinical population. *Heart Rhythm.* 2005;2:73–78.
18. Potter SL, Holmqvist F, Platonov PG, et al. Detection of hypertrophic cardiomyopathy is improved when using advanced rather than strictly conventional 12-lead electrocardiogram. *J Electrocardiol.* 2010;43:713–718.
19. Cortez D, Sharma N, Cavanaugh J, et al. The spatial QRS-T angle outperforms the Italian and Seattle ECG-based criteria for detection of hypertrophic cardiomyopathy in pediatric patients. *J Electrocardiol.* 2015;48:826–833.
20. Cortez D, Sharma N, Devers C, et al. Visual transform applications for estimating the spatial QRS-T angle from the conventional 12-lead ECG: Kors is still most Frank. *J Electrocardiol.* 2014;47:12–19.
21. Johnson JN, Grifoni C, Bos JM, et al. Prevalence and clinical correlates of QT prolongation in patients with hypertrophic cardiomyopathy. *Eur Heart J.* 2011;32:1114–1120.
22. Shi B, Ferrier KA, Sasse A, et al. Correlation between vectorcardiographic measures and cardiac magnetic resonance imaging of the left ventricle in an implantable cardioverter defibrillator population. *J Electrocardiol.* 2014;47:52–58.

Published online in Wiley Online Library (wileyonlinelibrary.com)
DOI:10.1002/clc.22549

Paper III

Cortez et al. BMC Cardiovascular Disorders (2017) 17:261
DOI 10.1186/s12872-017-0696-x

BMC Cardiovascular Disorders

RESEARCH ARTICLE Open Access

Right precordial-directed electrocardiographical markers identify arrhythmogenic right ventricular cardiomyopathy in the absence of conventional depolarization or repolarization abnormalities

Daniel Cortez[1,2*], Anneli Svensson[3], Jonas Carlson[1], Sharon Graw[4], Nandita Sharma[2], Francesca Brun[4,5], Anita Spezzacatene[4,5], Luisa Mestroni[4,5] and Pyotr G. Platonov[1,6]

Abstract

Background: Arrhythmogenic right ventricular dysplasia/cardiomyopathy (ARVD/C) carries a risk of sudden death. We aimed to assess whether vectorcardiographic (VCG) parameters directed toward the right heart and a measured angle of the S-wave would help differentiate ARVD/C with otherwise normal electrocardiograms from controls.

Methods: Task Force 2010 definite ARVD/C criteria were met for all patients. Those who did not fulfill Task Force depolarization or repolarization criteria (−ECG) were compared with age and gender-matched control subjects. Electrocardiogram measures of a 3-dimentional spatial QRS-T angle, a right-precordial-directed orthogonal QRS-T (RPD) angle, a root mean square of the right sided depolarizing forces (RtRMS-QRS), QRS duration (QRSd) and the corrected QT interval (QTc), and a measured angle including the upslope and downslope of the S-wave (S-wave angle) were assessed.

Results: Definite ARVD/C was present in 155 patients by 2010 Task Force criteria (41.7 ± 17.6 years, 65.2% male). -ECG ARVD/C patients (66 patients) were compared to 66 control patients (41.7 ± 17.6 years, 65.2% male). All parameters tested except the QRSd and QTc significantly differentiated -ECG ARVD/C from control patients ($p < 0.004$ to $p < 0.001$). The RPD angle and RtRMS-QRS best differentiated the groups. Combined, the 2 novel criteria gave 81.8% sensitivity, 90.9% specificity and odds ratio of 45.0 (95% confidence interval 15.8 to 128.2).

Conclusion: ARVD/C disease process may lead to development of subtle ECG abnormalities that can be distinguishable using right-sided VCG or measured angle markers better than the spatial QRS-T angle, the QRSd or QTc, in the absence of Taskforce ECG criteria.

Keywords: Arrhythmogenic right ventricular cardiomyopathy, Vectorcardiography, ECG, Cascade screening

* Correspondence: dr.danielcortez@gmail.com
[1]Department of Cardiology, Clinical Sciences, Lund University, Lund, Sweden
[2]Electrophysiology/Cardiology, Penn State Milton S. Hershey Medical Center, Hershey, USA
Full list of author information is available at the end of the article

Background

Arrhythmogenic right ventricular dysplasia/cardiomyopathy (ARVD/C) is an inherited cardiomyopathy characterized by fibro-fatty replacement of predominately the right ventricle, which predisposes patients to life-threatening ventricular arrhythmias and usually slowly progressive ventricular dysfunction [1]. The disease is inherited as an autosomal dominant trait with incomplete penetrance and highly variable expressivity [1]. Diagnosis is made by combining multiple sources of diagnostic information as prescribed by the Task Force criteria, which were updated in 2010 to increase diagnostic sensitivity while maintaining specificity [2].

First-degree relatives often have incomplete expression of the disease [3]. Clinical cascade screening of family members in genotype-negative ARVD/C is complicated by the lack of early specific signs of disease that would identify those individuals prone to development of disease. Electrocardiographic (ECG) changes may develop before histologic evidence of myocyte loss or clinical evidence of RV dysfunction [4, 5]. However, ECG depolarization and repolarization changes, based on current criteria, are typically only apparent in around half of family members who eventually progress to meet Definite ARVD/C by 2010 criteria [5].

The spatial QRS-T angle, a vectorcardiographic parameter easily derivable from the 12-lead ECG [6], has been shown to improve detection of left sided cardiomyopathy, particularly hypertrophic cardiomyopathy [7], as well as the prediction of susceptibility to ventricular tachycardia and cardiac death both in general populations [8–10] and in patients with known cardiac pathology [11–13]. Given this mainly right-sided heart disease, we hypothesize that right-precordial-directed vectorcardiographic parameters, particularly a right precordial-directed-orthogonal QRS-T angle (RPD angle), right-sided depolarization magnitude (right root mean square of the QRS, RtRMS-QRS) (Fig. 1) from a baseline ECG would improve detection of ARVD/C patients who have no depolarization or repolarization abnormalities otherwise but who still meet criteria for definite ARVD/C by 2010 taskforce criteria (by criteria other than ECG).

Methods

Population

A cross-sectional study of patients with ARVC/D from an international cohort from the University of Colorado (Denver, CO, USA), Skåne University Hospital (Lund, Sweden), Linköping University Hospital (Sweden) and the University of Trieste (Italy) undergoing routine follow-up, classified as definite ARVD/C by the 2010 Task Force criteria was performed [2]. Normal variant ECGs from patients, who did not have signs of bundle branch block and not fitting 12-lead ECG major or minor depolarization or repolarization criteria by 2010 Task Force guidelines (electrocardiographically concealed ARVD/C) were compared with ECGs recorded from 1:1 age- and gender-matched control subjects who were screened in cardiology clinic at the University of Colorado (Denver, CO) or at Skåne University Hospital (Lund, Sweden) for murmurs or chest pain without family history of ARVD/C and through ultrasound and clinical observations were deemed normal. None of the control subjects had other underlying cardiac disease (no cardiomyopathy or other notable cardiac disease) nor did they have obvious obstructive or restrictive lung disease or thromboembolisms. All ECG's were taken from the first time the patient had presented to the particular institution and no patients were on antiarrhythmic treatment at the time of their ECG. The study was approved by the Institutional Review Boards at each of the institutions noted above.

Electrocardiogram

The resting ECG closest to time of diagnostic echocardiogram or magnetic resonance imaging studies from ARVD/C patients at a speed of 25 mm/s and with voltages of 10 mm/mV were assessed (GE, WI, USA or Phillips Healthcare, MA, USA). Digital recordings were changed to PDF files and assessed at up to 150% magnification and used for vectorcardiographic derivations. Approximations of the Kors' quasi-orthogonal spatial peaks QRS-T angle (normally based on V6 defined as the X-axis, lead II as the Y-axis and −0.5*V2 as the Z-axis) were used with direction particularly toward the R-wave in V1 (as the Z-axis QRS vector magnitude) and S-wave in V5 (as the X-axis QRS vector magnitude) while ignoring magnitudes of the S-wave in V1 and the R-wave in V5 (as an attempt to have right-precordial-directed vector magnitude and angle). Lead II measures maximum deviation from baseline (whether R or S) was used as the Y-axis QRS vector magnitude, similar to Kors' quasi-orthogonal method [6]. Right-precordial-directed orthogonal QRS-T angles (RPD angle, degrees, Fig. 2), right-precordial-directed vector magnitudes (RtRMS-QRS, mV, Fig. 1), and spatial peaks QRS-T angles (SPQRS-T angle, degrees) were measured in ARVD/C and compared to the same parameters from control patients. The Bazett corrected QT interval (QTc) and the QRS duration (QRSd) were measured in milliseconds (ms).

The spatial QRS-T angle was calculated based on the visual transform estimation based on using selected leads and multipliers of those leads to approximate an orthogonal system. This is based on the Kors' visual estimations regression-related method, which has been described previously [6].

The RPD angle is similar in calculation to the Kors' quasi-orthogonal angle, but is a right-side restrictive measure meaning only the QRS maximum deviation in the orthogonal planes according to the following principles:

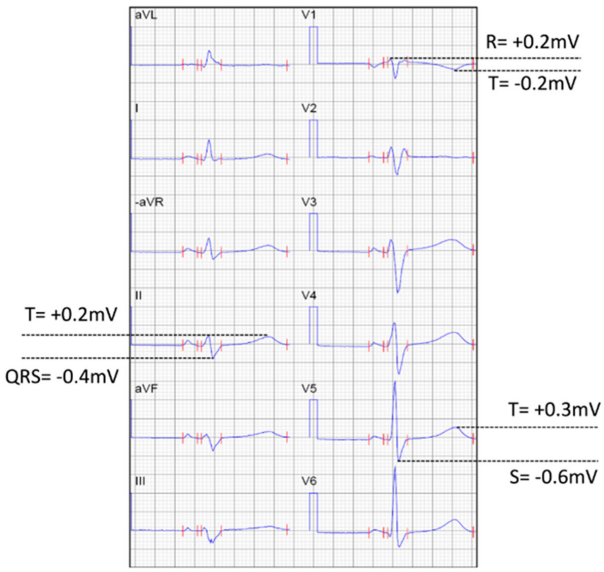

Fig. 1 Calculation of the right spatial peaks QRS-T angle (RtSPQRS-T angle) and the right root mean square QRS (RtRMSQRS). 0.1 mV × 40 ms = 1 little box. SV5 = Swave maximum deviation from baseline (negative number). QRSmaxII: QRS maximum deviation from baseline (positive or negative number) RV1: Rwave maximum deviation from baseline (positive number). RtRMS-QRS= $\sqrt{SV5^2 + QRSmaxII^2 + (-0.5 * RV1)^2}$ = $\sqrt{-0.6mV^2 + (-0.4mV)^2 + (-0.5 * 0.2mV)^2}$ = 0.73 mV. RtRMST=$\sqrt{TV5^2 + TII^2 + (-0.5 * TV1)^2}$ = $\sqrt{0.3mV^2 + 0.2mV^2 + (-0.5 * -0.2mV)^2}$ = 0.37 mV. RPD- angle= $\cos^{-1}$([(*SV5*∗*TV5*) + (*QRSmaxII*∗*TII*) − 0.5(*RV1*∗*TV1*)]/RtRMSQRS∗RtRMST) =$\cos^{-1}$([(−0.6*mV*∗0.3*mV*) + (−0.4*mV*∗0.2*mV*) − 0.5(0.2*mV*∗ −0.2*mV*)]/0.73 mV∗0.37 mV) = 172.4 degrees

- X-axis: the S-wave deviation only in V5 (ignoring the R-wave in V5, even if it has a greater deviation from baseline than the S-wave);
- Y-axis: the R or S maximum deviation from lead II;
- Z-axis: the negative one half of the deviation of the R in lead V1.

These measures are then applied in the equation (Fig. 1 legend) and inverse cosine is taken between the QRS deviations and the T-wave deviations (positive or negative in leads V6 (X-axis), II (Y-axis) and negative one half of the deviation in V1 (Z-axis)). Please see Fig. 1 for further detail.

The RtRMS-QRS is the vector magnitude of the QRS complex based on right-precordial-directed measures (please see equation noted above and Fig. 1).

V5 also more consistently demonstrated an S-wave than V6, thus the S-wave in V5 was used.

All parameters were assessed by the first author if not otherwise noted above, while 10% of the sample was assessed by the 5th author to calculate inter-observer variability (per below).

Statistics

Parametric measures are given as mean ± standard deviation, while non-parameteric measures are given as median (1st quartile to 3rd quartile) and were used to assess statistical significance between the two groups. A *p*-value of 0.05 or less was considered significant. Receiver operating characteristic curves were used to assess optimum cut-off values for sensitivity and specificity measures. Odds ratios were used. All data were de-identified. Intra-class correlation coefficients were used to determine inter−/intra-observer variability by the 1st and 5th authors' measurements of the RPD angle, and the RtRMS-QRS.

Results

Population

Of a total of 155 patients with the diagnosis of definite ARVD/C by 2010 Task Force criteria, 66 patients did not have depolarization or repolarization changes consistent with either major or minor criteria (ECG-negative patients) who were compared with 1:1 age- and gender matched control patients. Tables 1 and 2 summarize

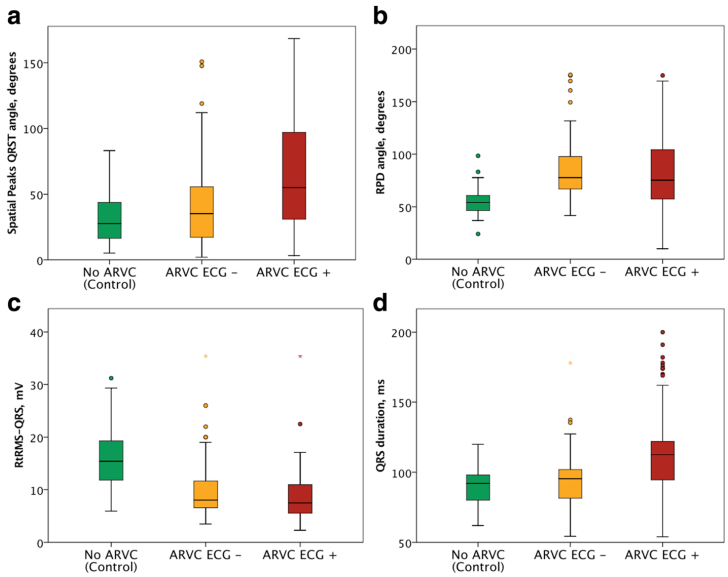

Fig. 2 a-d: Box plots comparing parameter values for controls, ECG-negative and ECG-positive comparisons of the **a**: Spatial peaks QRS-T angle (median with 1st to 3rd quartiles), **b**: RPD angle (mean with 2 standard deviations), **c**: RtRMS-QRS (mean with 2 standard deviations), **d**: QRS duration (mean with 2 standard deviations)

patient demographic data. Apart from the ECG-related differences between ECG-positive and ECG-negative ARVD/C patients, on which group definitions were based, no other diagnostic criteria appeared to demonstrate significant difference between the groups (Table 1). Borderline significant difference was observed in regard to the greater prevalence of patients fulfilling minor arrhythmia criterion in ECG-positive ARVD/C patients.

However, we observed significant differences in regard to the major MRI volume criteria, which was twice as common in ARVD/C patients who met ECG criteria (ECG-positive ARVD/C) than in those who did not meet 12-lead ECG criteria (ECG-negative ARVD/C). Figure 2 shows how the patients were sorted in various categories to determine the overall ability to detect ECG-negative ARVD/C patients. Figure 2a-d shows comparisons of various parameters for controls, ECG-negative and ECG-positive patients.

QTc and QRSd

Five of our ECG-negative ARVD/C patient had right bundle branch blocks. While QRSd did not significantly differentiate ECG-negative ARVD/C patients from controls (Table 2), the QTc was significantly longer in ECG-negative ARVD/C than in control subjects (Table 3), with resultant optimum sensitivity, specificity, positive and negative predictive values shown in Table 4 with an odds ratio of 5.3 for QTc (95% confidence interval 0.6 to 46.6). The QRSd and the QTc significantly differentiated the ECG-positive versus ECG-negative ARVD/C patients (p-values of <0.001 and 0.002, respectively).

Spatial peaks QRS-T angles

Both the SPQRS-T angle and the RPD angle demonstrated significant differences between ECG-negative ARVD/C patients and control subjects (p-value < 0.001, Table 3). The RPD angle showed much better sensitivity and specificity than the spatial QRS-T angle (Table 4) and with an odds ratio 34 times higher than that for the SPQRS-T angle at 41.3 l95% CI 13.1 to 130.2).

The SPQRS-T angle demonstrated stepwise increase from the lowest value in the control group to ECG-negative ARVD/C and the highest value observed in the ECG-positive ARVD/C patients.

Right root mean square QRS voltage

The right root mean square QRS (RtRMS-QRS) progressively and significantly decreased stepwise from the highest mean value observed in the control group to the lowest among the ECG-positive ARVD/C. In regard to discrimination between control subjects and ECG-negative ARVD/C patients, the ROC curve gave an

Table 1 All ARVD/C, ARVD/C with (+ECG) and without (−ECG) 2010 ECG taskforce criteria

	ARVC Total (*N* = 155)	ECG-positive ARVC (*N* = 89)	ECG-negative ARVC (*N* = 66)	*p*-value ECG-positive vs ECG-negative
Age	42.1 ± 17.3	42.0 ± 17.4	41.7 ± 17.6	0.861
Sex (% male)	106 (68.4%)	63 (70.8%)	43 (65.2%)	0.488
Proband (%)	111 (71.6%)	71 (79.8%)	30 (45.5%)	0.012
I. Imaging	155 (100%)	89 (100%)	66 (100%)	1.000
major, %	111 (71.6%)	68 (76.4%)	43 (65.2%)	0.082
minor, %	89 (57.4%)	60 (67.4%)	29 (43.9%)	0.005
II. Tissue characterization of the wall, biopsies performed (% of patients)	70 (45.2%)	39 (43.8%)	31 (47.0%)	0.745
major, %	53 (75.7%)	31 (79.1%)	22 (71.0%)	0.576
minor, %	63 (90.0%)	36 (92.3%)	27 (87.1%)	0.454
III. Repolarization abnormality				
major, %	54 (34.8%)	54 (60.7%)	0 (0.0%)	<0.001
minor, %	20 (12.9%)	20 (22.5%)	0 (0.0%)	<0.001
IV. Depolarization abnormality				
major, %	13 (8.4%)	13 (14.6%)	0 (0.0%)	<0.001
minor, %	17 (11.0%)	17 (19.1%)	0 (0.0%)	<0.001
V. Arrhythmia				
major, %	44 (28.4%)	26 (29.2%)	18 (27.3%)	0.858
minor, %	64 (41.3%)	42 (47.2%)	22 (33.3%)	0.1000
VI. Family history				
major, %	84 (54.2%)	48 (53.9%)	35 (53.0%)	1.000
VII. Genotype positive	48 (31.0%)	29 (32.6%)	19 (28.8%)	0.726
PLN (% genotype positive)	1 (2.1%)	0 (0.0%)	1 (5.3%)	0.396
TTN (% genotype positive)	11 (22.9%)	8 (27.6%)	3 (15.8%)	0.488
PKP2 (% genotype positive)	23 (47.9%)	17 (58.6%)	6 (31.2%)	0.083
DSC2 (% genotype positive)	2 (4.2%)	1 (3.5%)	1 (5.3%)	1.000
DSG2 (% genotype positive)	12 (25.0%)	6 (20.7%)	6 (31.5%)	0.501
DSG3 (% genotype positive)	2 (4.2%)	1 (3.5%)	1 (5.30%)	1.000
DSP (% genotype positive)	8 (16.7%)	6 (20.7%)	2 (10.56%)	0.4510

optimum cut-off value of 0.81 mV giving an odds ratio of 13.0 (4.6 to 36.4). Please see Tables 3 and 4.

Combined right-precordial directed parameters

Based on combined right-precordial-directed-sided parameters including the RPD angle and RtRMS-QRS, at the above noted cut-off values, the sensitivity, specificity and odds ratios were 90.9%, 83.3%, and 45.0 (95% CI 15.8 to 128.2), respectively. Figure 2a-d shows depolarization parameter box plots.

ECG-negative proband versus ECG-negative non-proband

Thirty patients without abnormalities on the 12-lead ECG were probands (45.5%). At the cut-off values above (70.2 degrees for RPD angle and 0.81 mV for the RtRMS-QRS, respectively), the sensitivity for probands was 86.7% and for non-probands 72.5% for identification of those without 12-lead ECG abnormalities otherwise, while of course maintaining specificity 92.4% and 94.0% respectively.

ECG-based 2010 taskforce criteria and their relationship to the right-precordial ECG parameters

When the whole ARVD/C cohort was assessed ($N = 155$), the RtRMS-QRS significantly differentiated those with TAD (upslope of the S-wave ≥55 ms, minor depolarization criterion) versus those ARVD/C patients with upslope of the S-wave <55 ms ($p = 0.006$).

Patients with and without epsilon waves did not demonstrate significant difference in regard to the novel right-precordial parameters (Table 5). Patients with different extent of repolarization abnormalities, such as no

Table 2 Detailed electrocardiographical and imaging characteristics of ECG-positive and ECG-negative ARVC/D patients including Epsilon waves, upslope S-wave, Signal Average ECG measurements (SAECG) including fractional QRS duration (fqrsd), low amplitude signal under 40 microV in the latter part of QRS (LAS40) and root mean square amplitude in the last 40milliseconds (RMS40), repolarization abnormalities and echocardiogram/magnetic resonance imaging (MRI) including right ventricular end-diastolic volumes (RVEDV)

	ARVD/C (n = 155)	ARVD/C ECG-positive (N = 84)	ARVD/C ECG-negative (N = 66)	P-value ECG positive/ negative
ECG: Depolarization				
- Epsilon waves	13 (8.4%)	13 (15.5%)	0 (0.0%)	<0.001
- upslope S-wave ≥55 ms V1,V2 or V3	17 (11.0%)	17 (20.2%)	0 (0.0%)	<0.001
Bundle branch blocks	22 (14.1%)	17 (20.2%)	0 (0.0%)	0.035
SAECG performed (% total)	63 (40.7%)	32 (38.1%)	31 (41.7%)	0.515
- fQRSd ≥114 ms (% of SAECG)	33 (52.4%)	17 (53.1%)	16 (51.6%)	1.000
- LAS40 ≥ 38 ms (% of SAECG)	31 (49.2%)	18 (56.3%)	13 (41.9%)	0.317
- RMS40 ≤ 20 μV (% of SAECG)	28 (44.4%)	13 (40.6%)	15 (48.4%)	0.616
ECG: Repolarization				
- T-wave inversions V1-V3 > 14 years no RBBB	54 (34.8%)	54 (64.3%)	0 (0.0%)	<0.001
- T-wave inversions V1-V4 with RBBB	12 (7.7%)	12 (14.3%)	0 (0.0%)	<0.001
- T-wave inversions V1 and V2 or in V4,V5,V6	8 (5.2%)	8 (9.5%)	0 (0.0%)	0.008
Imaging				
Echocardiograms performed (% total)	155 (100.0%)	84 (100.0%)	66 (100.0%)	1.000
- Regional akinesia/dyskinesia/aneurysm (% echo)	111 (71.6%)	65 (77.4%)	43 (65.2%)	0.108
MRI's performed (% total)	124 (80.0%)	72 (85.7%)	52 (73.2%)	0.070
- Regional akinesia/dyskinesia/aneurysm (% MRI)	89 (71.8%)	58 (80.6%)	31 (59.6%)	0.272
- RVEDV ≥110 ml/m^2 (M), 100 ml/m^2 (F) (%MRI)	65 (52.4%)	49 (68.1%)	16 (30.8%)	<0.001
- RVEDV ≥100 ml/m^2 but <110 ml/m^2 (M), ≥90 ml/m^2 but <100 ml/m^2 (F) (%MRI)	24 (19.4%)	10 (11.9%)	14 (26.9%)	0.106

T-wave inversion/T-wave inversion in V1 (repolarization criterion is not present), T-wave inversion in V1 and V2 only (minor repolarization criterion) or T-wave inversions in V1-V3 or beyond (major repolarization criterion) were not differentiated by the right--precordial parameters (Table 5). The spatial QRS-T angle was lower for those with only T-wave inversions in V1 and V2, versus those with more precordial T-wave inversions or those without T-wave inversions in the precordial leads (Table 5).

Left ventricular involvement and clinical parameters

Twelve total ARVD/C patients had left-sided disease (7.7%). Eleven had decreased left ventricular ejection

Table 3 Vector and protractor measured angles and their respective p-values for the QRS duration (QRSd, milliseconds), corrected QT interval (QTc, milliseconds), the right precordial directed angle (RPD angle), and right root mean square QRS (RtRMS-QRS)respectively for different subsets of patients including controls, arrhythmogenic right ventricular dysplasia/cardiomyopathy patients who meet 12-lead 2010 Taskforce criteria (ECG-positive), who don't meet 12-lead 2010 Taskforce criteria (ECG-negative), who are ECG-negative without bundle branch blocks (BBB) and who are ECG-negative who have signal average ECG's do not have any late potentials (SAECG-). P-values as compared to controls

Parameter	QRSd (ms),[p-value]	QTc (ms),[p-value]	SPQRS-T angle	RPD angle	RtRMS-QRS
Controls (N = 66)	91.5 (85.5 to 99.0)	405.0 (387.5 to 430.2)	24.1 (13.5 to 42.1)	54.4 (48.9 to 61.5)	1.54 (1.17 to 1.90)
ARVD/C ECG-positive (N = 89)	104.0 (94.0 to 122.0), [<0.001]*	425.0 (403.0 to 449.0), [0.022]*	43.8 (23.6 to 72.9), [0.228]	74.8 (58.4 to 94.7), [0.971]	0.81 (0.63 to 1.13), [0.371]
ARVD/C ECG- and no BBB (N = 66)	98.0 (86.0 to 104.0), [0.052]s	412.0 (399.0 to 430.0), [0.061]	33.6 (16.7 to 54.2), [0.004]	76.2 (62.3 to 92.9), [<0.001]	0.81 (0.64 to 1.15), [<0.001]
ARVD/C ECG-, no BBB, SAECG-negative (N = 20)	93.0 (85.5 to 100.0), [0.947]	420.5 (397.5 to 430.0), [0.057]	40.9 (22.3 to 55.7), [0.081]	71.2 (60.4 to 84.7) [<0.001]	0.77 (0.67 to 1.18), [<0.001]

*indicated significant p-value < 0.050

Table 4 Derived-vectorcardiographic angles and their respective sensitivities, specificities, positive and negative predictive values (PPV, NPV, respectively) and odds ratios (95% confidence intervals) for optimal cut-off values based on ROC curve analysis for the corrected QT interval (QTc), spatial peaks QRS-T angle (SPQRS-T angle), the right precordial directed angle (RPD angle angle), right root mean square QRS (RtRMS-QRS), and for both right parameters (RPD angle angle and RtRMS-QRS) at the above cut-off values) for ECG-negative ARVD/C versus controls

Parameter	Optimum cut-off	AUC	*p*-value	Sensitivity (%)	Specificity (%)	PPV (%)	NPV (%)	Odds ratio
QRSd	99.0 ms	0.64	0.026	48.5	83.3	74.4	61.8	4.7 (2.1 to 10.6)
QTc	451.0 ms	0.56	0.289	12.1	100.0	100.0	53.2	19.3 (1.1 to 342.1)
SPQRS-T angle	50.8°	0.68	<0.001	30.0	94.0	53.6	50.9	1.2 (0.5 to 2.7)
RPD angle	70.2°	0.86	<0.001	72.7	94.0	91.7	80.5	41.3 (13.1 to 130.2)
RtRMS-QRS	0.81 mV	0.85	<0.001	51.5	92.4	92.3	77.5	13.0 (4.6 to 36.4)
Both right parameters	N/A	N/A	N/A	81.8	90.9	90.0	83.3	45.0 (15.8 to 128.2)

fraction (median 52.5%, IQR 50.5 to 54.0%) and three had LVEDVi >100 ml/m^2 (median 30.8 ml/m^2, IQR 26.5 to 97.0 ml/m^2). Three patients were ECG-negative and one had no late potentials. There was only a significant difference in the QRSd with those without LV changes at median 100 ms (IQR 90-113 ms) versus those with left sided changes at a median of 97 ms (IQR 91.5 to 101 ms). The median values for ARVD/C patients with left-sided changes for the QTc, SPQRS-T angle, RPD angle and RtRMS-QRS were 417 ms (IQR 401 to 457 ms), 23.0 degrees (IQR 15.6 to 51.5 degrees), 79.4 degrees (IQR 70.0 to 99.8 degrees), and 0.91 mV (IQR 0.54 to 1.21 mV), respectively.

Intra-observer and inter-observer variability

Intra-class correlation coefficients for the intra−/inter-observer variability for the RPD angle were 0.93 and 0.92, for the RtRMS-QRS were 0.94 and 0.92. For the SPQRS-T angle, intra−/inter-observer variability has previously been described [6, 14, 15].

Variability between automated analyses and 1st author calculations gave intra-class correlation coefficients of 0.971 and 0.917 for RtRMS-QRS and RPD angle.

Magnetic resonance imaging correlates

MRI indexed volumes and ejection fractions were compared to the VCG/ECG parameters above. The highest R-squared value for a VCG or ECG parameter was 0.24 for the SPQRS-T angle correlating to left ventricular ejection fraction (EF). Otherwise the RPD angle and RtRMS-QRS correlated poorly to RV indexed volume (indexed RVEDV) with R-squared values at 0.15 and 0.07, respectively and with RV EF R-squared values of 0.06 and 0.19, respectively, all without significant *p*-values. QRSd also correlated poorly with indexed RVEDV and RVEF with R-squared values of 0.10 and 0.11, respectively without significant *p*-values.

Discussion

Main findings

We aimed to assess whether patients with definite ARVD/C diagnosed using the 2010 revised Task Force criteria exhibit subtle electrocardiographic abnormalities, which do not fit in the frame of the depolarization and repolarization criteria outlined in the Task Force 2010 document. By comparing with a cohort of healthy controls we found that ostensibly normal ECG pattern in patients with ECG-negative ARVD/C contain signs of abnormal ventricular depolarization and repolarization that can be quantified using novel right precordial-adjusted VCG markers. RPD angle, SPQRS-T angle, and the RtRMS-QRS demonstrated significant ability to differentiate patients with electrocardiographically concealed ARVD/C from healthy controls. In addition,

Table 5 Novel right-precordial and vectorcardiographic values compared to ARVD/C patients and 2010 Taskforce criteria values currently used

	SPQRS-T angle (degrees)	RPD angle (degrees)	RtRMS-QRS (millivolts)
Epsilon-wave +, *n* = 13	54.4 ± 31.3	100.5 ± 42.5	1.0 ± 0.8
Epsilon-wave -, *n* = 142	54.6 ± 42.0	81.2 ± 31.2	0.9 ± 0.4
TAD > = 55 ms, *n* = 17	67.0 ± 41.1	92.9 ± 40.7	0.7 ± 0.3[a]
TAD < 55 ms, *n* = 138	53.1 ± 41.1	81.7 ± 31.4	0.9 ± 0.5[a]
No T-wave inversion/only in V1, *n* = 26	56.7 ± 31.0	83.8 ± 33.8	1.0 ± 0.6
T-wave inversion V1-V2, *n* = 56	35.0 ± 28.0[a]	87.5 ± 31.8	0.9 ± 0.4
T-wave inversion V1-V3 or beyond, *n* = 73	67.7 ± 46.8	78.1 ± 32.4	0.8 ± 0.4

[a]indicates significantly different novel parameter values per 2010 Taskforce ECG parameter differentiation mentioned

SPQRS-T angle exhibited stepwise increase and RtRMS-QRS a decrease when control cohort was compared with ECG-negative and ECG-positive ARVD/C patients thus suggesting novel markers potential for quantification of electrocardiographic ARVD/C phenotype. These may aid in early detection in clinical cascade screening.

QRSd and QTc

The QRSd was not a specific marker for -ECG ARVC/D, which is not surprising, given the patients don't meet 2010 taskforce criteria including epsilon waves or delayed S-wave upstroke. It does significantly differentiate ECG-positive ARVD/C from ECG-negative ARVD/C. The QTc did significantly differentiate patients with ECG-negative ARVD/C with minimal diagnostic assistance. The QTc also prolongs significantly as the ARVD/C patients develop Taskforce 2010 ECG criteria, which may or may not assist in diagnosis.

Spatial angles

Although conventional VCG markers have shown use in left sided heart disease [7–11], they have shown limited use in right heart disease [13]. For instance, in hypertrophic cardiomyopathy, the spatial QRS-T angle improves diagnostic ability for detection of hypertrophic cardiomyopathy over conventional 12-lead ECG parameters, however only detected part of our ECG-negative ARVD/C cohort [7]. This same angle, however showed limited prognostic ability in other right-ventricle disease patients, namely those with Tetralology of Fallot [13, 14]. The RPD angle had the highest identification ability out of all parameters tested and gave the highest odds ratio for identification of ECG-negative ARVD/C. Although the SPQRS-T angle significantly differentiates controls from ECG-negative ARVD/C, it did not prove as clinically useful with less sensitivity and less specificity than the RPD angle. Although some cases of ARVD/C include left sided disease (12 patients in our cohort), more often than not a right-sided only phenotype is present [2]. Thus, even though the SPQRS-T angle has prognostic and diagnostic use [7–11], and specifically for a generally left sided cardiomyopathy [7], it is not surprising that a right-sided specific marker is more helpful in identification of disease in those without other depolarization/repolarization abnormalities in ARVD/C as suggested by our findings. This also seemed to be particularly a good marker for those family members detected by cascade screening, who likely represent an early ARVC/D phenotype. This may be a useful marker for screening and can be programmed in most ECG software.

Right root mean square

The RtRMS-QRS or right precordial-directed QRS vector magnitude is simply a measure of depolarization dispersion in the right ventricle which should become smaller as more fibrosis occurs. The lower the RtRMS-QRS, the more dispersion of depolarization in the right ventricle would likely occur. The RtRMS-QRS had significant identification ability in those with ECG-negative ARVD/C compared to control patients with a high specificity. This is useful as it is a simple parameter to calculate (Fig. 1). Similar to other right side-specific voltage parameters, it has low sensitivity for detection of right heart disease in this study, however as a non-invasive and cost-effective test, this simple method still detected over one half of patients who were not initially detected by ECG [15]. Given the fibro-fatty infiltration of right ventricular myocardium often observed in ARVD/C, it seems logical that dispersion of depolarization (ie. lower RtRMS-QRS) would be affected [1]. Again, this would also particularly be helpful in identification of those with early ARVC/D disease, as it was able to detect those non-proband family members who represent an early stage of ARVC/D and meet 1 of their major criteria by family association alone.

Combined right-sided parameters

Combined, the diagnostic value of these parameters demonstrated superior identification power than each parameter alone. Combined, without compromising specificity, these parameters identified 65/71 (91.6%) of patients who would not have otherwise been identified with ECG screening. A high odds ratio was determined. These right-sided specific parameters, although not perfectly sensitive, combined have an additive identification ability without compromising specificity for patients who might otherwise fit 2010 taskforce criteria for definite ARVD/C based on genetic testing or further imaging [2].

Novel right-precordial parameters and the degree of ARVD/C phenotype manifestation

In the case of the S-wave angle and RtRMS-QRS, there appears to be a significant step-wise progression from control patients to ECG-negative and further on to the ECG-positive ARVD/C patients, which suggests that these novel VCG/ECG markers may be considered as electrocardiographic equivalent of the disease substrate in ARVC/D. RtRMS-QRS appears to be related to the conventional electrocardiographic disease markers such as terminal activation delay in the right precordial leads, however they perform well in differentiating patients with ARVC/D from controls also in the "normal" TAD range. This demonstrates the ability of the novel VCG/ECG markers to detect ARVC/D manifesting with subtle depolarization abnormalities only and indicate their potential in identification of affected family members, which requires additional studies.

The RPD angle did not have a step-wise progression, but was similar in number between those ARVD/C patients with and those without other depolarization or repolarization abnormalities. Also, this parameter did not differentiate the degree of T-wave inversion (Table 5), thus must be more affected by depolarization versus repolarization abnormalities. Even though not a significant difference, the RPD angle (as well as the other right-precordial parameters) demonstrated trends with Epsilon wave differentiation, which seem to indicate dependence on dispersion of depolarization.

Regardless, all three parameters detect ARVD/C patients with electrographically concealed changes. Further studies are warranted to define these changes over time as well as genotype differences.

Limitations

The retrospective nature of this study gives inherent limitations. The study control patients were from the USA and from Sweden and did not include those from Italy, specifically, which may bias our control results to some extent. Furthermore, any type of estimation from an ECG of a parameter, if not automated carries some inherent error, although our correlation coefficients were reasonable for intra−/inter-observer variability.

Conclusion

Patients with ECG-negative ARVD/C bear subtle ECG abnormalities that can be detected using right-sided measures including the RPD angle and the RtRMS-QRS. In combination these parameters can identify almost all patients with ECG-negative ARVD/C without compromising specificity. Future studies are warranted to identify changes in these parameters over time as well as to identify their utility in clinical cascade screening. If independently reproduced, these parameters should be considered for addition to current ARVD/C guidelines and may help to cost-effectively screen for ARVD/C in family members or those at risk.

Abbreviations

ARVC/D: Arrhythmogenic right ventricular cardiomyopathy/dysplasia; BBB: Bundle branch blocks; DSC2: Desmocollin 2; DSG2: Desmoglein 2; DSG3: Desmoglein 3; DSP: Desmoplakin; ECG: Electrocardiogram; F: Female; fQRSd: Filtered QRS duration; ICD: internal cardiac defibrillator; LAS40: Low amplitude duration < 40 mV; M: Male; Mri: Magnetic resonance imaging; Ms.: millisecond; mV: millivolt; NPV: Negative predictive value; OR: Odds ratio; PKP2: Plakophilin 2; PLN: Phospholamban; PPV: Positive predictive value; QRSd: QRS duration; QTc: Corrected QT interval; RMS40: Root mean square voltage last 40 milliseconds of the QRS; ROC: receiver operating characteristic curve; RPD angle: Right precordial-directed angle; RtRMS-QRS: Right root mean square QRS (millivolts); RVEDV: Right ventricular end-diastolic volume; SAECG: Signal average electrocardiogram; SPQRS-T angle: Spatial peaks QRS-T angle; TTN: Titin

Acknowledgements

Not otherwise applicable.

Funding

This work was supported by the Swedish National Health Service, Donation funds at Skåne University Hospital, Lund, Sweden, the Swedish Heart-Lung Foundation (20140734), and the Region Skåne.

Availability of data and materials

The data supporting the results and conclusions of the survey might be available from the corresponding author on reasonable request.

Authors' contributions

DC made substantial contributions to data conception, design, analysis and interpretation; he wrote the manuscript. AS was responsible a good portion of the data collection, and was thoroughly involved in drafting the manuscript. JC was responsible for the data, analysis and interpretation; he was involved in drafting the manuscript. SG made substantial contributions to data collection, and revision of the manuscript. NS was responsible for inter-observer variability, conception and design of the project and manuscript revision. FB made substantial contributions to the data collection and manuscript revision. AS made substantial contributions to the data collection and manuscript revision. LM made substantial contributions to the conception, design, data acquisition and manuscript revision PP made substantial contributions to conception, design, data acquisition, analysis and interpretation; he was involved in drafting and revising the manuscript; agreed to be accountable for all aspects of work in ensuring that any questions related to accuracy or integrity are appropriately investigated and resolved. All authors read and approved the final manuscript.

Ethics approval and consent to participate

This study was part of the Lund (568/2010), Colorado (COMIRB 99-177) and Italian Registries (43/2009) Stroke Register and thus all patients were consented and the study was approved by the Internal Review Board of Lund University and Skane Hospital, the University of Colorado and the University of Trieste and conformed to the Declaration of Helsinki and which included analysis of ECG variables.

Consent for publication

Not applicable.

Competing interests

The authors declare that they have no competing interests.

Publisher's Note

Author details

[1]Department of Cardiology, Clinical Sciences, Lund University, Lund, Sweden. [2]Electrophysiology/Cardiology, Penn State Milton S. Hershey Medical Center, Hershey, USA. [3]Department of Cardiology and Department of Medical and Health Sciences, Linkoping University, Linkoping, Sweden. [4]Cardiovascular Institute and Adult Medical Genetics Program, University of Colorado Denver AMC, Aurora, CO, USA. [5]Cardiovascular Department, Ospedali Riuniti and University of Trieste, Trieste, Italy. [6]Arrhythmia Clinic, Skåne University Hospital, Lund, Sweden.

Received: 12 July 2017 Accepted: 6 October 2017
Published online: 13 October 2017

References

1. Basso C, Corrado D, Fl M, Nava A, Thiene G. Arrhythmogenic right ventricular cardiomyopathy. Lancet. 2009;373:1289–300.
2. Fl M, McKenna WJ, Sherrill D, Basso C, Bauce B, Bluemke DA, Calkins H, Corrado D, Cox MG, Daubert JP, Fontaine G, Gear K, Hauer R, Nava A, Picard MH, Protonotarios N, Saffitz JE, Sanborn DM, Steinberg JS, Tandri H, Thiene G, Towbin JA, Tsatsopoulou A, Wichter T, Zareba W. Diagnosis of arrhythmogenic right ventricular cardiomyopathy/dysplasia: proposed modification of the task force criteria. Circulation. 2010;121:1533–41.
3. Hamid MS, Norman M, Quraishi A, .Firoozi S, Thaman R, Gimeno JR, Sachdev B, Rowland E, Elliott PM, McKenna WJ: Prospective evaluation of relatives for familial arrhythmogenic right ventricular cardiomyopathy/dysplasia reveals a need to broaden diagnostic criteria. J Am Coll Cardiol 2002; 40: 1445-1450.

4. Kaplan SR, Gard JJ, Protonotarios N, Tsatsopoulou A, Spiliopoulou C, Anastasakis A, Squarcioni CP, McKenna WJ, Thiene G, Basso C, Brousse N, Fontaine G, Saffitz JE. Remodeling of myocyte gap junctions in arrhythmogenic right ventricular cardiomyopathy due to deletion in plakoglobin. Heart Rhythm. 2004;1:3–11.
5. Te Riele AS, James CA, Rastegar N, Bhonsale A, Murray B, Tichnell C, Judge DP, Bluemke DA, Zimmerman SL, Kamel IR, Calkins H, Tandri H. Yield of serial evaluation in at-risk family members of patients with ARVD/C. J Am Coll Cardiol. 2014;64:293–301.
6. Cortez D, Sharma N, Devers C, Devers E, Schlegel TT. Visual transform applications for estimating the spatial QRS-T angle from the conventional 12-lead ECG: Kors is still most frank. J Electrocardiol. 2014;47:12–9.
7. Poplock Potter SL, Holmqvist F, Platonov PG, Steding K, Arheden H, Pahlm O, Starc V, McKenna WJ, Schlegel TT. Detection of hypertrophic Cardiomyopathy is improved when using advanced rather than strictly conventional 12-lead electrocardiogram. J Electrocardiol. 2010;43:713–8.
8. Kardys I, Kors JA, van der Meer IM, Hofman A, van der Kuip DA, Witteman JC. Spatial QRS-T angle predicts cardiac death in a general population. Eur Heart J. 2003;24:1357–64.
9. Kors JA, Kardys I, van der Meer IM, van Herpen G, Hofman A, van der Kuip DA, Witteman JC. Spatial QRS-T angle as a risk indicator of cardiac death in an elderly population. J Electrocardiol. 2003;36(Suppl):113–4.
10. Yamazaki T, Froelicher VF, Myers J, Chun S. Wang pl: spatial QRS-T angle predicts cardiac death in a clinical population. Heart Rhythm. 2005;2:73–78.16.
11. Borleffs CJ, Scherptong RW, Man SC, van Welsenes GH, Bax JJ, van Erven L, Swenne CA, Schalij MJ. Predicting ventricular arrhythmias in patients with ischemic heart disease: clinical application of the ECG-derived QRS-T angle. Circ Arrhythm Electrophysiol. 2009;2:548–54.
12. Cortez D, Graw S, Mestroni L. Hypertrophic cardiomyopathy, the spatial peaks QRS-t angle identifies those with sustained ventricular arrhythmias. Clin Cardiol. 2016;39:459–63.
13. Cortez D, Ruckdeschel E, McCanta AC, Collins K, Sauer W, Kay J, Nguyen D. Vectorcardiographic predictors of ventricular arrhythmia inducibility in patients with tetralogy of Fallot. J Electrocardiol. 2015;48:141–4.
14. Cortez D, Barham W, Ruckdeschel E, Sharma N, McCanta AC, von Alvensleben J, Sauer WH, Collins KK, Kay J, Patel S, Ngueyen DT. Noninvasive predictors of ventricular arrhythmias in patients with tetralogy of Fallot undergoing pulmonary valve replacement. JACC Clin Electrophysiol. 2017;3:162–170.
15. Whitman IR, Patel VV, Soliman EZ, Bluemke DA, Praestgaard A, Jain A, Herrington D, Lima JA, Kawut SM. Validity of the surface electrogram criteria for right ventricular hypertrophy: the MESA-RV study (multi-ethnic study of atherosclerosis-right ventricle). J Am Coll Cardiol. 2014;63:672–8.

Paper IV

Received: 25 April 2019 | Revised: 14 September 2019 | Accepted: 18 September 2019

DOI: 10.1111/jce.14210

ORIGINAL ARTICLE

WILEY

Quantitative T-wave morphology assessment from surface ECG is linked with cardiac events risk in genotype-positive KCNH2 mutation carriers with normal QTc values

Daniel Cortez MD[1,2] | Wojciech Zareba MD, PhD[3] | Scott McNitt MS[3] | Bronislava Polonsky MS[3] | Spencer Z. Rosero MD[3] | Pyotr G. Platonov MD, PhD[1]

[1]Clinical Sciences, Cardiology, Lund University, Lund, Sweden

[2]Pediatric Cardiology and Electrophysiology, University of Minnesota/Masonic Children's Hospital, Minneapolis, Minnesota

[3]Heart Research Follow-up Program, University of Rochester Medical Center, Rochester, New York

Correspondence
Daniel Cortez, MD, PhD, Lund University, Department of Pediatric Cardiology, University of Minnesota, 22450 Riverside Avenue, Minneapolis, MN 55454.
Email: dcortez@umn.edu

Disclosures: None.

Funding information
National Institutes of Health Grant, Grant/Award Number: HL-123483; Swedish Heart Lung Foundation, Grant/Award Number: 20150574; Fulbright Commission; Maggie Stephens Foundation; Swedish Society of Medicine, Grant/Award Number: SLS-551761; Skåne University Hospital, Grant/Award Number: 96332

Abstract

Introduction: Long QT syndrome (LQTS) mutation carriers have elevated the risk of cardiac events even in the absence of QTc prolongation; however, mutation penetrance in patients with normal QTc may be reflected in abnormal T-wave shape, particularly in KCNH2 mutation carriers. We aimed to assess whether the magnitude of a three-dimensional T-wave vector (TwVM) will identify KCNH2-mutation carriers with normal QTc at risk for cardiac events.

Methods: Adult LQT2 patients with QTc < 460 ms in men and <470 ms in women (n = 113, age 42 ± 16 years, 43% male) were compared with genotype-negative family members (n = 1007). The TwVM was calculated using T-wave amplitudes in leads V6, II, and V2 as the square root of $(TV6^2 + TII^2 + (0.5*TV2)^2)$. Cox regression analysis adjusted for gender and time-dependent beta-blocker use was performed to assess cardiac event (CE) risk, defined as syncope, aborted cardiac arrest, implantable cardioverter-defibrillator therapy, or sudden death.

Results: Dichotomized by median of 0.30 mV, lower TwVM was associated with elevated CE risk compared to those with high TwVM (HR = 2.95, 95% CI, 1.25-6.98, $P = .014$) and also remained significant after including sex and time-dependent beta-blocker usage in the Cox regression analysis (HR = 2.64, 95% CI, 1.64-4.24, $P < .001$). However, these associations were found only in women but not in men who had low event rates.

Conclusion: T-wave morphology quantified as repolarization vector magnitude using T-wave amplitudes retrieved from standard 12-lead electrocardiogram predicts cardiac events risk in LQT2 women and appears useful for risk stratification of KCNH2-mutation carriers without QTc prolongation.

KEYWORDS
cardiac events, long QT syndrome, T-wave vector magnitude

1 | INTRODUCTION

Long QT syndrome (LQTS) is one of the most lethal inheritable arrhythmias and the most common causes of sudden cardiac death without autopsy finding.[1,2] LQTS affects 1 in 2000 people.[3] There are three main subtypes of LQTS defined by mutations in KCNQ1, KCNH2, and SCN5A with different T-wave patterns and arrhythmogenic triggers as well as specific treatment based strategies.[4] For instance, patients with LQT1 typically have broad-based T-waves, while LQT2 patients typically have biphasic or flattened T-waves.[4]

Although in patients with LQT1, the arrhythmogenic risk is associated with prolongation of the heart rate corrected QT intervals, the second most common type of LQTS, LQT2, does not necessarily have arrhythmogenic risk associated with the degree of QTc prolongation.[5] About 20% to 50% of patients with LQTS do not have prolonged QTc.[6,7] Although mutation carriers have a higher risk of cardiac events than genotype-negative family members and therefore the risk of sudden death is still present for anyone with mutation, assessment for risk of cardiac events is not always straight forward or apparent for those without QTc prolongation.[6,8] Recently, qualitative measures of the T-wave appear to demonstrate risk stratification capability in LQT2 without QTc prolongation, however quantifiable methods are needed.[9]

Electrocardiogram (ECG)-derived vectorcardiographic (VCG) repolarization parameters offer the possibility of objective T-wave morphology measure and have demonstrated significant diagnostic and prognostic value in patients at risk for sudden cardiac death.[10-19] ECG-derived VCG has shown prognostic utility in LQTS patients with prolonged QTc values, while in LQTS patients without QTc prolongation, neither spatial durations nor the spatial QRS-T angle was able to differentiate symptomatic from asymptomatic LQTS patients.[20,21]

Assessment of the shape of the T-wave can be a way to identify patients with LQT2 without QTc prolongation at risk for cardiac events[4,9]; however, qualitative methods may be operator-dependent and subject to interindividual variability. The T-wave vector magnitude (TwVM) defined as the maximum distance from the origin of the 3-dimensional T-wave loop and calculated from the amplitudes of the T-wave in the orthogonal leads offers and attractive quantitative measure of T-wave polarity, amplitude and shape and has demonstrated diagnostic utility in other populations but not in LQTS patients.[22]

Given the flattening or biphasic shape of T-waves in LQT2, we hypothesized that the TwVM, a quantifiable measure of T-wave flattening, will identify those LQT2 patients without QTc prolongation at risk for cardiac events.

2 | METHODS

2.1 | Study population

Patients in this study were from the Rochester-based LQTS Registry; enrollment into the registry has been previously described.[22-24] Patients were selected to the current analysis if they were shown to be carriers of the disease-causing mutation in KCNH2 (LQT2), had Bazett-corrected QT interval (QTc) of less than 470 ms for female and less than 460 ms for male, and were 18 years or older to exclude variation of the T-wave morphology that may be observed in children and adolescents. The first recorded ECG at age 18 or older was used and the Bazette-corrected QTc was calculated based on digital caliper QT measurement by an electrophysiologist. Ten-second recordings were used. Patients were excluded from the study if they had more than one LQTS-associated mutation. The presence of LQTS-causing KCNH2 mutations was verified with the use of standard genetic tests performed in the academic molecular genetic laboratories reported previously.[8]

The study population also required the patients who met the above criteria to have ECGs (at time of enrollment in the prospective registry) with flat baselines in leads I, II, and V1-V6 (<0.1 mV movement), adequate for assessment of voltage parameters. Poor quality ECGs, with movement artifacts, were excluded.

Patients with LQT2 without QTc prolongation were compared with a control population of 1007 individuals who belonged to families with genotype-positive probands, but who were genetically tested and found to be negative for LQT-associated mutations and who also had normal QTc intervals (per above).

2.2 | Clinical data

Clinical data were collected on prospectively designed forms with information on demographic characteristics, personal and family medical history, ECG findings, therapy, including QT-prolonging medications, and events during long-term follow-up. Information about beta-blocker use was also collected to allow time-dependent assessment of their possible impact on the incidence of cardiac events.

2.3 | T-wave morphology characterization

At enrollment in the registry, all incoming ECGs were assessed by a cardiologist (WZ or SZR), who were blinded to subjects' clinical characteristics, in regard to the T-wave morphology in leads V5 and II, which was classified as either normal, broad, flat, notched, negative, or biphasic.[20,24] For the purpose of this analysis, T-wave morphologies, which were not assessed as normal in either lead II (L2) or V5, were classified as abnormal, indicating the possible presence of manifesting ventricular repolarization abnormality.

2.4 | ECG and derived-vector evaluation

ECG measurements were performed by the first author who was blinded to the clinical characteristics of the patients. ECGs were recorded at a speed of 25 mm/s with 10 mm/mV reference for limb and precordial leads. The corrected QT-intervals (QTc) from Bazette's formula, spatial QRS-T angles, and TwVM were assessed on all ECGs. The spatial QRS-T angle was calculated by the peaks method, utilizing the visually estimated method by Kors' et al.[25,26] TwVM was calculated as the square root of the sum of the squared T waves in leads V6, II and one half of the T wave amplitude in V2, given by the equation TwVM = *SQRT*[*Twavell*)^2 + (TwaveV6)^2 + (0.5*TwaveV2)^2], based on the T-wave magnitude as defined by the transformed Kors' Quasi-orthogonal method, utilizing the beat with a stable baseline (median when it met this standard).[25,26] Please see Figure 1, for example, TwVM calculation.

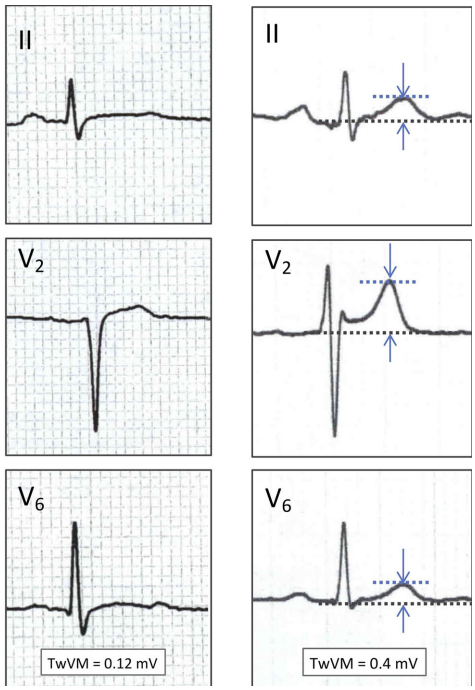

FIGURE 1 Examples of ECG leads II, V2, and V6 used for assessment of the vectrocardiographic T wave vector magnitude from two LQT2 mutation carriers with low TwVM of 0.12 mV (left) and higher Twvm at 0.40 mV (right). ECG, electrocardiogram; TwVM, T-wave vector magnitude

2.5 | Endpoints

The primary endpoint of the study was the occurrence of a first cardiac event that included syncope (transient loss of consciousness that was abrupt in onset/recovery), aborted cardiac arrest requiring defibrillation as part of resuscitation (ACA), LQTS-related sudden cardiac death (SCD, defined as abrupt in onset, if witnessed-not explained by other cause, if not witnessed-was not explained by any other cause) or implantable cardioverter-defibrillator (ICD) therapy including anti-tachycardia pacing (ATP) or shock therapy.

2.6 | Statistical analysis

Data were assessed for normality using Shapiro–Wilk testing. Normally distributed continuous data are presented as mean and standard deviation. Student *t*-tests, χ^2, and analysis of variance were used to identify significant differences between groups. Receiver operating characteristic (ROC) curve analysis was performed to identify threshold values for VCG parameters associated with cardiac events. The cumulative probability was assessed by the Kaplan–Meier method with significance testing by the log-rank statistic. The Cox proportional hazard model was used to evaluate the independent contribution of clinical and genetic factors to the first occurrence of time-dependent cardiac events from the age of 18 years through the end of follow-up. The Cox regression model was adjusted for the time-dependent beta-blocker use (the age at which patients were on and off beta-blocker therapy) and stratified by sex. As preselected QTc inclusion overlapped with borderline QTc prolongation, the model was adjusted for QTc duration wit 440 ms selected as a cutoff for normal vs borderline QTc values. The proportionality assumption was tested using time-dependent covariates created from interactions between survival time and various covariates. Pearson and Spearman correlation coefficients were used as appropriate for parametric and non-parametric data. Intraobserver and interobserver variability were estimated by intraclass correlation coefficients based on a 10% sample of the population. Repeatability was performed by Daniel Cortez, MD and Pyotr Platanov, MD/PhD. Data analysis was performed using SPSS (IBM, Chicago, IL).

3 | RESULTS

3.1 | Clinical characteristics

One hundred and fifty-four patients met clinical inclusion criteria, of whom 113 patients had ECG's suitable for assessment. These 113 patients with LQT2 with normal QTc values (mean age 42 ± 16 years, 43% male) comprised the study group and were compared with 1007 normal QTc control patients (mean age 41 ± 15 years, 41% male). LQT2 mutation carriers did not differ from the control group in regard to the age at enrollment or gender distribution, however, they had significantly lower heart rate, longer QTc (even though still within normal range), QTpeak and Tpeak-Tend intervals in comparison with the genotype-negative subjects (Table 1). As previously reported,[9] the proportion of subjects demonstrating visually abnormal T wave morphology at inclusion in the registry was nearly five times higher among LQT2 mutation-positive patients than in the control group. The proportion of individuals experiencing syncopal episodes was significantly higher among LQT2 mutation carriers, however, very few were treated with beta-blockers or had more serious events by the age of 18 (baseline), as shown in Table 1.

3.2 | Derived T-wave vector magnitude and clinical characteristics of LQT2 mutation carriers

Among patients carrying LQT2 mutation who had ECG available for TwVM assessment, median TwVM was 0.30 mV, which was used as a cut-off for analyses of associations between TwVM and clinical characteristics and study endpoints. TwWM was significantly higher in LQT2 men than women: 3.8 ± 1.8 vs 3.0 ± 1.3 mV, respectively ($P = .020$). Intraclass correlation coefficients for the TwVM measurements for a 10% sample of the population gave interobserver variability of 0.94.

LQT2 mutation carriers with TwVM ≤ 0.30 mV were more likely to be female, have lower heart rates, have syncope and receive beta-blocker treatment (Table 2). Low TwVM was strongly associated with

TABLE 1 Clinical characteristics for genotype negative LQTS family members with normal QTc values and genotype positive LQT2 patients with normal QTc values at baseline (18 years)

Clinical characteristics	Normal QTc Genotype-negative family members n = 1007	Normal QTc LQT2 carriers n = 113	*P* value
Male, #(%	414 (41)	49 (43)	.645
Age at ECG, y	41 ± 15	42 ± 16	.242
Pore Mutation	N/A	18 (16)	N/A
ECG characteristics			
RR, msec	893 ± 166	951 ± 176	**.001**
PR, msec	161 ± 28	163 ± 23	.807
QRS, msec	85 ± 14	85 ± 14	.919
QTp, msec	305 ± 31	326 ± 42	**<.001**
QT, msec	391 ± 34	421 ± 38	**<.001**
QTc, msec	417 ± 26	434 ± 25	**<.001**
TpTe, msec	86 ± 21	95 ± 30	**.004**
Abnormal T-wave in V5/L2	64 (7)	35 (34)	**<.001**
Treatment, #(%)			
Beta-blockers	3 (0)	2 (2)	**<.001**
LCTSD	0(0)	0 (0)	N/A
Pacemaker	1 (0)	0 (0)	1.000
ICD	1 (0)	1 (1)	.192
Cardiac Events, # (%)			
Syncope	62 (6)	15 (13)	**.009**
ACA	1 (0)	0 (0)	1.000
Appropriate Shock	0 (0)	0 (0)	N/A

Abbreviations: ACA, aborted cardiac arrest; ECG, electrocardiogram; ICD, implantable cardioverter-defibrillator; LCTSD, left cervicothoracic sympathectomy; LQTS, long QT syndrome.
Bold values indicate significance, $P < .05$.

the visually assessed abnormal T-wave morphology: of 35 LQT2 mutation carriers demonstrating abnormal T-wave morphology, 26 (75%) had low TwVM ($P < .001$). There was a trend indicating greater proportion of LQT2 pore-mutation carriers among patients with low TwVM, though the difference was not significant (21% vs 11%, $P = .144$).

3.3 | Clinical course in LQT2 patients with normal QTc values

During follow up, 27 LQT2 mutation carriers had CE, of which 5 were ACA and 22 syncopal episodes (compared with 62 syncopal episodes and 1 ACA in the control group), which were assessed using Kaplan–Meier curve analysis and Cox regression analysis as outlined in the Methods. Four ACA events were observed among female LQT2 carriers who had low TwVM and one ACA event occurred to a male patient with high TwVM.

Figure 2A-C show Kaplan–Meier curve analysis of the risk of cardiac events in normal QTc LQT2 mutation carriers dichotomized by the median TwVM and compared with the genotype-negative controls shown for the entire study cohort (Figure 2A) and separately for men (Figure 2B) and women (Figure 2C). In the entire cohort, low TwVM was associated with a high risk of cardiac events among the LQT2 patients with normal QTc values, while the curve indicating the cumulative risk of cardiac events among these same patients with high TwVM was overlapping with the one corresponding to the genotype-negative controls. In the univariate Cox regression analysis, TwVM ≤ 0.30 mV was associated with the increased risk of cardiac events (HR = 2.95, 95% CI, 1.25-6.98, $P = .014$) compared to LQT2 patients (with normal QTc values) with TwVM > 0.30 mV. After including sex and time-dependent beta-blockade use in the multivariate Cox regression analysis, low TwVM remained a significant predictor of cardiac event risk (HR = 2.55, 95% CI, 1.07-6.04, $P = .034$). This difference was primarily due to the differences observed among women (HR_{female} = 3.18, 95% CI, 1.91-5.98, $P = < .001$; HR_{male} = 1.05, 95% CI, 0.25-4.37, $P = .947$, Table 3). After including sex and time-dependent beta-blockade use in the Cox regression analysis, low TwVM remained a significant predictor of cardiac event risk within the LQT2 cohort (HR = 2.55, 95% CI, 1.07-6.04, $P = .034$). There were no differences in LQT2 patients with TwVM > 0.30 mV compared to controls in respect to survival to CE, and whether men and women, just women, or just men were evaluated (Table 3).

TABLE 2 Characteristics of electrocardiographically concealed LQT2 patients (genotype positive KCNH2 with normal QTc values), based on cut-offs of the median product of the T wave vector magnitude (TwVM) at baseline (18 years)

Clinical characteristics	TwVM ≤ median N = 57	TwVM > median N = 56	*P* value
Male, # (%)	17 (30)	32 (57)	**.003**
Age at ECG, y	44 ± 16	40 ± 15	.230
Pore Mutation, # (%)	12 (21)	6 (11)	.144
ECG characteristics			
RR, msec	912 ± 168	991 ± 177	**.017**
PR, msec	163 ± 22	162 ± 24	.850
QRS, msec	83 ± 12	87 ± 15	.102
QTp, msec	326 ± 45	327 ± 39	.885
QT, msec	417 ± 43	425 ± 33	.202
QTc, msec	438 ± 22	430 ± 27	.091
TpTe, msec	92 ± 33	98 ± 27	.404
Abnormal T-wave in V5/L2	26 (50)	9 (17)	**<.001**
TwVM	0.22 ± 0.05	0.45 ± 0.14	**<.001**
Treatment, # (%)			
Beta-blockers	1 (2)	1 (2)	1.000
LCTSD	0	0	N/A
Pacemaker	0	0	N/A
ICD	0	1(2)	.495
Cardiac Events, # (%)			
Syncope	10 (18)	5 (9)	.269
ACA	0	0	N/A
Appropriate Shock	0	0	N/A

Abbreviations: ACA, aborted cardiac arrest; ECG, electrocardiogram; ICD, implantable cardioverter-defibrillator; LCTSD, left cervicothoracic sympathectomy.
Bold values indicate significance, $P < .05$.

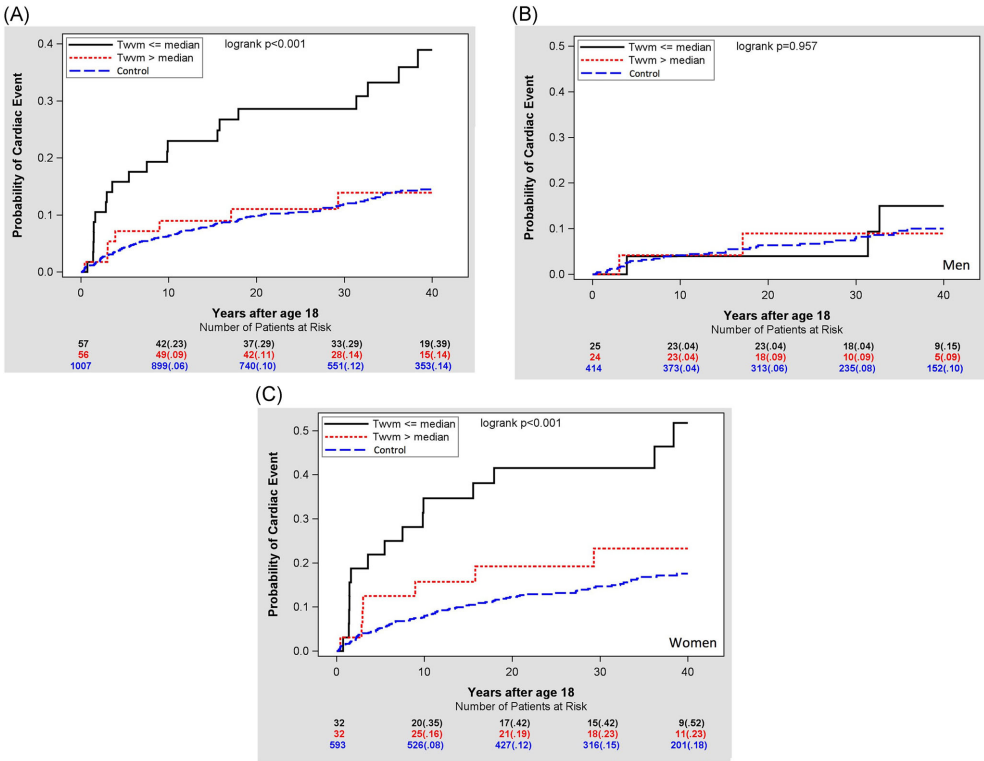

FIGURE 2 A, Probability of cardiac events dichotomized by the median T-wave vector magnitude (TwVM of 0.30 mV) among the LQT2 patients with normal QTc values compared with genotype-negative control individuals. B, Probability of cardiac events based on the median (0.3 mV) T-wave vector magnitudes (TwVM) for men only. C, Probability of cardiac events based on the median (0.3 mV) T-wave vector magnitudes (TwVM) for women only

It is worth stressing that these associations were present in women but not in men who presented with low risk of cardiac events. As sensitivity analysis we repeated the above Cox analyses while using sex-specific median TwVM values as cut-offs in males (≤0.37 mV) and females (≤0.27 mV) and the results were very similar: hazard ratio of 3.30 ($P < .001$) in females and 0.78 ($P = .732$) in males when comparing risk of events in individuals with lower vs higher than median TmVM values.

TwVM demonstrated a significant association with the risk of ACA/SCD (HR = 2.64, 95% CI, 1.64-4.24, $P < .001$) compared to genotype-negative family members (Figure 3).

TABLE 3 Probability of cardiac events in the Cox regression analysis in the ECG concealed LQT2 patients with adjustment for time-dependent beta-blocker usage based on T-wave vector magnitude cut-off of 0.3 mV with female and male cohorts also presented separately. The hazard ratio for the genotype-negative control population versus the entire genotype negative cohort is also presented

	All			Females			Males		
	HR	95% CI	*P* value	HR	95% CI	*P* value	HR	95% CI	*P* value
ecLQT2 TwVM ≤0.30 mV vs ecLQT2 TwVM > 0.30 mV	2.55	1.07-6.04	.034	3.18	1.08-9.40	.036	0.99	0.17-5.95	.993
ecLQT2 TwVM ≤0.30 mV vs Genotype-negative control	2.64	1.64-4.24	<.001	3.18	1.91-5.28	<.001	1.05	0.25-4.37	.947
ecLQT2 TwVM > 0.30 mV vs Genotype-negative control	1.38	0.72-2.62	.333	1.37	0.64-2.95	.422	1.39	0.43-4.52	.589

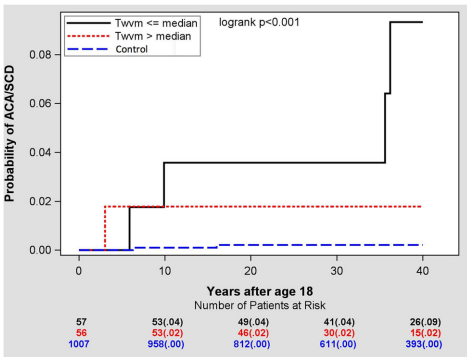

FIGURE 3 Probability of sudden cardiac death or ACA in genotype positive KCNH2 mutation carriers with normal QTc values based on T-wave vector magnitude (TwVM) cut-off value of 0.30 mV as compared to genotype negative control individuals. ACA, aborted cardiac arrest

4 | DISCUSSION

Our study demonstrates the ability of an easily calculated, quantifiable parameter, the TwVM, to identify LQT2 patients with normal QTc values at risk for cardiac events with increased cardiac events risk being associated with reduced TwVM. While an earlier study by our group suggested abnormal T wave morphology, which included qualitatively assessed flat, broad or notched T waves, as an indicator of mutation penetrance associated with cardiac event risk,[9] the current analysis has demonstrated the value of a quantitative measure of three-dimensional T-wave magnitude for risk stratification of LQT2 patients with unaffected QTc. To our knowledge, this is the first study to demonstrate this particular risk factor in the LQTS context.

Earlier attempts to quantify T-wave morphology in patients with LQTS involved VCG studies and standard 12-lead ECG based measures such as measured T-wave slope or T-wave center of gravity.[19,27] An advantage of VCG is its ability to address three-dimensional T wave morphology while other T wave measures are bound to specific surface ECG leads. For example, the significant association with cardiac events in LQTS patients with prolonged QTc values was shown regarding the slope of the T-wave in lead V6.[27] The earlier reported VCG measures, however, have been limited to computed eigenvector values. More complicated compared to TwVM, the eigenvector values appeared to be able to differentiate symptomatic from asymptomatic LQTS patients but are difficult to conceptualize and most of the commonly used ECG systems are not able to calculate them.[19] On the other hand, not all T wave morphology markers have performed as significant risk indicators in the context of LQTS with normal QTc values. The center of gravity x-axis (last 25% of T-wave) in lead I,[27] for example, was an independent predictor of cardiac events in LQTS patients with prolonged QTc but not in unaffected mutation carriers.[27]

Our study demonstrated that cardiac event risk stratification was similarly determined for female patients with LQT2 (with normal QTc values) by our quantitative parameter as by the T-wave morphology as read by electrophysiologist.[9] As noted in Table 2, there were more patients of female sex with Twvm of less than or equal to 0.3 mV. Similar to our earlier report, the T-wave changes were not significant for risk stratification in males, although the number of male patients with cardiac events were generally low.[9] In LQT2 patients with normal QTc values, male sex male was associated with higher TwVM values. Lower T-wave amplitudes have been demonstrated in females after oophorectomy with improvement once estrogen replacement was given, thus, likely sex hormonal variation affects the TwVM to some degree as well.[28] Differences in corrected QT interval have also been demonstrated in healthy males and females, including menstrual cycle phase-dependent for females.[29-31] However, in a population of LQTS patients with normal QTc values, it is difficult to know if subtle prolongation would have any significant effect. Otherwise, utilizing the control group of genotype negative family members allows a true risk of events within families of patients with LQT2 based on their genotype status and ECG findings.

Given a similar effect on I_{kr}, implications for risk stratification of patients with QTc prolongation on particular medications may be of significance. The TwVM may help identify those at risk for torsades, who take QTc prolonging agents given similar T-wave morphologies and effect on Ikr. Future studies should consider this approach for risk assessment.

4.1 | Limitations

Almost all events were in females, thus it is unknown how helpful this tool is in QTc unaffected men with genotype positive KCNH2, as more events would be needed to eliminate a type 2 error. The number of ACA/SCD events was too low for robust statistical assessment. The observed association of reduced TwVM with ACA/SCD in the univariable analysis should, therefore, be interpreted with caution. Furthermore, mutation-negative family members were included in the analysis as a control group to compare the incidence of clinical events rather than for assessment of T-wave characteristics in the genetically unaffected individuals. Therefore, no comparison of TwVM between LQT2 patients and the control group could be performed, which is a limitation of the study.

5 | CONCLUSION

T-wave morphology quantified as repolarization vector magnitude using T-wave amplitudes retrieved from standard 12-lead ECG predicts cardiac event risk in LQT2 patients and appears to be useful for risk stratification of KCNH2-mutation carriers without QTc prolongation. This association was found in women but not in men with LQT2.

ACKNOWLEDGMENTS

The study was performed with support from National Institutes of Health grant (No. HL-123483). Dr. Platonov was supported by the research grant from the Swedish Heart-Lung Foundation (grant no. 20150574) and scholarship grants from the Fulbright Commission, Maggie Stephens Foundation, Swedish Society of Medicine, (grant no. SLS-551761)

and donation funds at Skåne University Hospital (Lund, Sweden) (grant no. 96332).

CONFLICT OF INTERESTS

The authors declare that there are no conflict of interests.

ORCID

Daniel Cortez http://orcid.org/0000-0001-9874-0733

REFERENCES

1. McGorrian C, Constant O, Harper N, et al. Family-based cardiac screening in relatives of victims of sudden arrhythmic death syndrome. *Europace*. 2013;15:1050-1058.
2. Behr ER, Dalageorgou C, Christiansen M, et al. Sudden arrhythmic death syndrome: familial evaluation identifies inheritable heart disease in the majority of families. *Eur Heart J*. 2008;29:1670-1680.
3. Schwartz PJ, Stramba-Badiale M, Crotti L, et al. Prevalence of the congenital long-QT syndrome. *Circulation*. 2009;120:1761-1767.
4. El-Sherif N, Turitto G, Boutjdir M. Congenital Long QT syndrome and torsade de pointes. *Ann Noninvasive Electrocardiol*. 2017;22:e12481. https://doi.org/10.1111/anec.12481
5. Mathias A, Moss AJ, Lopes CM, et al. Prognostic implications of mutation-specific QTc standard deviation in congenital long QT syndrome. *Heart Rhythm*. 2013;10:720-725.
6. Vincent GM, Timothy KW, Leppert M, Keating M. The spectrum of symptoms and QT intervals in carriers of the gene for the long-QT syndrome. *N Engl J Med*. 1992;327:846-852.
7. Vink AS, Neumann B, Lieve KVV, et al. Determination and interpretation of the QT Interval: comprehensive analysis of a large cohort of long QT syndrome patients and controls. *Circulation*. 2018;138:2345-2358.
8. Goldenberg I, Horr S, Moss AJ, et al. Risk for life-threatening cardiac events in patients with genotype-confirmed long-QT syndrome and normal-range corrected QT intervals. *J Am Coll Cardiol*. 2011;57:51-59.
9. Platonov PG, McNitt S, Polonsky B, et al. Risk stratification of type 2 long-QT syndrome mutation carriers with normal QTc interval: the value of sex, T-wave morphology, and mutation type. *Circ Arrhythm Electrophysiol*. 2018;11:e005918. https://doi.org/10.1161/CIRCEP.117.005918
10. Voulgari C, Pagoni S, Tesfaye S, Tentolouris N. The spatial QRS-T angle: implications in clinical practice. *Curr Cardiol Rev*. 2013;9:197-210.
11. Cortez D, Graw S, Mestroni L. In hypertrophic cardiomyopathy, the spatial peaks QRS-T angle identifies those with sustained ventricular arrhythmias. *Clin Cardiol*. 2016;39:459-463.
12. Rautaharju PM, Prineas RJ, Wood J, Zhang ZM, Crow R, Heiss G. Electrocardiographic predictors of new-onset heart failure in men and in women free of coronary heart disease (from the Atherosclerosis in Communities [ARIC] study). *Am J Cardiol*. 2007;100:1437-1441.
13. Yamazaki T, Froelicher VF, Myers J, Chun S, Wang P. Spatial QRS-T angle predicts cardiac death in a clinical population. *Heart Rhythm*. 2005;2:73-78.
14. Poplock Potter SL, Holmqvist F, Platonov PG, et al. Detection of hypertrophic cardiomyopathy is improved when using advanced rather than strictly conventional 12-lead electrocardiogram. *J Electrocardiol*. 2010;43:713-718.
15. Cortez D, Sharma N, Cavanaugh J, et al. The spatial QRS-T angle outperforms the Italian and Seattle ECG-based criteria for detection of hypertrophic cardiomyopathy in pediatric patients. *J Electrocardiol*. 2015;48:826-833.
16. Cortez D, Sharma N, Cavanaugh J, et al. Lower spatial QRS-T angle rules out sustained ventricular arrhythmias in children with hypertrophic cardiomyopathy. *Cardiol Young*. 2017;27:354-358.
17. Cortez D, Ruckdeschel E, McCanta AC, et al. Vectorcardiographic predictors of ventricular arrhythmia inducibility in patients with tetralogy of Fallot. *J Electrocardiol*. 2015;48:141-144.
18. Cortez D, Barham W, Ruckdeschel E, et al. Noninvasive predictors of ventricular arrhythmias in patients with tetralogy of fallot undergoing pulmonary valve replacement. *JACC: Clin Electrophysiol*. 2017;3:162-170.
19. Priori SG, Mortara DW, Napolitano C, et al. Evaluation of the spatial aspects of T-wave complexity in the long-QT syndrome. *Circulation*. 1997;96:3006-3012.
20. Cortez D, Bos JM, Ackerman MJ. Vectorcardiography identifies patients with electrocardiographically concealed long QT syndrome. *Heart Rhythm*. 2017;14:894-899.
21. Cortez D, Patel S, Sharma N, et al. Repolarization vector magnitude differentiates Kawasaki disease from normal children. *Ann Noninvasive Electrocardiol*. 2016;21:493-499.
22. Goldenberg I, Mathew J, Moss AJ, et al. Corrected QT variability in serial electrocardiograms in long QT syndrome. *J Am Coll Cardiol*. 2006;48:1047-1052.
23. Migdalovich D, Moss A, Lopes CM, et al. Mutation and gender-specific risk in type 2 long QT syndrome: implications for risk stratification for life-threatening cardiac events in patients with long QT syndrome. *Heart Rhythm*. 2011;8:1537-1543.
24. Cortez D, Sharma N, Devers C, Devers E, Schlegel TT. Visual transform applications for estimating the spatial QRS-T angle from the conventional 12-lead ECG: Kors is still most Frank. *J Electrocardiol*. 2014;47:12-19.
25. Kors JA, van Herpen G, Sittig AC, van Bemmel JH. Reconstruction of the Frank vectorcardiogram from standard electrocardiographic leads: diagnostic comparison of different methods. *Am J Cardiol*. 1990;11(12):1083-1092. https://www.ncbi.nlm.nih.gov/pubmed/2292255
26. Moss AJ, Zareba W, Benhorin J, et al. ECG T-wave patterns in genetically distinct forms of the hereditary long QT syndrome. *Circulation*. 1995;92:2929-2934.
27. Sugrue A, Noseworthy PA, Kremen V, et al. Identification of concealed and manifest long QT syndrome using a novel T wave analysis program. *Circ Arrhythm Electrophysiol*. 2016;9:e003830.
28. De Leo V, la Marca A, Agricola E, Morgante G, Mondillo S, Setacci C. Resting ECG is modified after oophorectomy and regresses with estrogen replacement therapy in premenopausal women. *Maturitas*. 2000;36:43-47.
29. Burke JH, Ehlert FA, Kruse JT, Parker MA, Goldberger JJ. Gender-specific differences in the QT interval and the effect of autonomic tone and menstrual cycle in healthy adults. *Am J Cardiol*. 1997;79:178-181.
30. Zareba W, Moss AJ, Locati EH, et al. International Long QT Syndrome Registry. Modulating effects of age and gender on the clinical course of long QT syndrome by genotype. *J Am Coll Cardiol*. 2003;42:103-109.
31. Kutyifa V, Daimee UA, McNitt S, et al. Clinical aspects of the three major genetic forms of long QT syndrome (LQT1, LQT2, LQT3). *Ann Noninvasive Electrocardiol*. 2018;23:e12537. https://doi.org/10.111/anec

How to cite this article: Cortez D, Zareba W, McNitt S, Polonsky B, Rosero SZ, Platonov PG. Quantitative T-wave morphology assessment from surface ECG is linked with cardiac events risk in genotype-positive KCNH2 mutation carriers with normal QTc values. *J Cardiovasc Electrophysiol*. 2019;30:2907–2913. https://doi.org/10.1111/jce.14210